



Analysis of the molecular basis of herbicide resistance in plants

Fatemeh Abdollahi

► To cite this version:

Fatemeh Abdollahi. Analysis of the molecular basis of herbicide resistance in plants. Organic chemistry. Université de Strasbourg; University of Mohaghegh Ardabili (Ardabil, Iran), 2020. English. NNT : 2020STRAF012 . tel-03504141

HAL Id: tel-03504141

<https://theses.hal.science/tel-03504141>

Submitted on 28 Dec 2021

HAL is a multi-disciplinary open access archive for the deposit and dissemination of scientific research documents, whether they are published or not. The documents may come from teaching and research institutions in France or abroad, or from public or private research centers.

L'archive ouverte pluridisciplinaire **HAL**, est destinée au dépôt et à la diffusion de documents scientifiques de niveau recherche, publiés ou non, émanant des établissements d'enseignement et de recherche français ou étrangers, des laboratoires publics ou privés.

ÉCOLE DOCTORALE DES SCIENCES CHIMIQUES

Equipe de Synthèse Organique et Phytochimie (SOPhy), UMR 7177

THESE présentée par :

Fatemeh ABDOLLAHI

Soutenue le : 16 Septembre 2020

Pour obtenir le grade de : **Docteur de l'université de Strasbourg**

Discipline/ Spécialité : **Chimie Organique**

**Analyse des bases moléculaires de la
résistance aux herbicides chez les
plantes**

THÈSE dirigée par :

Dr. MIESCH Laurence, Directrice de Recherche CNRS, Université de Strasbourg

CODIRECTEUR DE THÈSE :

Dr. ALEBRAHIM Mohammad Taghi, Associate Professor, University of Mohaghegh Ardabili

RAPPORTEURS :

Dr. BOUCHER Jean Luc, Directeur de Recherche CNRS, Université Paris Descartes
Dr. GHAVIDEL Akbar, Associate Professor, University of Mohaghegh Ardabili

AUTRES MEMBRES DU JURY :

Dr. NAVROT Nicolas, Maître de Conférence, Université de Strasbourg

Acknowledgments

I would like to thank Dr. Laurence Miesch, Dr. Daniele Werck, Dr. Francois Andre and Dr. Nicolas Navrot for continued guidance. Without them, and their patience and immense knowledge, this thesis would not have been possible, and thank them for always being available to answer my questions and have a good chat, I am very grateful for their friendship, support and advice. I would like to thank Dr. Mohammad Thaghi Alebrahim for provided financial support to complete this degree.

I would also like to thank the committee members: Dr. Jean Luc Boucher and Dr. Akbar Ghavidel. It is a pleasure to thank my fellow lab members in past and present, for their intimate contacts to make a happy and warm environnement that makes the everyday lab work easier. I am extremely grateful to both the university of Strasbourg and university of Mohaghegh Ardabili for providing me with the best educational possibility. Now, I wish to thank all the persons who accompanied and supported me during the long journey of PhD thesis research.

Finally, I owe my deepest gratitude to my parents and my brothers not only have they always encouraged me to continue my education, they have taught me the importance of hard work and keeping a positive attitude. To them I am forever grateful.

Fatemeh ABDOLLAHI

Table of contents

List of figures.....	iii
List of tables.....	vi
Chapter 1	1
General Introduction	2
Herbicide Resistance	3
Mechanisms of herbicide resistance	6
Target-site herbicide resistance (TSR).....	6
Non-target-site herbicide resistance (NTSR)	7
Glutathione S-transferases (GSTs)	8
Cytochrome P450 monooxygenases.....	9
Structure of the cytochrome P450 enzymes	9
Nomenclature of cytochromes P450	10
Classification of cytochromes P450	11
Functions of cytochrome P450 enzymes	12
The catalytic reaction.....	12
Role of P450 enzymes in drug metabolism.....	15
Role of P450 enzymes in plants.....	17
Role of plant P450s in the metabolism of endogenous compounds	17
Role of plant P450s in the metabolism of exogenous compounds.....	17
Metabolism of herbicides.....	17
Synergists and P450 inhibitors.....	20
Safeners and P450 inducers	21
Dinitroaniline herbicides	22
Research objective.....	24
Chapter 2	26
Herbicides assayed for plant P450 metabolism.....	27
Transgenic plant lines	30

Enzyme expression in yeast and isolation of recombinant enzyme-containing microsomal fractions	30
Quantification of P450 expression.....	31
Assays of herbicide conversion <i>in vitro</i>	31
Herbicide conversion in whole yeast	31
Leaf disc assay.....	34
Tests of herbicide tolerance	35
Thin-layer and silica column chromatography	35
LC-Q-TOF acquisition	37
Nuclear magnetic resonance (NMR)	37
Homology modeling of CYP706A3	37
Docking of herbicide	38
Chapter 3	39
Relaxed substrate specificity of the CYP706 family of P450 enzymes provides a suitable context for the evolution of dinitroaniline resistance.....	40
Summary	41
Introduction	42
Methods	46
Results	52
Discussion	72
References	Error! Bookmark not defined.
Supplemental material.....	78
Chapter 4	98
General Discussion and Conclusion.....	98
References	103
Appendix	109
Résumé en français.....	111
Introduction	112
Résultats et discussion.....	113
Conclusion générale.....	123

List of figures

Chapter 1

Figure 1. Evolution of herbicide-resistant weed biotypes by year from 1955 until 2019 (from http://weedsicence.org , February 2020).	4
Figure 2. Number of herbicide-resistant species for the top ten weed families (from http://weedsicence.org , February 2020).	5
Figure 3. Number of resistant weed species for several herbicide sites of action, from 1955 until 2019 (from http://weedsicence.org , February 2020).	6
Figure 4. Diagrammatic representation of one of the mechanisms of target site resistance (from Cobb and Reade, 2010).	7
Figure 5. Diagrammatic representation of enhanced metabolic resistance (from Cobb and Reade, 2010).	8
Figure 6. Typical structure of cytochrome P450 active site (from Groves, 2015).	10
Figure 7. Naming of P450 protein (from Bak et al., 2011).	11
Figure 8. Reaction mechanism of cytochrome P450 monooxygenases (from Werck-Reichhart et al., 2000).	13
Figure 9. Oxidation reactions catalyzed by P450s (from Mansuy, 1998).	14
Figure 10. Non-oxidation reactions catalyzed by P450s (from Mansuy, 1998).	14
Figure 11. Monooxygenation reactions catalyzed by P450 (from Mansuy, 1998).	15
Figure 12. Contribution of human P450s to drug metabolism (from Zanger and Schwab, 2013).	16

Chapter 2

Figure 1. Assay of herbicide conversion in whole yeast	33
Figure 2. Solid-phase extraction	33

Figure 3. Leaf disc assay.....	35
Figure 4. Characterization and purification of the products for NMR analysis	36

Chapter 3

Figure 1. Carbon monoxide-reduced versus reduced difference spectra of recombinant P450 investigated.	53
Figure 2. Conversion of pendimethalin by CYP706A3 in recombinant yeast microsomes.	55
Figure 3. Pendimethalin conversion by CYP706A3 in whole yeast and <i>N. benthamiana</i> leaf discs.....	57
Figure 4. LC-MC characterization of the pendimethalin oxidation products.....	59
Figure 5. NMR characterization of the pendimethalin oxidation products.....	61
Figure 6. Dinitroaniline herbicides tested as substrates of CYP706A3.....	62
Figure 7. CYP706A3-mediated dinitroaniline conversion in whole yeast assay.....	63
Figure 8. <i>A. thaliana</i> ectopically expressing CYP706A3 is tolerant to dinitroaniline herbicides.	65
Figure 9. Evaluation of the gain in herbicide resistance conferred by the ectopic overexpression of CYP706A3 in <i>A. thaliana</i>	66
Figure 10. Binding mode of dinitroanilines pendimethalin and oryzalin in CYP706A3 active site.....	69
Figure 11. Dinitroaniline conversion by other sesquiterpene-metabolizing enzymes.....	72
Supplemental Figure 1. <i>CYP706A3</i> -mediated pendimethalin conversion products detected in cell yeast extract.	82
Supplemental Figure 2. Optimization of the incubation time for the production of <i>CYP706A3</i> oxidation products in the whole yeast culture.....	83
Supplemental Figure 3. LC-MS profiling of the pendimethalin conversion products of <i>CYP706A3</i>	84

Supplemental Figure 4. The TLC-purified products correspond to the peak 1 and 2 detected by HPLC-DAD and LC-MS.....	85
Supplemental Figure 5. Binding mode of other dinitroanilines in CYP706A3 active site.	94
Supplemental Figure 6. View of the best affinity score pose of Oryzalin in model AtCYP706A3 active site showing the H-bonding interactions between sulfonamide group and Asn 122 and Glu 128 residues on the top of the active site	94
Supplemental Figure 7. Dinitroaniline conversion by other sesquiterpene-metabolizing enzymes.	95

List of tables

Chapter 1

Table 1. Investigated P450 enzymes.....	25
---	----

Chapter 2

Table 1. Herbicides tested as substrates of the plant P450 enzymes	27
--	----

Chapter 3

Table 1. Cytochrome P450 enzymes tested for herbicide conversion.	45
--	----

Table 2. Screening for CYP-dependent herbicide oxidation.	54
--	----

Table 3. Physical properties of dinitroaniline herbicides and natural substrates of CYP706A3 and CYP76 enzymes.....	70
---	----

Supplemental Table 1. Herbicides tested as substrates of the plant P450 enzyme	78
--	----

Supplemental Table 2. Quantification of P450 expression in yeast.	81
--	----

Supplemental Table 3. Estimated gain in herbicide tolerance of the CaMV 35S:CYP706A3 transformed Arabidopsis plant versus wild-type (WT).	81
--	----

Chapter 4

Appendix Table 1. Investigated P450 enzymes.....	116
--	-----

Appendix Table 2. Summary of docking poses found by Autodock 4.2.6 experiments performed on other dinitroanilines.	117
---	-----

Chapter 1

Introduction and Literature review

General Introduction

The human race farmed for over 10,000 years. Weeds would have been an unwelcome presence alongside crops ever since the first farmers saved and planted seeds. The most obvious problem caused by weeds is the reduction of yield through direct competition for light, space, nutrients and water. Weed control techniques are therefore aimed at the reduction in the competitive ability of weeds in a crop and the prevention of weed problems in a future crop. Weed control technologies have evolved from hand weeding to include primitive hoes (6000 B.C.), animal-powered implements (1000 B.C.), mechanically powered implements (1920 A.D.), biological control (1930 A.D.), and chemical (herbicide) control (1947 A.D.) (Powles and Shaner 2001). Some approaches have been retired after several years and others still, being adopted, such as biocontrol. Herbicide application is one of the approaches that still remains durable and efficient. Herbicides are often the most reliable and least expensive method of weed control available, especially on large fields, and the success of herbicides is largely responsible for the abundant and sustained food production necessary to support an increasing world population. The efficacy and cost-effectiveness of herbicides has led to heavy reliance on them in the developed world. Nevertheless, there are some real and perceived problems with herbicides. In recent years, there has been increased concern about residues and associated health and food safety issues, their adverse impact on the environment, and the widespread occurrence of herbicide-resistance. Herbicide resistance has evolved through persistent herbicide selection exerted on huge weed populations across vast areas (Powles and Shaner 2001; Alebrahim *et al.*, 2017).

The mechanisms of herbicide resistance are generally grouped into two categories: target-site and non-target-site herbicide tolerance. Target site herbicide resistance is caused by the mutation within in the target enzyme for herbicide binding, or by overproduction of the target enzyme. Non-target-site resistance involves mechanisms such as reduced herbicide uptake or translocation, increased herbicide sequestration, or enhanced herbicide metabolism, that minimizes the amount of active herbicide reaching the target site. Among these mechanisms, enhanced herbicide metabolism is certainly the most studied aspects of non-target-site resistance. Although several enzymatics are known to be involved in herbicide metabolism, endogenous cytochrome P450 monooxygenases, glucosyl transferases (GTs) and glutathione S-transferases (GSTs)

have the highest relevance. In particular, cytochrome P450 monooxygenases are an important driver of the increased metabolism of herbicides in weeds. From the point of view of weed control, non-target-site herbicide resistance is a greater threat to crop production, because it often results in resistance to multi herbicides of different chemical classes and different modes of action (Yuan *et al.*, 2007; Powles and Yu, 2010; Saika *et al.*, 2014; Iwakami *et al.*, 2014; Vrbničanin *et al.*, 2017; Alebrahim *et al.*, 2017).

Herbicide Resistance

Since the introduction of 2,4-dichlorophenoxyacetic acid (2,4-D) is a first selective herbicide in 1947, herbicides have had a major positive impact on weed management in all over the world. Unfortunately, herbicide resistance developed shortly after the introduction of the herbicides. The phenomenon of resistance can be defined as the decreased response of a species population to one or several herbicide(s). It is also defined as a 'survival of a segment of the population of a weed species following an herbicide dose lethal to the normal population'. In addition, resistance can be defined as 'the inherited ability to survive treatment by an herbicide', or also a 'phenomen which occurs as a result of heritable changes to biochemical processes that enable weed species survival when treated with an herbicide' (Vrbničanin *et al.*, 2017).

Weed resistance to herbicides is a normal and predictable outcome of natural selection. In that context, rare mutations that confer herbicide resistance exist in wild/weed populations before any herbicide introduction. These mutations increase over time after each herbicide application until they become predominant, at what time the weed population is called resistant (Heap, 2014). The first confirmed herbicide-resistant weed species was *Senecio vulgaris* that had developed resistance to PS II inhibitors (atrazine and simazine) after the herbicides had been applied once or twice annually for 10 years (Ryan, 1970). Some weed species, such as *Lolium rigidum*, *Echinochloa crus-galli* var. *crus-galli*, *Poa annua*, *Alopecurus myosuroides*, *Echinochloa colona*, *Eleusine indica*, or *Amaranthus* sp. have a high propensity to develop resistance especially due to their congenital genetic variability. Currently, herbicide resistance has been reported in 510 weed biotypes within 262 weed species (152 dicots and 110 monocots) in 70 countries (**Figure 1**). The highest number of confirmed resistant weed species belongs to the families: *Poaceae* (82 species), *Asteraceae* (42), *Brassicaceae* (22), *Cyperaceae* (12),

Amaranthaceae (11), *Scrophulariaceae* (9), *Chenopodiaceae* (7), *Alismataceae* (7), *Polygonaceae* (8) and *Caryophyllaceae* (6) (**Figure 2**). Many of those families are resistant to acetolactate synthase (ALS) inhibitors, photosystem II (PS II) inhibitors, acetyl CoA carboxylase (ACCase) inhibitors and 5-enolpyruvylshikimate-3-phosphate (EPSP) inhibitors (**Figure 3**) (<http://weedsicence.org/>).

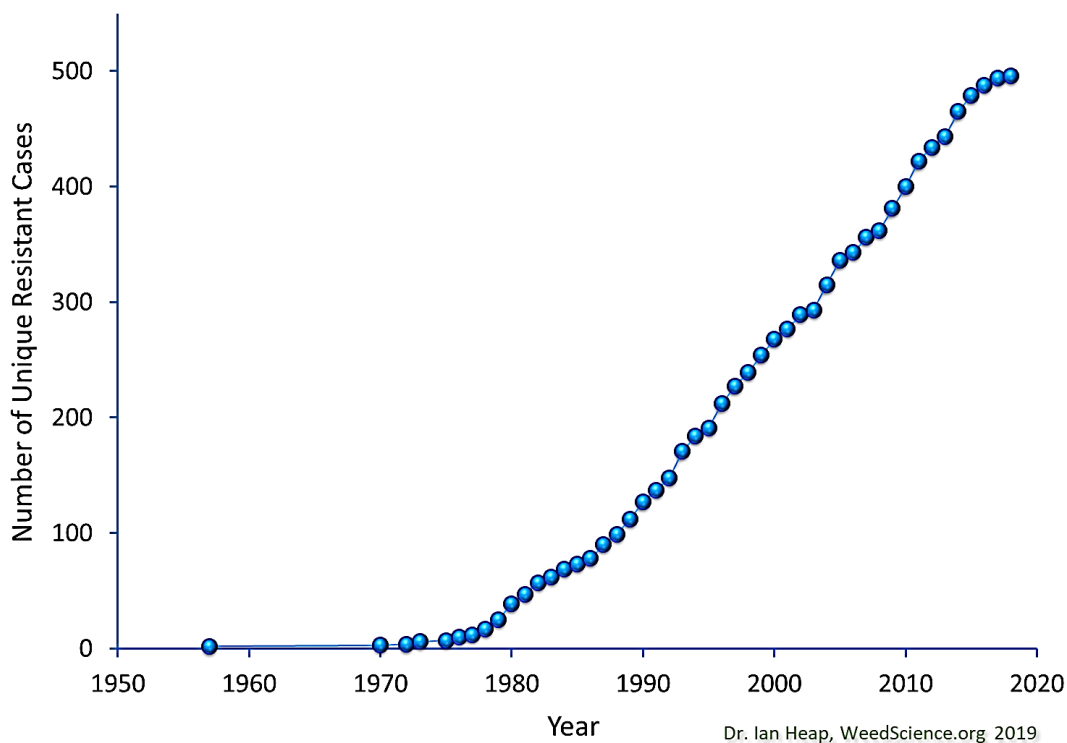
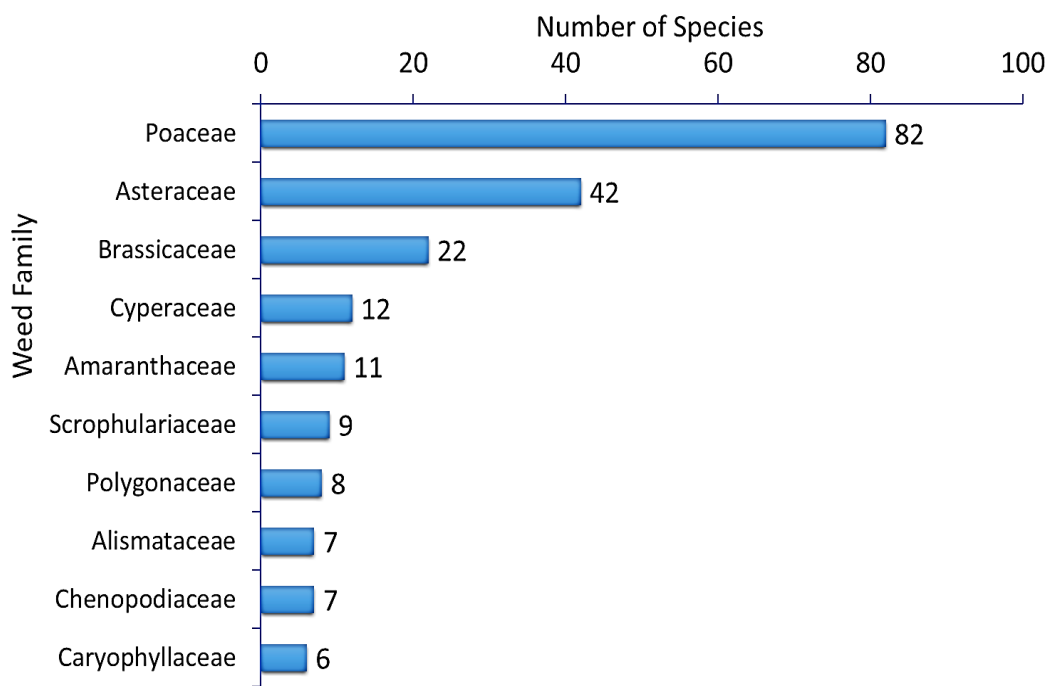


Figure 1. Evolution of herbicide-resistant weed biotypes by year from 1955 until 2019 (from <http://weedsicence.org>, February 2020).



Dr. Ian Heap, WeedScience.org 2019

Figure 2. Number of herbicide-resistant species for the top ten weed families (from <http://weedsicence.org>, February 2020).

Herbicides with different modes of action (e.g. sulfonylurea and synthetic auxins) can largely differ in their risk levels for resistance. However, different chemical groups with the same mode of action such as herbicide inhibitors of acetolactate/acetohydroxyacid synthase (ALS/AHAS) can also be distinguished in their risk level for resistance.

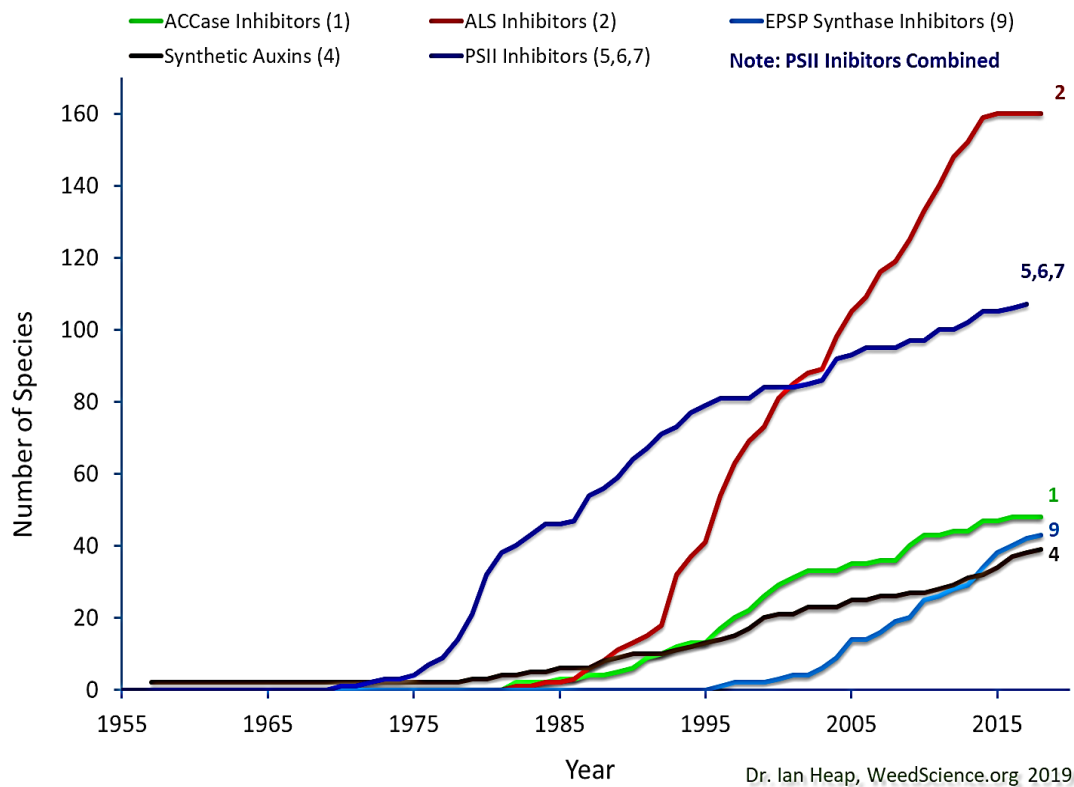


Figure 3. Number of resistant weed species for several herbicide sites of action, from 1955 until 2019 (from <http://weedsicence.org>, February 2020).

Mechanisms of herbicide resistance

Two types of mechanisms, target-site resistance and non-target-site resistance are involved in herbicide resistance.

Target-site herbicide resistance (TSR)

Target site resistance can be caused by changes in the tridimensional structure of the herbicide target protein that decrease herbicide binding, by increased activity of the target protein, or by increased expression of the gene encoding the target protein. Mutations endowing TRS can be classified in two types.

The first type is a change in the DNA sequence encoding the target protein. Such mutations are expected to cause a structural modification in the tridimensional structure of the target that will lead to a decrease in the efficacy of an herbicide or increased target activity.

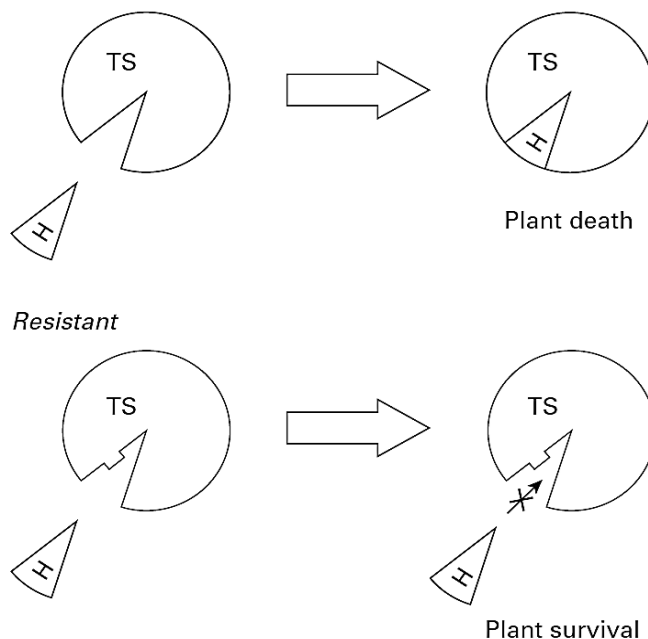


Figure 4. Diagrammatic representation of one of the mechanisms of target site resistance (from Cobb and Reade, 2010).

For example, mutations leading to an amino acid substitution at the herbicide-binding site of a target protein can decrease the affinity of the herbicide for the target protein (**Figure 4**). In the case of structural changes in the target, seeking the cause for resistance means being able to detect and identifying the relevant mutation in the target-encoding gene and associated structural changes in the protein of resistant plants.

The second type of mutations result in a difference in the expression of one or several genes in resistant plants compared to sensitive plants, either due to modification of the non-coding sequence of the target-encoding gene, or due to a regulatory gene mutation (Devine *et al.*, 1997; Yuan *et al.*, 2015). These mutations are changes in a DNA sequence that can cause an increase in the expression of the target protein that compensates for the herbicide inhibitory action.

Non-target-site herbicide resistance (NTSR)

Non-target-site resistance is generally due to reduced amount of active compound reaching the target protein caused by mechanisms such as reduced absorption (penetration), altered translocation, increased herbicide sequestration, or enhanced herbicide metabolism (detoxification), where the herbicide does not reach its site of action in sufficient concentration to cause plant mortality. Enhanced herbicide metabolism

(Figure 5) accounts for the majority of non-target-site resistance cases. Metabolism-based resistance thus most often relies on plant endogenous enzymes such as cytochrome P450 monooxygenases, glucosyl transferases (GTs) or glutathione S-transferases (GSTs). In particular, cytochrome P450 monooxygenases (P450s) are most frequently responsible for the increased metabolism of herbicides in plants.

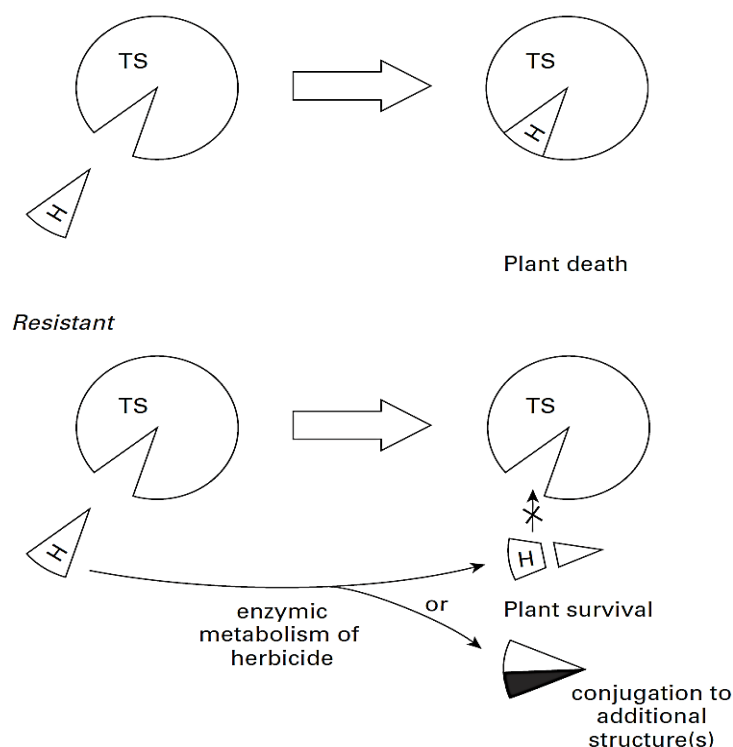


Figure 5. Diagrammatic representation of enhanced metabolic resistance (from Cobb and Reade, 2010).

Glutathione S-transferases (GSTs)

The glutathione S-transferases form a widespread superfamily of homo- or hetero-dimeric proteins that play an essential role in the detoxification, metabolism and transport of xenobiotic and endogenous compounds (Perperopoulou *et al.*, 2017). Glutathione transferases are involved in the phase II of herbicide detoxification in crops and weeds by conjugating electrophilic herbicides with the tripeptide glutathione (GSH) (Nianiou-Obeidat *et al.*, 2017; Perperopoulou *et al.*, 2017). It has been reported that GSTs mediate herbicide resistance to major herbicides such as imazamox, fluorodifen, atrazine, chlorimuronethyl, trisulfuron methyl, alachlor, S-ethyl dipropylthiocarbamate sulfoxide and metolachlor (Ma

et al., 2013; Nianiou-Obeidat *et al.*, 2017; Duhoux *et al.*, 2015, 2017; Li *et al.*, 2017). For example, Cummins *et al.* (2009) reported the role of GSTs in black-grass resistance to fenoxaprop-*p*-ethyl. It was also demonstrated that a GST-enzyme was directly responsible for the metabolism of mesotrione and atrazine in a resistant population of waterhemp (Ma *et al.*, 2013). Another study by Duhoux *et al.* (2015) identified a GST involved in ALS-inhibitor metabolism in resistant populations of *Lolium spp.* But the best illustration was provided by Cummins *et al.* (2013) who unraveled the direct and central role of *AmGSTF1* in the detoxification of several herbicides, including chlorotoluron, alachlor, and atrazine in black-grass. In this work, *AmGSTF1*-transformed *A. thaliana* was shown to acquire multi-herbicide tolerance.

Cytochrome P450 monooxygenases

Structure of the cytochrome P450 enzymes

Cytochromes P450 are hemoproteins formed out of 400-500 amino acid residues and an iron-protoporphyrin IX (heme) prosthetic group located in the core of the protein forming the active site (**Figure 6**). P450 proteins have molecular masses ranging from 45 to 62 kDa. However, their overall tridimensional structure is conserved, as are a few residues located on both sides of the heme. A Phe-x-x-Gly-x-Arg-x-Cys-x-Gly motif near the C-terminus is the most conserved sequence in P450 proteins. It includes the cysteine that serves as a fifth ligand to the heme iron. Another Ala/Gly-Gly-x-Asp-/Glu-Thr-Thr/Ser consensus, located ~150 residues upstream, corresponds to the oxygen binding and activation groove in the I helix on the distal side of the heme. A few other less conserved motifs, such as a Pro-Pro-x-Pro hinge near the N-terminus, or a Pro-Glu/Asp-Arg/His-Phe/Trp sequence between I helix and heme-binding cysteine are found in most P450 proteins. These conserved motives and their locations are considered as signatures for P450 proteins. Other characteristics of P450 enzymes include O₂- and NADPH-dependence, inhibition by carbon monoxide reversed by light, endoplasmic reticulum location (for most of them in Eukaryotes) and inhibition by antibodies directed against P450 reductase (Werck-Reichhart *et al.*, 2000; Schuler and Werck-Reichhart, 2003; Bak *et al.*, 2011).

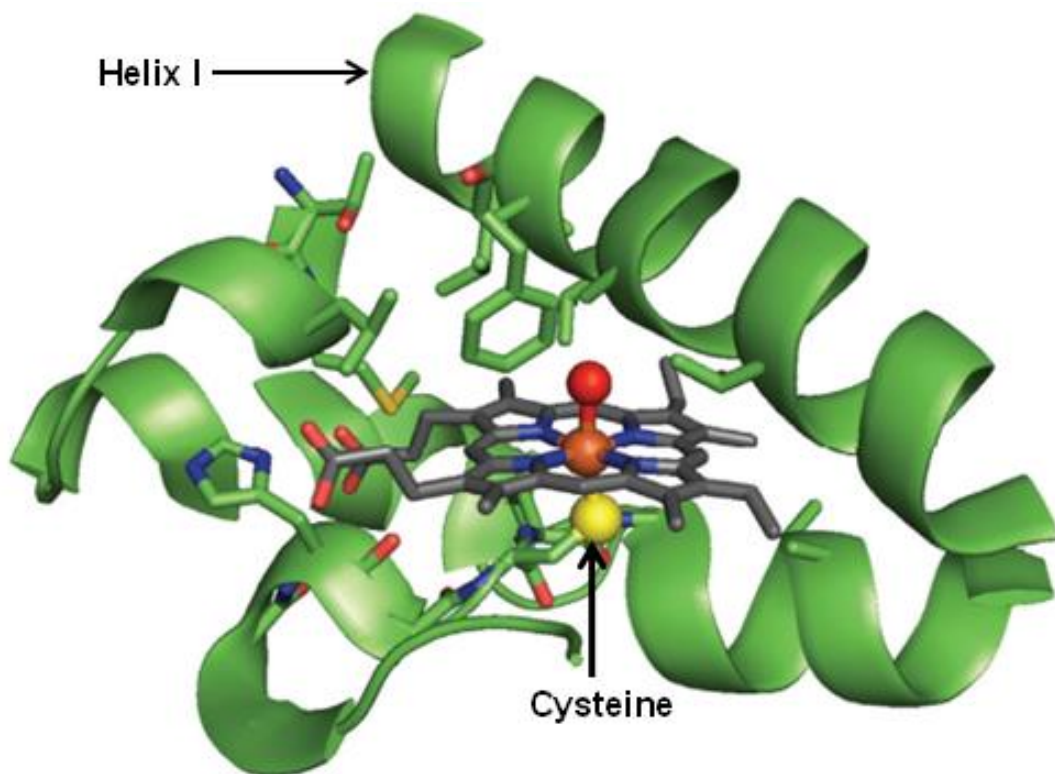


Figure 6. Typical structure of cytochrome P450 active site (from Groves, 2015).

The protein is represented as cartoon (green). Heme is represented in sticks. Oxygen atoms are shown in red, nitrogen in blue, and iron in orange.

Nomenclature of cytochromes P450

The nomenclature of the P450 genes of from all organisms is established on the basis of protein sequence identity and phylogeny. The term CYP refers to haem-containing proteins characterized by a maximum absorption wavelength of 450 nm in the reduced state in the presence of carbon monoxide. In the standardized P450 nomenclature, the CYP enzymes are designated by the letters "CYP" and an Arabic numeral denoting the CYP family (e.g. CYP1, CYP2, CYP3), followed by a capital letter representing the subfamily (e.g. CYP1A) and another number that indicates the individual gene/enzyme (e.g. CYP1A1). For example, CYP1A1 designates the CYP belonging to family 1, subfamily A and protein 1 in the subfamily (Bak *et al.*, 2011; Manikandan and Nagini, 2018) (**Figure7**).

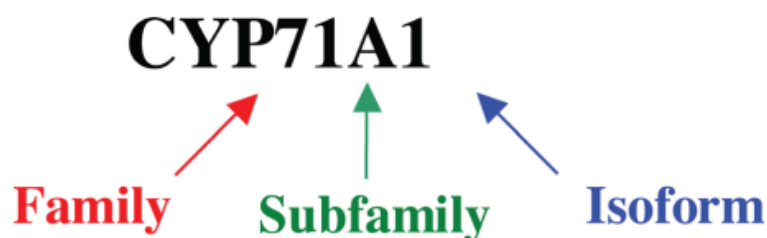


Figure 7. Naming of P450 protein (from Bak *et al.*, 2011).

Classification of cytochromes P450

Cytochromes P450 form one of the largest enzyme families, found in most organisms, such as viruses, bacteria, fungi, mammals, and plants. In 2017, Nelson reported that over 300,000 P450 sequences had been annotated and that this number kept increasing. From these sequences, animals (insects, non-insect invertebrates, mammals and other vertebrates) had over 13,000 and plants had more than 16,000 named P450s. Cytochromes P450, based on their electron transport chain, can be divided into three main classes. Class I type cytochromes P450 obtain electrons from NADP(H) via a Fe_2S_2 ferredoxin (Fdx) and a FAD-containing reductase (FdR). This type of cytochromes P450 is usually found in bacterial and some mitochondrial systems. For Class II, electrons are transported from NADPH to the heme of P450 by a NADPH cytochrome P450 reductase (CPR) which contains a flavin adenine dinucleotide (FAD) and flavin mononucleotide (FMN). Class II P450s are usually found anchored on the membranes of endoplasmic reticulum. The class III type do not need any additional source of electrons i.e. are self-reliant since the reductase fused to the P450 protein (e.g. the bacterial P450 BM3). For the class IV type, electrons are directly received from reduced pyridine nucleotides (Hannemann *et al.*, 2007; Gray and Winkler, 2010). Plant P450s involved in herbicide metabolism belong to the class II.

In plants, the cytochrome P450 superfamily is one of the largest families of enzymes. 246 P450 genes have been annotated in the Arabidopsis genome and 356 in rice. Plant P450s were initially grouped in two main types including, the A-type and non-A-type. They were re-classified into 11 clans based on the numerous available genome sequences. The A-types now corresponds to the CYP71 clan, whereas the non-A types according to

a common nomenclature standard were subdivided into 10 clans (CYP51, CYP72, CYP74, CYP85, CYP86, CYP97, CYP710, CYP711, CYP727, and CYP746) (Nelson and Werck-Reichhart, 2011; Du *et al.*, 2016).

Functions of cytochrome P450 enzymes

The catalytic reaction

A typical cytochrome P450 catalytic cycle occurs in several steps. In resting cytochromes P450, heme is in a ferric (Fe^{+3}), six-coordinated, low spin state, with its iron axially coordinated to a thiolate ($-\text{S}^-$) of a conserved cysteine of the protein and a molecule of water. Binding of a substrate (RH) induces a change in the conformation of the active site and displaces the water molecule with a change in the spin of Fe^{+3} from low spin to high spin. To be active, the ferric CYP-substrate complex needs to be coupled to an electron donor that transfers electrons from NADPH to the P450 protein: most often a cytochrome P450 reductase, or another associated reductase. Afterwards, the addition of an electron leads to the ferrous state (Fe^{2+}), and molecular oxygen binds to the reduced iron to form a ferrous superoxo-complex. A second reduction step leads to the formation of a peroxo form. One oxygen binds two protons and leaves as a molecule of water, which generates a ferryl-oxo-complex also called compound I. The compound I is highly reactive and unstable, attacks the substrate, yielding the hydroxylated product. Dissociation of the hydroxylated product restores the resting state of the P450 (**Figure 8**) (Werck-Reichhart and Feyereisen, 2000; Bak *et al.*, 2011; Manikandan and Nagini, 2018).

The resulting overall reaction is usually a hydroxylation:



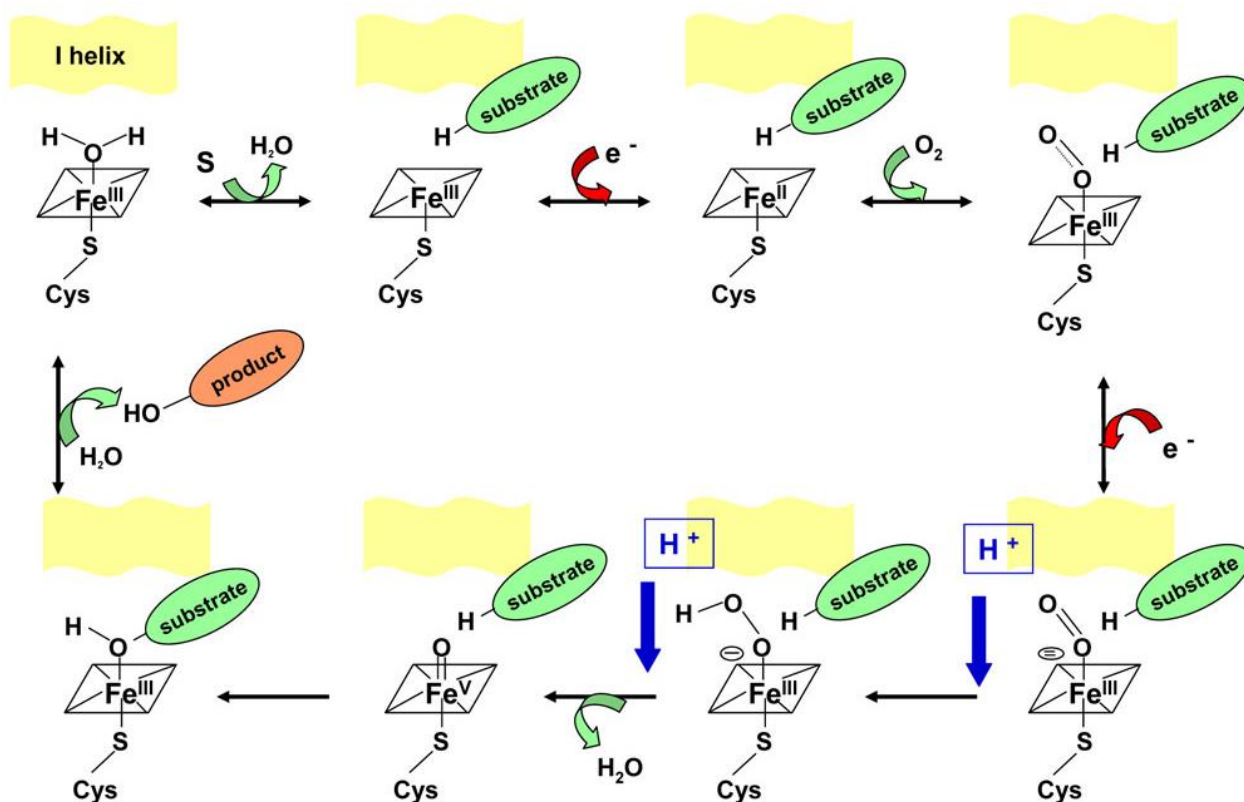


Figure 8. Reaction mechanism of cytochrome P450 monooxygenases (from Werck-Reichhart *et al.*, 2000).

Cytochrome P450 enzymes in fact catalyze a diversity of reactions, their function were classified by Mansuy (1998) into oxidation (**Figure 9**) and non-oxidation (**Figure 10**) reactions. Most of the P450 reactions are of the oxidation type. They lead to biodegradation or biosynthesis of endogenous compounds like steroids, fatty acids, most plant secondary metabolites, drug or pesticide metabolism. Most typically, the monooxygenation reactions involve the transfer of an oxygen atom to substrates as described above. The oxygen atom can be inserted into a C-H or C=C double bond leading to carbon hydroxylation or epoxidation of the product, or on a heteroatom like N in amides or amines, or S in thioethers. Rearrangement of the primary oxidation products can lead to *N*-, *O*- or *S*-dealkylation reactions (**Figure 11**) as frequently encountered in herbicide metabolism.

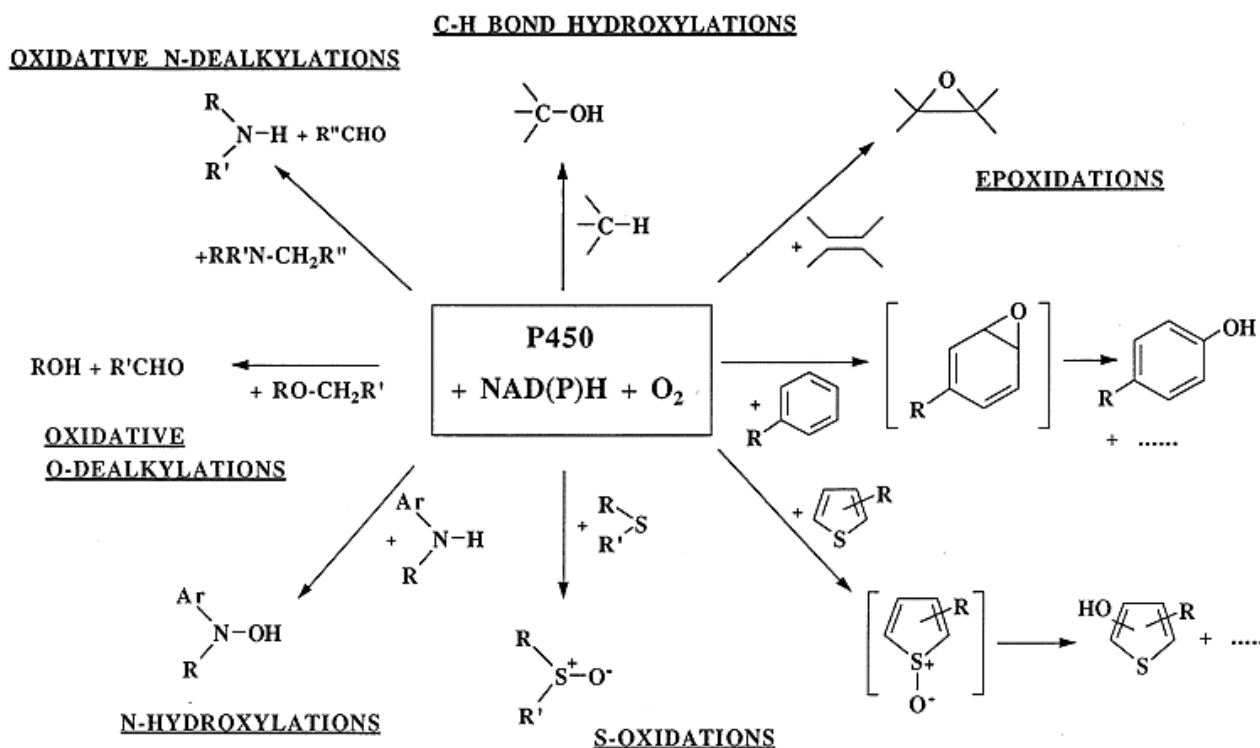


Figure 11. Monooxygenation reactions catalyzed by P450 (from Mansuy, 1998).

Role of P450 enzymes in drug metabolism

Drug metabolism is the mechanism of biotransformation and elimination of undesirable and foreign compounds in the body. It proceeds in two phases called I and II, mostly in the liver. In phase I, drugs are metabolized by different non-synthetic reactions including aromatic or aliphatic hydroxylations, oxidative *N*-dealkylation, *S*-oxidation, oxidative *O*-dealkylation, hydrolysis and reduction. Cytochromes P450 are the most common and important enzymes involved in phase I metabolism of drugs. Approximately 30 P450 enzymes are responsible for drug metabolism in humans, however, six main enzymes such as CYP1A2, 2C9, 2C19, 2D6, 2E1 and 3A4/5 are able to metabolize the majority (90 %) of them. Among those, CYP2D6 and CYP3A4 metabolize the largest number of drugs (**Figure 12**).

CYP2D6 is responsible for the metabolism of wide range of drugs. It metabolizes ~ 25% of the drugs, such as flecainide, propafenone, mexiletine, venlafaxine, paroxetine, amitriptyline, risperidone, aripiprazole, metoprolol, bufuralol, as well as anti-cancer drugs

and tramadol, and many others, in spite of a low expression level in the liver. In addition, some substances called pro-drugs, such as codeine, are activated by CYP2D6. The CYP3A enzymes have the main role in drug metabolism in man. They are responsible for metabolization of ~50% of the drugs and of more than 120 different medications. The large and flexible active site of the CYP3A4 enzyme allows the processing of a wide range of lipophilic compounds with large structures such as cyclosporin A, antibiotics, and anticancer drugs (taxol) (Bibi, 2008; Zanger and Schwab, 2013).

In phase II, synthetic reactions such as sulfation, glucuronidation, amino acid conjugation, methylation, acetylation or glutathione conjugation, form more polar compounds that can be excreted easily by the kidneys (in urine) and the liver (in bile). Similar processes are encountered in pollutant and pesticide (insecticide, fungicide and herbicide) metabolism.

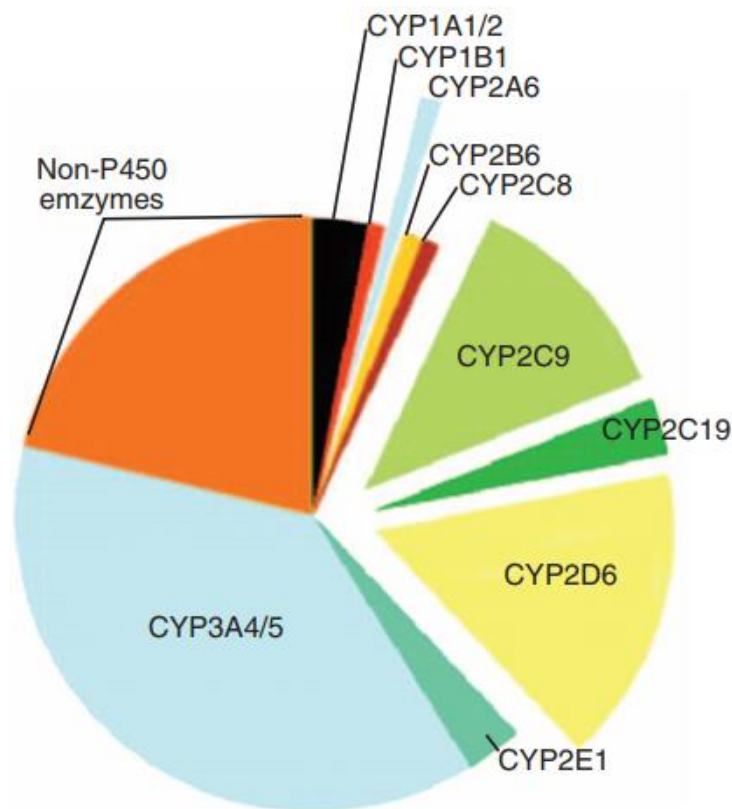


Figure 12. Contribution of human P450s to drug metabolism (from Zanger and Schwab, 2013).

Role of P450 enzymes in plants

Plant cytochrome P450 enzymes are involved in the metabolism of several hundreds of different substrates. Their primary role is the biosynthesis and catabolism of endogenous compounds, but incidentally, they can also metabolise exogenous molecules, which has a significant impact on herbicide activity and tolerance.

Role of plant P450s in the metabolism of endogenous compounds

Plants are able to produce and synthesize a variety of organic compounds. Those have been initially grouped into two major classes: 1) primary metabolites, such as, sugars, fatty acids, sterols, amino acids, vitamins, hormones, which are directly involved in plant growth and development, and, 2) secondary metabolites, long considered not essential to growth and life, but playing an important role in the interaction of the plant with their environment, and often generated in response to stress. This view is now largely reconsidered since many of the so-called “secondary metabolites” have been recently shown to be essential for normal plant development. Accordingly, there now coined “specialized metabolites”. Plant specialized metabolites are usually classified into three major classes: terpenoids, phenylpropanoids and nitrogen-containing compounds, of which the nitrogen-containing group can be subdivided into cyanogenic glucosides, alkaloids and glucosinolates. Plant P450s play paramount roles in the synthesis or catabolism of primary and specialized metabolites: structural precursors of membranes, cutin and suberin like oxygenated fatty acids and sterols, hormones such as gibberellins, brassinosteroids, cytokinins, strigolactones, jasmonates, and more specialized compounds like lignin building blocks, pigments, volatiles, antioxidants, allelochemicals and defense compounds (Mizutani and Ohta, 2010; Bak *et al.*, 2011).

Role of plant P450s in the metabolism of exogenous compounds

Metabolism of herbicides

In addition to biosynthetic activities, plant P450s metabolize a range of toxic exogenous compounds encountered in the environment such as herbicides, insecticides, and some pollutants. Herbicide metabolism most often leads to the production of less phytotoxic compounds that can be either further metabolized and fully degraded or conjugated and stored in the vacuole. Metabolism can also lead to more phytotoxic

compounds, but examples of herbicide activation are not available yet for plant P450 enzymes. So far O'Keefe *et al.*, (1994) reported that, the transgenic tobacco (*Nicotiana tabacum*) overexpressing cytochrome P450 CYP105A1 from *Streptomyces griseolus* was killed by a sulfonylurea pro-herbicide 2-methylethyl-2,3-dihydro-N-[(4,6-dimethoxypyrimidin-2-yl) aminocarbonyl]-1,2-benzothiazole-7-sulfonamide-1,1-dioxide (R7402) treatment, demonstrating that the R7402 pro-herbicide was metabolized to highly phytotoxic compound by CYP105A1. In the same way, Xie *et al.* (2010) demonstrated the capacity of human CYP2A5 to activate the herbicide 2,6-dichlorobenzonitrile.

Numerous studies have demonstrated plant P450 involvement in herbicide detoxification and increased herbicide tolerance in weeds. The first reports involving plant P450 enzymes in herbicide metabolism were published in 1985 and 1986, suggesting contribution to resistance to acetyl CoA carboxylase (diclofop-methyl) and photosystem II (chlortoluron and isoproturon) inhibitors in annual ryegrass (*Lolium rigidum*) and black-grass (*Alopecurus myosuroides*), respectively (Moss and Cussans, 1985; Heap and Knight, 1986). Since then, many studies have reported P450-mediated herbicide resistance in several weeds, such as *Descurainia sophia* (flixweed), *Amaranthus hybridus*, *Bromus tectorum*, *Avena sterilis*, *Phalaris minor*, *Echinochloa phyllopogon*, *Stellaria media*, *Digitaria sanguinalis*, or *Sinapis arvensis*. *Descurainia sophia* is one of the most challenging broadleaf weeds in winter fields, and has evolved remarkably resistant to ALS-inhibiting sulfonylurea herbicide tribenuron-methyl due to both target-site (ALS gene mutations) and non-target-site (enhanced metabolism) mechanisms. Yang *et al.* (2016, 2018) obtained evidence of the involvement the two cytochromes P450 in metabolic tribenuron-methyl resistance by showing correlation between CYP96A146 and CYP96A13 expression and herbicide metabolism. In *Lolium rigidum*, enhanced P450-dependent metabolism was suggested to be responsible herbicide resistance to herbicides with different modes of action such as diclofop-methyl (acetyl CoA carboxylase inhibitor), prosulfocarb and triallate (lipid synthesis inhibitor), pyroxsulam (acetolactate synthase inhibitor), trifluralin (tubulin assembly inhibitor) and pyroxasulfone (long chain fatty acid inhibitor) (Moss and Cussans, 1985; Busi and Powles, 2013; Duhoux *et al.*, 2015; Chen *et al.*, 2018; Busi *et al.*, 2017). In addition, plant treatment with one class of herbicides can result in resistance to another class of active compounds. For example, Han *et al.* (2013) have demonstrated that pre-treatment of a susceptible biotype of *L.*

rigidum with 2,4-D, an auxinic herbicide, enabled plant survival to application of the P450-metabolized diclofop-methyl (ACCase inhibitor). P450-dependent aryl-hydroxylation had been previously shown to be responsible for 2,4-D tolerance in grasses, including *L. rigidum* (Coupland, 1994). Gaines *et al.*, (2014) therefore set up to identify the metabolic gene(s) responsible for herbicide tolerance in an Australian diclofop-resistant *L. rigidum* population. RNAseq (RNA sequencing, i.e. particular technology which uses next-generation sequencing (NGS) to examine the quantity and sequences of RNA in a sample), genetic and physiological approaches converged for pointing to four contigs including two CYP72 P450s, one GT and one nitronate monooxygenase as the best candidates potentially responsible for the herbicide resistance. While the direct involvement of these candidates is still not confirmed, direct evidence for a single P450 conferring herbicide cross-resistance has been recently obtained for another weed *Echinochloa hylopopogon* prominent in rice cultures (Iwakami *et al.*, 2019; Dimaano *et al.*, 2020). In the latter case, several P450 enzymes belonging to the grass-specific CYP81A subfamily were shown able to confer multiple resistance to herbicides classes as diverse as ALS inhibitors (most pronounced), photosystem II, phytoene desaturase, protoporphyrinogen desaturase, 4-hydroxyphenylpyruvate dioxygenase and 1-deoxy-D-xylulose 5-phosphate synthase inhibitors (Dimaano *et al.*, 2020). The physiological function(s) and enzyme activity(ies) of the grass CYP81A enzymes and reason for their unusual promiscuity are however still to be uncovered.

Many studies also demonstrated that P450s are responsible for metabolism of herbicides in crops. For example, it was shown that CYP81A6, CYP72A18 and CYP72A31 from rice (*Oryza sativa*) could metabolize several herbicides including PSII and ALS-inhibitors. Thanks to the characterization of a rice population susceptible to bentazon and sulfonylurea (Zhang *et al.*, 2002), it could be demonstrated that CYP81A6 was responsible for rice bentazon and sulfonylurea tolerance (Zhang *et al.*, 2006). Accordingly, expression of CYP81A6 conferred a significant increase in tolerance to bentazon and bensulfuron-methyl in mutant rice and its suppression in wild-type resulted in a loss of tolerance (Pan *et al.*, 2006). Expression of CYP81A6 also conferred an increase in herbicide tolerance to Arabidopsis, and tobacco (Liu *et al.*, 2012). Similarly, the differential sensitivities of indica and japonica rice varieties to bipyridac sodium (acetolactate synthase inhibitor) allowed the map-based identification of CYP72A31 as the gene responsible for the indica variety

resistance to this herbicide (Saika *et al.*, 2014). *CYP72A31* expression in *Arabidopsis* confirmed the capacity of *CYP72A31* to confer bispyribac sodium tolerance and in addition demonstrated its potential to confer bensulfuron-methyl cross-tolerance (different class of acetolactate synthase inhibitors).

A role of cytochrome P450s in herbicide metabolism has also been demonstrated for enzymes isolated from model plants using more direct biochemical approaches. It was for example shown that *CYP76B1* from Jerusalem artichoke (*Helianthus tuberosus*), catalyzed oxidative dealkylation of the PSII inhibitors phenylurea (isoproturon, diuron, linuron and chlortoluron) to yield nonphytotoxic products (Robineau *et al.*, 1998). Overexpression of *CYP76B1* in tobacco and *Arabidopsis* conferred a 20-fold increase in tolerance to linuron, and a 10-fold increase in tolerance to isoproturon or chlortoluron (Didierjean *et al.*, 2002). In the same way, the yeast-expressed *CYP76C1*, *CYP76C2*, and *CYP74C4* isolated from *A. thaliana* were shown to metabolize a subset of phenylurea forming both ring-methyl hydroxylated and *N*-demethylated metabolites. Accordingly, ectopic expression of *CYP76C1*, *CYP76C2*, and *CYP76C4* conferred phenylurea tolerance to *A. thaliana* (Höfer *et al.*, 2014). Screening recombinant enzyme activity has also been used to demonstrate that soybean *CYP71A10* was able to convert phenylurea: fluometuron, diuron and chlorotoluron into *N*-demethylated and the ring-methyl hydroxylated products (Siminszky *et al.*, 1999). Overexpression of *CYP71A10* in tobacco resulted in a significant tolerance to chlortoluron and linuron (Siminszky *et al.*, 1999).

Synergists and P450 inhibitors

P450 inhibitors can be used as herbicide synergists and have been extensively used to demonstrate cytochrome P450 dependence of metabolism-based resistance. In particular, piperonyl butoxide (PBO), 1-aminobenzotriazole (ABT), phorate, and malathion have been used to indicate P450-mediated metabolic resistance to herbicides. For example, pre-treatment with PBO or malathion dramatically decreased the Asia minor bluegrass (*Polypogon fugax*) and Japanese foxtail (*Alopecurus japonicus*) resistance to fenoxaprop and pyroxsulam (Feng *et al.*, 2016; Zhao *et al.*, 2019). In the same way, Zhao *et al.* (2018) reported a decrease in resistance to fenoxaprop-*P*-ethyl and mesosulfuron-methyl in shortawn foxtail (*Alopecurus aequalis* Sobol.) when pre-treated with PBO and malathion. Many other studies using enzyme inhibitors demonstrated the involvement of P450 in herbicide resistance of other weed populations, in rigid ryegrass, barnyardgrass,

rigid brome, palmer amaranth, or common waterhemp (Burnet, *et al.*, 1993; Riar, *et al.*, 2012; Oliveira *et al.*, 2017; Kleinman *et al.*, 2017; Busi *et al.*, 2017; Nakka *et al.*, 2017; Shergill *et al.*, 2018).

Safener and P450 inducers

Cytochromes P450 and other detoxifying enzymes have been repeatedly described to be induced by exogenous compounds. This also true for plant P450 enzymes involved in herbicide metabolism. P450 inducers, can be exploited as herbicide safeners to enhance herbicide metabolism in crop plants via selective treatment like seed coating. Safeners are an important chemically group of agrochemicals used to reduce the phytotoxicity of herbicides in crops by accelerating the metabolism of herbicides into less active or inactive compounds, without compromising weed control efficacy (Hatzios and Burgos, 2004; Riechers *et al.*, 2010; Brazier-Hicks *et al.*, 2020) Thereby, they also permit to increase the selectivity of weed control. For example, Scalla and Roulet, (2002) observed an increase of fenoxaprop metabolism in barley when treated with the safener mefenpyr-diethyl. Several other studies confirmed that safeners were responsible for herbicides enhanced detoxification in wheat, maize, rice and sorghum. Zhang *et al.* (2007) showed that the safener cloquintocet-mexyl protected seedlings of wheat from injury by the herbicide dimethenamid. Treatment with the herbicide safener fenclorim induced the expression of genes encoding P450s and glutathione transferases in rice (Brazier-Hicks *et al.*, 2018), Goodrich *et al.* (2018) observed that the application of the saferener fluxofenim in combination with the herbicide pyroxasulfone provided effective weed control and reduced sorghum injury by herbicide. Conversely, a few studies revealed negative effects of safeners on weed species, accelerating herbicide metabolism and non-target-site-based resistance. DeBoer *et al.* (2011) and Rosenhauer *et al.* (2016) reported a decrease in sensitivity to pyroxsulam, iodosulfuron and mesosulfuron when combined to the safeners cloquintocet-mexyl and mefenpyr-diethyl in *Alopecurus myosuroides* (black-grass). Another study reported that both safeners mefenpyr-diethyl and cloquintocet-mexyl reduced the sensitivity of *Lolium* sp. to ALS-inhibitor herbicides and significantly increases herbicide degradation (Duhoux *et al.*, 2017).

Dinitroaniline herbicides

Dinitroanilines are pre-emergence, soil-incorporated microtubule assembly inhibitors with a structure containing an aniline ring attached to two nitro groups, used to control annual grass and certain dicot weeds in several major crops, especially wheat, soybean and cotton. They were first reported as herbicides in 1960. This herbicide group includes trifluralin, pendimethalin, ethalfluralin, benefin, fluchloralin, oryzalin, dinitramine, methal propaline, prodiamine, profluraline, nitratine, benfluraline, butraline, clonidine, dinitramine, dipropylène and isopropylène. Trifluralin is the most commonly used dinitroaniline herbicide. It was commercialized in the 1960s and is largely used as a pre-emergence herbicide in soybean cultures to control grass weeds. Dinitroaniline herbicides are highly volatile and easily subject to photodegradation. Consequently, these herbicides need to be incorporated into the soil to prevent loss via photodegradation and volatilization (Alder *et al.*, 1960; Grover *et al.*, 1997; Epp *et al.*, 2017). Dinitroanilines have negative effects on plant growth by inhibiting cell division, specifically, they inhibit microtubulin polymerization. Dinitroanilines specifically bind tubulin and inhibit cell division in plants and protozoans, but not in animal cells. They are also used to control protozoal parasite-mediated diseases, for example for malaria treatment (Dempsey *et al.*, 2013).

Dinitroaniline-resistant populations have been reported in weeds as diverse as *Alopecurus myosuroides* (James *et al.*, 1995), *Lolium rigidum* Eleusine indica (Mudge *et al.*, 1984), *Setaria viridis* (Morrison *et al.*, 1989), *Amaranthus palmeri* (Gossett *et al.*, 1992), *Poa annua* (Lowe *et al.*, 2001) and *Alopecurus aequalis* (Hashim *et al.*, 2012). In many cases, this resistance was shown to result from mutations in the gene encoding the target-site, α/β -tubulin (Hashim *et al.*, 2012; Anthony *et al.*, 1998; Yamamoto *et al.*, 1998; Délye *et al.*, 2004; Chen *et al.*, 2018, 2020; Chu *et al.*, 2018; Chen *et al.*, 2020). Still, NTSR and enhanced metabolism was also reported. James *et al.* (1995) revealed a metabolic resistance to pendimethalin in the black grass population, leading to hydroxylation of the 4-methyl group of pendimethalin. Tardif and Powles then found that pendimethalin resistance in annual ryegrass was partly reversed by a P450 inhibitor, malathion (Tardif and Powles, 1999). A more recent investigation on Australian trifluralin resistant populations of *L. rigidum* pointed to metabolism as the most frequent cause of the resistance in this weed (Chen *et al.*, 2018b). A synergy between trifluralin and the insecticide phorate in addition supported P450-mediated metabolism in several

multi-resistant populations (Busi *et al.*, 2017). But no P450 enzyme was so far associated with dinitroaniline metabolism.

Research objective

The problem of herbicide resistance is a major challenge for agriculture. Several resistance mechanisms exist in plants, but NTRs and more specifically herbicide metabolism is the most challenging of them (Powles & Yu 2010). Therefore, the present study was focused on the molecular mechanism and evolution of P450-mediated herbicide resistance. In particular, my objective was to determine if P450-mediated herbicide metabolism could be related to innate plant P450 catalytic promiscuity.

Drug metabolism in mammals largely relies on a small number of P450 enzymes showing a very relaxed substrate specificity. Plants encode a much larger number of P450 genes than animals (200 to 500 in vascular plants versus 57 in human genome), required to orchestrate a very complex metabolism. The first plant P450 enzymes functionally investigated showed narrow substrate specificity, more reminiscent of animal P450 enzymes involved in essential functions like hormonal metabolism, which seemed to indicate high specialization. More recent work, however, starts to reveal more promiscuous plant P450 enzymes, usually contributing to defense and adaptive pathways.

Therefore, my task was here to start investigating if such promiscuous plant P450 enzymes might be more prone to support herbicide metabolism. To this end, I compared the metabolism of a set of active compounds representative of the most commonly used classes of herbicide (dinitroanilines, triazines, imidazolinones, sulfonylureas, phenylureas, benzoic acids, nitriles, aryloxyphenoxy, propionates, piridazinone, benzothiadiazinone, chlorinated anilide, diphenyl ethers and phenoxy-carboxylic-acids) by six plant cytochromes P450 enzymes with documented biochemical activities and known biological functions in plant (**Table 1**). These candidates were selected to be representative of P450s with very low to high promiscuity with regard to natural substrates. The yeast-expressed enzymes were first screened for their capacity to metabolize herbicides. A novel herbicide-metabolizing CYP706A3 enzyme was identified. The functional and structural properties of the positive candidate were then extensively investigated to test the relevance of my starting hypothesis and to determine the molecular bases of CYP706A3 and related P450 herbicide metabolism.

Table 1. Investigated P450 enzymes.

CYP	Plant	In plant	Promiscuity	Reference
CYP73A92	<i>Brachypodium distachyon</i>	<i>Phenolics</i>	-	(Renault <i>et al.</i> , 2017)
CYP98A23	<i>Populus trichocarpa</i>	<i>Phenolics</i>	-	(Alber <i>et al.</i> , 2019)
CYP72A224	<i>Catharanthus roseus</i>	<i>Iridoids</i>	-	(Miettinen <i>et al.</i> , 2014)
CYP98A27	<i>Populus trichocarpa</i>	<i>Phenolics</i>	+/-	(Alber <i>et al.</i> , 2019)
CYP76B1	<i>Helianthus tuberosus</i>	<i>Alkoxycoumarins,</i> <i>Alkoxyresorufins,</i> <i>Phenylurea</i>	++	(Batard <i>et al.</i> , 1998; Robineau <i>et al.</i> , 1998)
CYP706A3	<i>Arabidopsis thaliana</i>	<i>Terpenoids</i>	+++	(Boachon <i>et al.</i> , 2019)

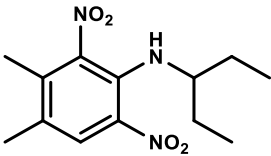
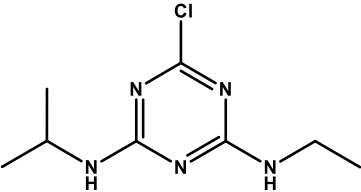
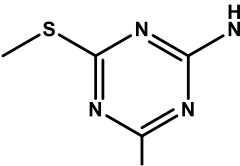
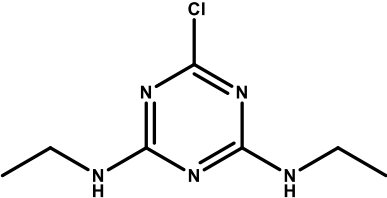
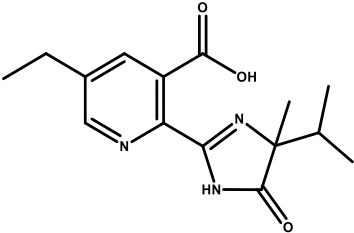
Chapter 2

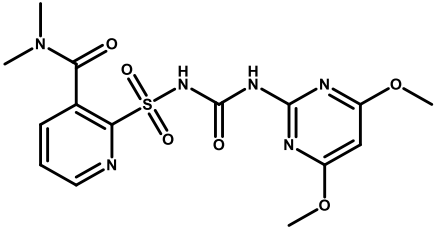
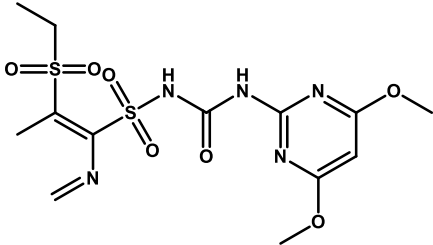
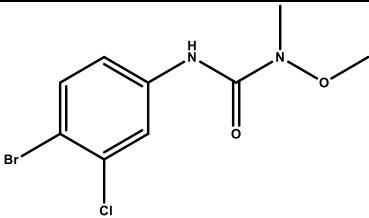
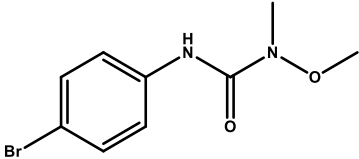
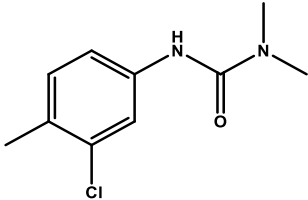
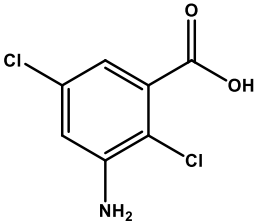
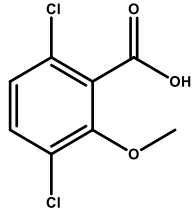
Material and Method

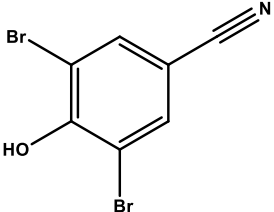
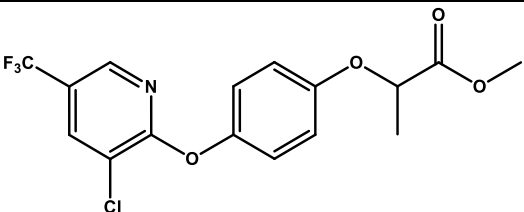
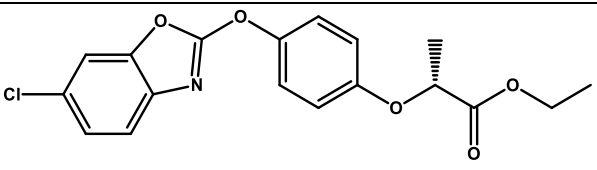
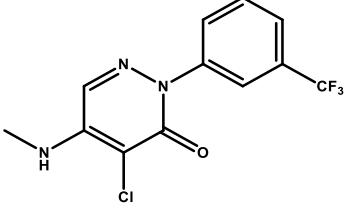
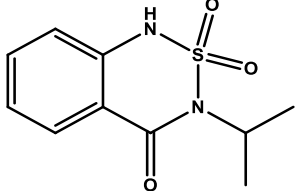
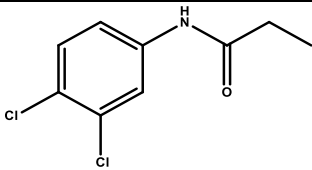
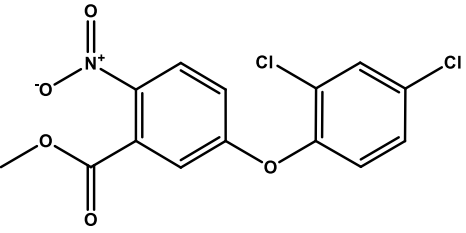
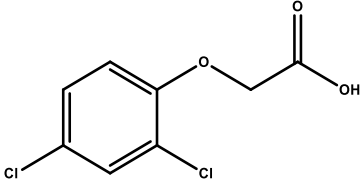
Herbicides assayed for plant P450 metabolism

All of herbicides were purchased from Sigma-Aldrich (Saint Louis, USA). The full lists of herbicides used in this experiment are listed in **Table 1**, Stock solutions at 2 mM were prepared in methanol 96 % (v/v) and stored in the dark at 5 °C.

Table 1. Herbicides tested as substrates of the plant P450 enzymes

Chemical Family	Active Ingredients	MW (g/mol)	Structure
Dinitroanilines	Pendimethalin	281.3	
	Atrazine	215.6	
Triazines	Terbutryn	241.3	
	Simazine	201.6	
Imidazolinones	Imazethapyr	289.3	

	Nicosulfuron	410.4	
Sulfonylureas	Rimsulfuron	431.4	
	Chlorbromuron	293.5	
Phenylureas	Metobromuron	259.1	
	Chlortoluron	212.7	
Benzoic acids	Chloramben	206.1	
	Dicamba	221.1	

Nitriles	Bromoxynil	276.9	
Aryloxyphenoxy propionates	Haloxypop-methyl	375.7	
	Fenoxaprop- <i>p</i> -ethyl	361.8	
Pridazinone	Norflurazon	303.6	
Benzothia diazinone	Bentazon	240.3	
Chlorinated anilide	Propanil	218.1	
Diphenyl ethers	Bifenox	342.2	
Phenoxy-carboxylic-acids	2,4-D	221.1	

Transgenic plant lines

The source and validation of *Arabidopsis thaliana* CYP706A3 T-DNA insertion and 35S:CYP706A3 overexpressing lines are described in Boachon *et al.* (2019).

Enzyme expression in yeast and isolation of recombinant enzyme-containing microsomal fractions

For the production of recombinant enzymes, the WAT11 yeast strain and pYeDP60 vector were used. In the WAT11 strain, the ATR1 *A. thaliana* NADPH-P450 reductase gene was inserted in the chromosome under the control of the *GAL10-CYC1* promoter (Pompon *et al.*, 1996). pYeDP60 is a multicopy expression vector with an expression cassette under control of the galactose-inducible and glucose-repressed yeast hybrid promoter *GAL10-CYC1*. Construction of the expression vector of CYP76B1, CYP72A224, CYP73A92, CYP98A23/A27, CYP706M1, CYP71D51, CYP81D11, CYP81F1, CYP81F2, CYP81F4, CYP81H1 and CYP706A1/A2/A3/A7 were previously described in Robineau *et al.*, 1998, Gavira *et al.*, 2013, Cankar *et al.*, 2014, Miettinen *et al.*, 2014, Renault *et al.*, 2017, Hansen *et al.*, 2018, Alber *et al.*, 2019, and Boachon *et al.*, 2019. Yeast transformation with the expression vectors was previously described (Ginglinger *et al.*, 2013).

Transformed yeast colonies were inoculated into 30 mL SGI medium (0.7% (w/v) yeast extract, 0.1% (w/v) Bacto Casamino Acids, 0.002% (v/v) tryptophan, 2% (w/v) glucose) and grown at 28°C for 24 h with shaking (180 rpm) to reach an optical density of 1 at 600 nm. The overnight culture was diluted into 200 mL of YPGE medium (1% (w/v) yeast extract, 1% (w/v) peptone, 3% (v/v) ethanol, 0.5% (w/v) glucose), and cells were grown at 28°C with shaking (180 rpm) until cell density reached OD₆₀₀ of 0.7 to 0.9. Ten mL of 200 g.L⁻¹ galactose were then added for induction of P450 expression and cells were then further grown at 20°C with shaking (180 rpm) overnight. The yeast cells were harvested by centrifugation (15 min, 4,500 rpm, 4°C), washed in 30 mL of TEK buffer (50 mM Tris HCl pH7.5, 1 mM EDTA, 100 mM KCl), centrifuged at 7,000 rpm for 10 min at 4°C, and resuspended in 1 mL of cold TES buffer (50 mM Tris HCl pH7.5, 1 mM EDTA, 600 mM sorbitol). Cells were broken by vigorous shaking with glass beads (250 to 500 µm diameter) five times for a total of 5 min. The crude extract was recovered, and the beads were washed twice with 20 mL of cold TES. The homogenate was centrifuged for

20 min at 7,000 rpm and 4°C and the resulting supernatant was centrifuged for 1h at 30,000 rpm and 4°C. The resulting pellets were then resuspended in 2 mL of TEG (50 mM Tris HCl pH 7.5, 0.5 mM EDTA, and 30% (v/v) glycerol) and stored at -20°C (Liu *et al.*, 2016).

Quantification of P450 expression

Microsomal suspensions were diluted in TEG buffer to record CO-bound reduced versus reduced differential absorption spectra using a Cary 300 UV-Visible spectrophotometer. To this end, each sample was reduced with Na₂SO₄ and dispatched between the two cuvettes for setting a baseline between 380 and 500 nm, before bubbling carbon monoxide in the assay cuvette for about 30 seconds. The absorbance spectrum of the CO-bound ferrous P450 was then recorded and used for the calculation of the P450 concentration according to Omura and Sato (1964).

Assays of herbicide conversion *in vitro*

The screening for herbicide conversion was carried out in a final volume of 100 μ L containing 80 μ L Na phosphate buffer 20 mM pH 7.4, containing 100 μ M of herbicide in the presence of 300 μ M NADPH and 10 μ L yeast microsomal membranes. The incubation was carried out at 25°C for 20 min and stopped by adding 200 μ L of acetonitrile: HCl (99:1, v/v). The mixture was then centrifuged at 13,000 rpm for 5 min to remove precipitated proteins. The supernatant was transferred to 250 μ L HPLC vials and analyzed on an Alliance 2695 Waters HPLC apparatus set with a C18 column (5 μ m, 100 Å, 150 mm, 4.6 mm, Kinetex) using a binary gradient system of solvents A (water containing 0.1% (v/v) formic acid) and B (100% HPLC-grade acetonitrile containing 0.1% (v/v) formic acid) as follows: 0 to 5 min 10% to 50% B, then, 5 to 15 min 50% to 95% B, hold for 2 min, followed by 95% to 10% for 1min, hold for 1 min. Flow rate was 1 mL.min⁻¹ and column temperature 35°C. The formation of products was monitored with a diode array absorbance detector from 220 to 400 nm. All solvents were HPLC grade and filtered and degassed before use. All assays were conducted in triplicates.

Herbicide conversion in whole yeast

Yeast colonies were inoculated into 30 mL SGI medium and grown at 28°C for 24 h with shaking (180 rpm). The overnight culture was diluted into 200 mL of YPGE, and cells

were grown at 28°C with shaking at 180 rpm until the cell density reached an OD₆₀₀ of 0.7 to 0.9. Ten mL of 200 g.L⁻¹ galactose were then added for induction of P450 expression at room temperature with shaking at 180 rpm for 24 hours. To test herbicide conversion by living P450-expressing yeasts, 5 mL of 200 µM herbicide were added to the culture medium, which was further incubated overnight at room temperature with shaking at 180 rpm. The yeast cells were then harvested by centrifugation (15 min at 4,500 rpm and 4°C), and the supernatant was collected. The yeast cells were resuspended in 500 µL methanol (99:1, v/v), then vortex and left 30 minutes at room temperature. Finally, they were centrifuged for 10 min at 13,000 rpm. The supernatant was recovered and analyzed by high performance liquid chromatography (HPLC) (**Figure 1**). The supernatants from 50 mL whole yeast cultures were extracted and concentrated using solid-phase extraction (SPE) before analysis. The SPE cartridges (Oasis HLB 1 cc, 60 mg; Waters) were conditioned with 5 mL of methanol, then 5 mL of water. The passage of the samples (50 mL) through the cartridges was carried out at a flow-rate of 7 mL.min⁻¹ with a peristaltic pump. The column was washed with 5 mL of 5% methanol, and compounds retained then eluted with 2 mL of methanol (**Figure 2**). 200 µL of the eluates were transferred to HPLC vials and analyzed on an Alliance 2695 Waters HPLC apparatus, as described in the herbicide *in vitro* conversion section. In some cases, when handling of a large number of samples was required, the culture medium was directly analysed by HPLC without prior concentration.

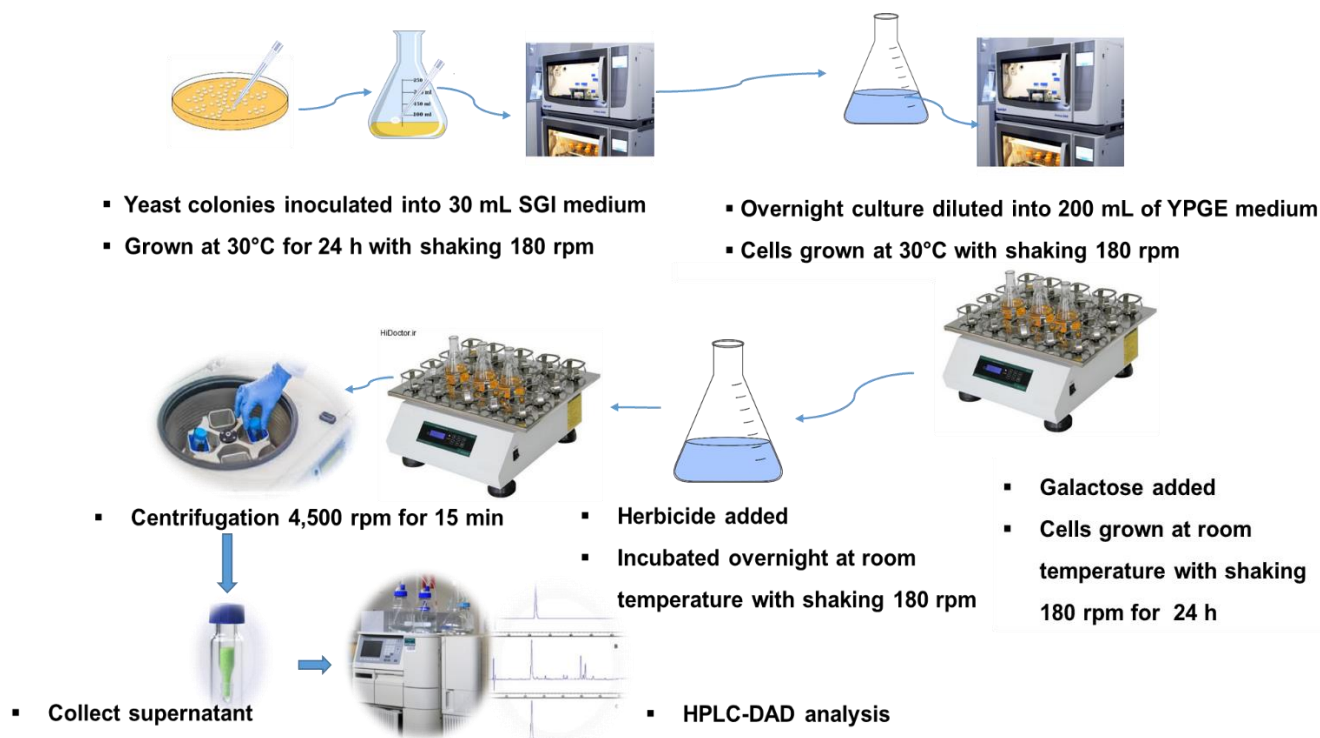


Figure 1. Assay of herbicide conversion in whole yeast

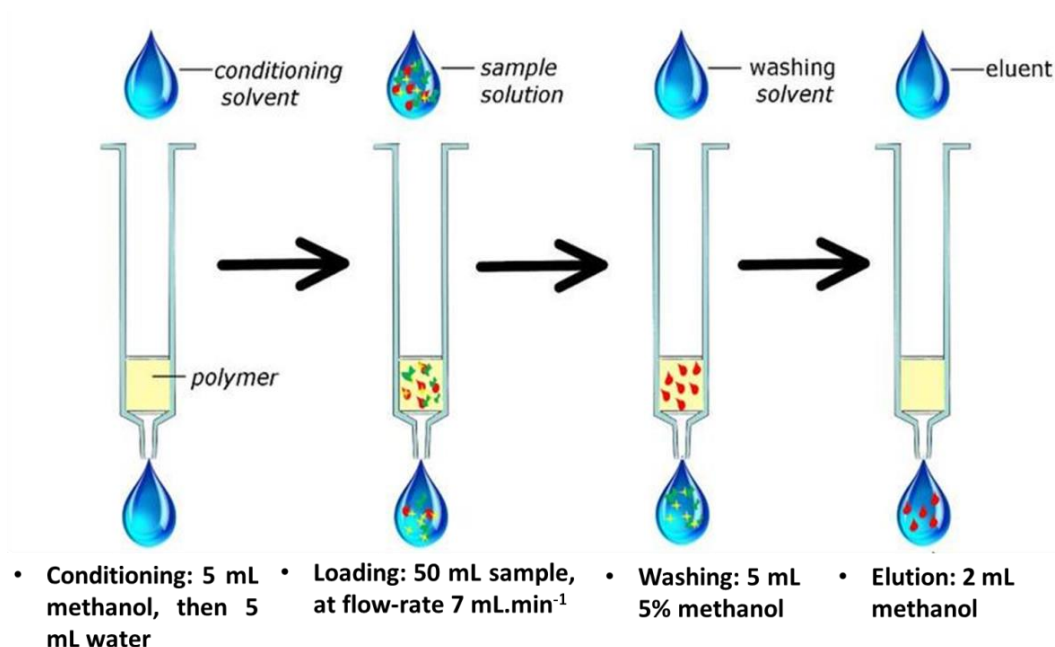


Figure 2. Solid-phase extraction

The supernatants of *CYP706A3*- or empty vector-transformed whole yeast cultures were purified and concentrated via solid-phase extraction before analysis by HPLC. The Oasis HLB 1 cc, 60 mg; Waters cartridge was conditioned with 5 mL of methanol, then 5 mL of water, and then loaded 50 mL of the samples at a flow-rate of 7 mL.min⁻¹ with a peristaltic pump. The cartridge was

washed with 5 mL of 5% methanol, and compounds eluted with 2 mL of methanol. Finally, 200 μ L of the eluates were transferred to HPLC vials and analyzed on an Alliance 2695 Waters HPLC.

Leaf disc assay

For transient expression of the genes of interest in *Nicotiana benthamiana* leaves, the plant expression constructs (pCAMBIA3300u, 35S:CYP706A3, empty vector) (Boachon *et al.*, 2019) were introduced into the *Agrobacterium tumefaciens* strain GV3101 (van der Fits *et al.*, 2000) by electroporation as described by Weigel and Glazebrook (2006). The *Agrobacterium* cells carrying the expression vectors were then grown in 5 mL Luria broth (LB) medium overnight in a shaker operated at 180 rpm and 30 °C with appropriate antibiotic selection (gentamycin, kanamycin and rifampicin). Bacteria were pelleted by centrifugation for 20 min at 4,500 rpm, washed twice with water, and resuspended in tap-water to OD₆₀₀ = 0.5. Young, fully expanded leaves of 6-week-old *N. benthamiana* plants, cultivated in a growth chamber at 20° C with a photoperiod of 16/8 h light/dark cycle, were infiltrated with the bacterial mix on the abaxial side using a needleless syringe. After 5 days, 14 mm diameter discs were excised from the infiltrated leaves with a cork borer. The leaf discs (20 per sample) were placed on 10 mL 20 mM Na phosphate citrate buffer pH 7.4 and containing 200 μ M of herbicides in a Petri dish, exposed to vacuum twice, and placed in a growth chamber at 20° C with a photoperiod of 16/8 h light/dark for 24 h. The leaf discs were directly ground in 4 ml methanol with a mortar and pestle. The extracts and growth medium were centrifuged 5 min at 12,000 rpm, and 200 μ L of the supernatants were transferred to HPLC vials and analyzed on an Alliance 2695 Waters HPLC system as described above. Incubation media of the leaf discs were separately analyzed by HPLC after centrifugation for 5 min at 12,000 rpm. All assays were conducted in triplicates (**Figure 3**).

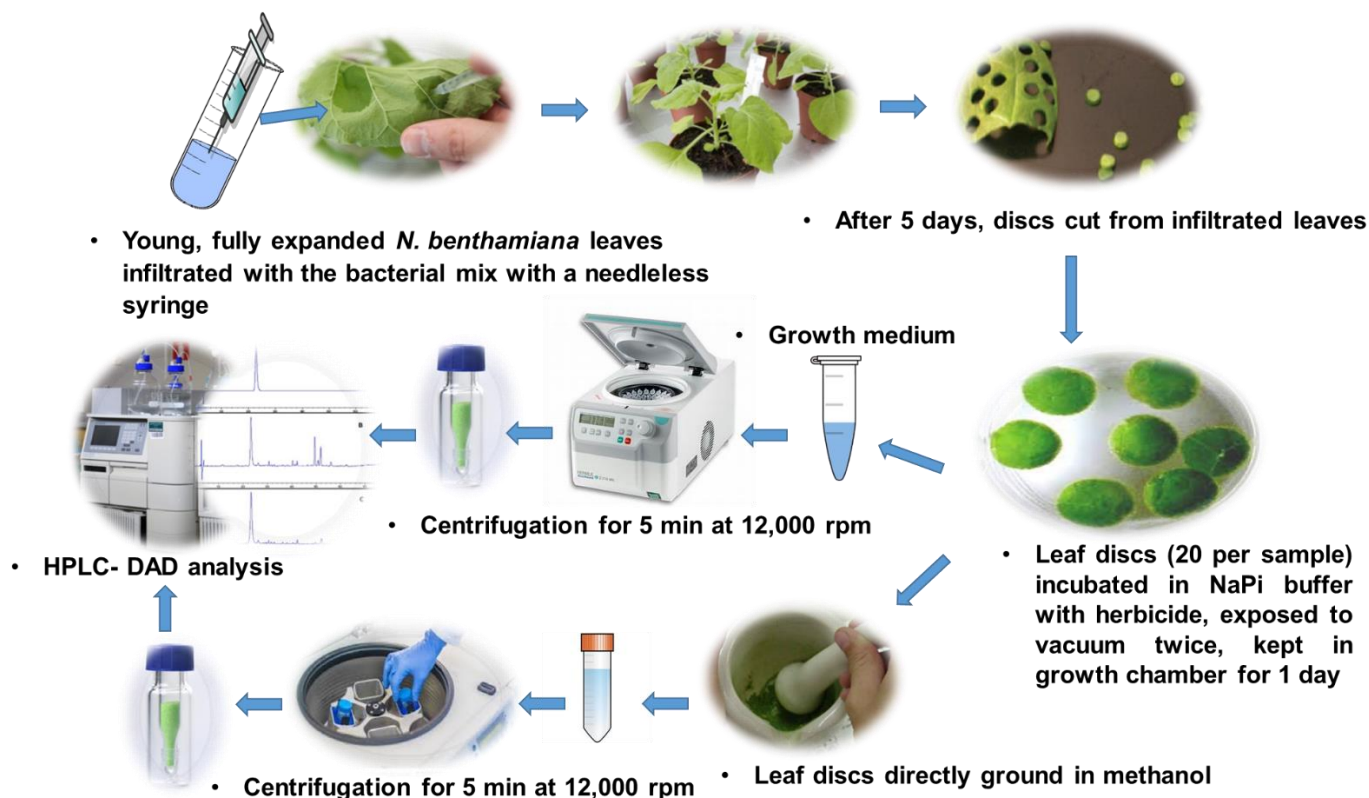


Figure 3. Leaf disc assay

Tests of herbicide tolerance

Seeds of *A. thaliana* Col-0 ecotype and of the *CYP706A3* T-DNA insertion and overexpression lines were sterilized in ethanol 70% (v/v), SDS 0.05% (w/v) for 20 min. Sterilized seeds were sown on solid medium containing 8 g.L⁻¹ agar and 2.45 g.L⁻¹ Murashige and Skoog including vitamins (Duchefa-Biochemie), adjusted to pH 5.8. Plants were grown in growth chambers with a light intensity of 70 to 90 mmol m⁻².s⁻¹ at 22°C during the 16 h day period and at 20°C during the 8 h night period. After germination, plantlets were transferred to a new plate of the same medium with 0, 0.05, 0.1, 0.2, 0.5, 1, 2, 3, 4, 6, 8, 10, 12 µM of herbicides. Plants were placed in the growth chamber previously described for 15 days.

Thin-layer and silica column chromatography

Thin-layer chromatography (TLC) was performed using Merck-TLC Silica gel 60 F₂₅₄ aluminum plates. The plates developed in a mobile phase containing petroleum ether and

ethyl acetate in ratio 70:30 (v/v). After that, plates were revealed either with sulfuric vanillin, with a KMnO_4 solution, or with a mixture of phosphomolybdic acid-cerium sulfate followed by heating using a heat gun and then read under UV light. The crude material was then purified by column chromatography on Merck Geduran® 40-63 μm silica gel using a step gradient of EtOAc in petroleum ether (0 to 10% v/v) to afford a mixture of two diastereomeric hydroxylated pendimethalin compounds. To separate the two diastereoisomers with close retention factors (R_f), preparative thin-layer chromatography, was performed using silica gel 60 F254 Merck-glass plates 20 X 20 cm, 0.5 mm thick and a 30:70 EtOAc/petroleum ether mixture (v/v) as mobile phase (**Figure 4**). NMR analysis confirmed the purity of each diastereoisomer.

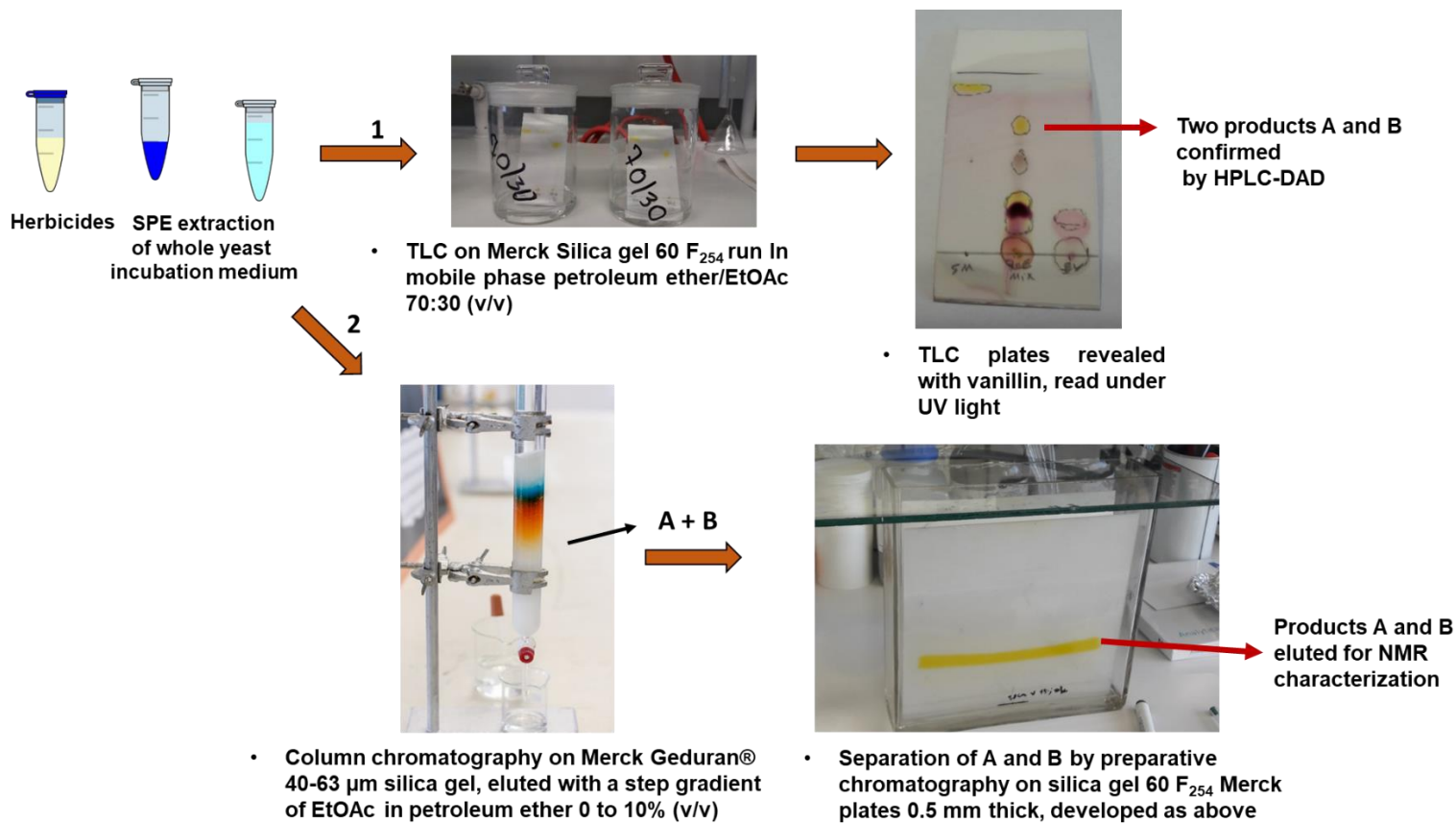


Figure 4. Characterization and purification of the products for NMR analysis

LC-Q-TOF acquisition

Extracts were analyzed using liquid chromatography (LC) coupled to high resolution mass spectrometry (HRMS) on a DioneX Ultimate 3000 (Thermo) coupled to a Q-TOF Impact II (Bruker). Chromatographic separation was achieved using an Acquity UPLC BEH C18 column (100 x 2.1 mm, 1.7 μ m; Waters) and pre-column. The mobile phase consisted of (A) water and (B) methanol, both containing 0.1 % formic acid. The run started by 2 min of 95% A, then a linear gradient was applied to reach 100% B at 10 min, followed by isocratic run using B during 3min. Return to initial conditions was achieved in 1 min, with a total runtime of 15 min. The column was operated at 35°C with a flow-rate of 0.30mL min⁻¹.

The spectrometer was used in positive ion mode, with a spectra rate of 2 Hz on a mass range from 20 to 1000 Da. The capillary voltage was set at 2500 V, the nebulizer at 2 Bars and the dry gas at 8 L min⁻¹, with a dry temperature of 200 °C. Fragments were obtained via auto-MS/MS with a MS/MS collision energy ramping from 18 to 45 eV depending on the mass of the parent ion.

Nuclear magnetic resonance (NMR)

NMR spectra were recorded using a Bruker AV-300 or AV-400 or AV-500 spectrometer with the solvent residual peak as internal standard. Splitting patterns were reported as s, singlet; d, doublet; t, triplet; q, quartet; qu, quintet; sex, sextet; m, multiplet and br, broad singlet.

Homology modeling of CYP706A3

Homology modeling and preparation of CYP706A3 structure for docking studies were performed according to the protocol described in Boachon *et al.* (2019), modified with the following adjustments. The multiple sequence alignment of the three templates CYP2R1 (pdb 3czh), CYP17A1 (pdb 5irq), and CYP1A2 (pdb 2hi4) used for Modeller 9v18 was that calculated solely by Promals3D (Pei *et al.*, 2008), to which was added a new template corresponding to a single heme compound with the geometry and charges calculated by DFT by Shahrokh *et al.* (2012). The resulting alignment with the heme parametrized was then submitted to Modeller, and a python script was subsequently applied to the best model for assigning to the heme the electrostatic charges of Shahrokh *et al.* (2012), in the Fe(III) ground or compound I states. The model selected was the best compromise

between the Dope score of Modeller and the QMEANDisco score (0.68) calculated by Swissmodel (Studer *et al.*, 2020).

Docking of herbicide

Molecular docking experiments with herbicide molecules into the CYP706A3 active site were performed using AutoDock 4 (release 4.2.6) in the semi-flexible mode, and prepared with AutoDock Tools (Morris *et al.*, 2009). Ligand molecules were built using ChemDraw molecular sketcher, and optimized and parameterized under the UCSF Chimera molecular modeling suite using AM1-BCC charges model, and the structure files saved under MOL2 format as input files for AutoDock. The MOL2 format files, created by Chimera for the receptor (charges generated with AMBER ff14) and the ligands, were converted into the PDBQT format file by AutoDockTools (ADT), without using the charge calculation provided by ADT. For ligand structures, partial charges were finally assigned using MMF94 force field under Avogadro software after different tests based on the pendimethalin know metabolism. In all docking runs, the receptor was kept rigid, and the ligand fully flexible. The docking box, in which grid maps were computed using program AutoGrid4, included the active site with the iron-protoporphyrin group on one edge, and the whole distal moiety of the enzyme, including access channels and protein surface, to allow a large sampling of potential poses. The grid built by AutoGrid included 60, 60 and 60 points in x, y and z directions, with a grid spacing of 0.37 Å. For each herbicide conformer, 100 independent runs were performed using the Lamarckian genetic algorithm (Fuhrmann *et al.*, 2010). The default settings were applied for all other parameters (maximum number of evaluations set to 2500000). The resulting poses were assigned a score calculated by Autodock that can be considered as an estimated free energy of ligand binding (indicative of binding affinity), then clustered as a function of the closeness of their positions and conformations with Root Mean Square Deviation (RMSD) set between 2.0 Å or 2.5 Å, and finally ranked by their binding score (for the best pose in the cluster).

Chapter 3

Results

The results have been drafted as a paper to be submitted to New Phytologist.

Relaxed substrate specificity of the CYP706 family of P450 enzymes provides a suitable context for the evolution of dinitroaniline resistance

Fatemeh Abdollahi^{a,b,c}, Mohammad Taghi Alebrahim^b, Chheng Ngov^c, Etienne Lallemand^d, Claire Villette^a, François André^d, Nicolas Navrot^a, Danièle Werck-Reichhart^{a*}, Laurence Miesch^{c*}

^a Institut de Biologie Moléculaire des Plantes du Centre National de la Recherche Scientifique (CNRS), Unité Propre de Recherche 2357, Université de Strasbourg, France.

^b Department of Agronomy and Plant Breeding, Faculty of Agricultural Sciences & Natural Resources, University of Mohaghegh Ardabili, Ardabil, Iran.

^c Equipe de Synthèse Organique et Phytochimie, Institut de Chimie, Unité Mixte de Recherche 7177, CNRS, Université de Strasbourg, France.

^d Institute for Integrative Biology of the Cell (I2BC), iBiTec-S/SB²SM, Commissariat à l'Energie Atomique, CNRS, Université Paris Sud, Université Paris-Saclay, Gif-sur-Yvette, France.

*Corresponding authors:

Danièle Werck: werck@unistra.fr

Laurence Miesch: lmiesch@unistra.fr tel:

Keywords: cytochrome P450 monooxygenases, dinitroanilines, herbicide metabolism, herbicide resistance, sesquiterpene metabolism

Summary

- Increased metabolism is one of the main causes for the evolution of herbicide resistance in weeds, a major challenge for sustainable food production. The molecular drivers of this evolution are poorly understood. We tested here the hypothesis that a suitable context for the evolution of herbicide resistance could be provided by plant enzymes with innate high promiscuity with regard to their natural substrates.
- A selection of yeast-expressed plant cytochrome P450 enzymes with well documented narrow to broad promiscuity when metabolizing natural substrates was tested for herbicide metabolism competence. The positive candidate was assayed for capacity to confer herbicide tolerance in *Arabidopsis thaliana*.
- Our data demonstrate that CYP706A3 from *A. thaliana*, with the most promiscuous activity on mono- and sesqui-terpenes for flower defense, is also able to metabolize the plant microtubule assembly inhibitors dinitroanilines. Ectopic expression of CYP706A3 confers dinitroaniline resistance. We show, in addition, that the capacity to metabolize dinitroanilines is shared by other members of the CYP706 family from plants as diverse as eucalyptus and cedar.
- Supported by 3D modelling of CYP706A3, the properties of the enzyme active site and substrate access channel are discussed together with the shared physicochemical properties of the natural and exogenous substrates to explain herbicide metabolism.

Introduction

Evolution of herbicide resistance in weeds provides a good example of ongoing, human-driven evolution. Although weeds are the primary cause of crop yield loss worldwide, in the context of growing demand for food and pesticide use reduction, it is essential to understand how herbicide resistance occurs. Herbicide resistance has been spreading around the world, since the introduction of 2,4-dichlorophenoxyacetic acid (2,4-D) as a first selective herbicide in 1947 (Switzer, 1957; Whitehead and Switzer, 1963). Two types of mechanisms can endow herbicide resistance. Target site herbicide resistance (TSR) is caused either by a mutation within the target that hampers herbicide binding, or by an increased production of the target enzyme protein. Non-target-site resistance (NTSR) involves reduced herbicide uptake or translocation, increased herbicide sequestration or enhanced herbicide metabolism, all resulting in a reduction of the amount of active herbicide reaching the target site. It can also result from protection against collateral damage of the herbicide action (Powles and Yu, 2010; Délye *et al.*, 2013; Cummins *et al.*, 2014). Herbicide target sites are well documented, and their limited number facilitates the description of the molecular mechanisms leading to TSR as stated by Iwakami *et al.*, 2019. In addition, TSR does not compromise efficiency of herbicides active on other targets. NTSR is more complex and challenging, especially when supported by herbicide metabolism. Its complexity results from the herbicide treatment-selected accumulation of multiple dominant or semi-dominant alleles conferring mild herbicide tolerance. Such complexity is particularly favored in outcrossing species. NTSR is considered as a major threat because it is supported by large families of enzymes with often redundant and/or promiscuous activities, which potentially leads to cross-resistance to herbicides with different modes of action, including not yet marketed compounds (Délye *et al.*, 2013; Yu and Powles, 2014). Enzyme families involved in NTSR are usually glutathione transferases, glucosyl transferases or, most often, cytochrome P450 monooxygenases.

Complementary strategies can be employed to discover the molecular determinants of metabolic resistance. One is a genetic, biochemical, and transcriptomic approach of resistant weed populations to identify the candidate's enzymes responsible for the herbicide metabolism. The transcriptomic approach was in particular explored to identify the determinants of NTSR and cytochrome P450-mediated herbicide resistance in the

Australian grass weed populations of *Lolium rigidum* (Yu and Powles, 2014; Gaines *et al.*, 2014). In the case of the Californian cross-resistant populations of *Echinochloa phyllopogon*, the discovery of the enzymes responsible for herbicide resistance was guided by the prior identification of CYP81 enzymes conferring bentazon tolerance in rice (Pan *et al.*, 2006; Iwakami *et al.*, 2014). This second approach recently led to the characterization of a subfamily of grass-specific P450 enzymes with a puzzling promiscuity, with the capacity to metabolize a broad range of active compounds with different mode of actions and contrasting physicochemical properties (Iwakami *et al.*, 2014; Iwakami *et al.*, 2019; Guo *et al.*, 2019). It also demonstrated that the knowledge accumulated on herbicide metabolism in crops and model plants is a useful support to the discovery of the metabolic determinants of weed cross-resistance.

Another strategy to disclose the molecular determinants of herbicide resistance is to screen for herbicide metabolism a range of representative and functionally characterized (sub)families of enzymes. This second strategy holds the potential to link the metabolism of specific classes of herbicides with the physicochemical and catalytic properties of some enzyme clades, and to document their physiological and ecological functions. It is expected to reveal the genetic backgrounds allowing evolution of herbicide metabolism, and will provide a support to appraise the ecological side-effects of herbicide treatments on weeds and crops. The best documented example of this approach is provided by the CYP76 family of P450 enzymes involved in the metabolism of monoterpenols in many plant species. When CYP76B1 was first shown to metabolize phenylurea herbicides, no physiological function was associated with this enzyme from Jerusalem artichoke (*Helianthus tuberosus*). CYP76B1-mediated herbicide metabolism resulted in nonphytotoxic di-*N*-dealkylated metabolites and in significant tolerance to phenylurea herbicides in transgenic tobacco (*Nicotiana tabacum*) and *Arabidopsis thaliana* (Robineau *et al.*, 1998; Didierjean *et al.*, 2002). It was then reported that several members of the CYP76 family in *Catharanthus roseus*, *A. thaliana*, or grapevine catalyzed different oxidation reactions on monoterpenols, including sequential reactions and conversion of different related compounds (Collu *et al.*, 2001; Hoefer *et al.*, 2013; Miettinen *et al.*, 2014; Ginglinger *et al.*, 2013; Ilc *et al.*, 2017). Most notably, CYP76C1 from *A. thaliana* was associated with the conversion of volatile linalool into more soluble carboxylinalool and lilac oxides in the opening flower for protection against florivorous insects (Boachon *et al.*,

2015). Meanwhile, the work of Höfer *et al.* (2014) bridged Arabidopsis CYP76C activities on monoterpenols and phenylurea herbicides, demonstrating that the enzymes of the CYP76C subfamily supported both the hydroxylation of monoterpenols and the dealkylation or hydroxylation of phenylurea (but no conversion of other classes of herbicides) and conferred phenylurea tolerance to ectopically over-expressing *A. thaliana* lines. CYP76s form a fast-blooming family of genes (Nelson and Werck-Reichhart, 2011) encoding moderately promiscuous enzymes. This led us to postulate that P450s in highly diversified families or encoded by recent gene duplicates under relaxed selective pressure, which show more promiscuous catalytic properties, might be more prone to metabolize exogenous compounds, and thus to contribute to the evolution of herbicide resistance.

The aim of this study was to investigate if P450-mediated herbicide metabolism could be related to innate catalytic promiscuity. We assessed the metabolism of a set of active compounds representative of the most commonly used classes of herbicides by six plant cytochrome P450 enzymes with documented biochemical activities and, for most of them, known physiological functions in plant (**Table 1**). These candidates were selected to be representative of P450s with very low to high promiscuity with regard to natural substrates. This investigation reveals a novel activity of the promiscuous terpenoid-oxidizing P450 enzymes CYP706A3 of *Arabidopsis thaliana* on dinitroanilines, and demonstrates that CYP706A3 holds the innate capacity to enhance the plant tolerance to most of the members of this class of herbicides. We show that the capacity to metabolize dinitroanilines extends to other sesquiterpenoids metabolizing CYP706 enzymes from cedar and eucalyptus. Results are discussed in light of enzyme and substrate structural/biophysical properties and adaptive evolution.

Table 1. Cytochrome P450 enzymes tested for herbicide conversion.

CYP	Plant	Reported substrates	Promiscuity	References
CYP73A92	<i>Brachypodium distachyon</i>	<i>Phenolics</i>	-	(Renault <i>et al.</i> , 2017)
CYP98A23	<i>Populus trichocarpa</i>	<i>Phenolics</i>	-	(Alber <i>et al.</i> , 2019)
CYP72A224	<i>Catharanthus roseus</i>	<i>Iridoids</i>	-	(Miettinen <i>et al.</i> , 2014)
CYP98A27	<i>Populus trichocarpa</i>	<i>Phenolics</i>	+/-	(Alber <i>et al.</i> , 2019)
CYP76B1	<i>Helianthus tuberosus</i>	<i>Monoterpenols</i> <i>Alkoxycoumarin</i> <i>Alkoxyresorufin</i>	+	(Batard <i>et al.</i> , 1998; Robineau <i>et al.</i> , 1998; Hoefer <i>et al.</i> , 2014)
CYP706A3	<i>Arabidopsis thaliana</i>	<i>Terpenoids</i>	+++	(Boachon <i>et al.</i> , 2019)

Methods

Herbicides assayed for plant P450 metabolism

All the herbicides were purchased from Sigma-Aldrich (Saint Louis, USA). The full list of herbicides used in this experiment is provided in Supplemental Table 1. Two mM stock solutions were prepared in methanol 96 % (v/v) and stored in the dark at 5°C.

Transgenic plant lines

The source and validation of *Arabidopsis thaliana* CYP706A3 T-DNA insertion and 35S:CYP706A3 overexpressing lines are described in Boachon *et al.* (2019).

Enzyme expression in yeast and isolation of recombinant enzyme-containing microsomal fractions

For the production of recombinant enzymes, the WAT11 yeast strain and pYeDP60 vector system were used (Pompon *et al.*, 1996). In the WAT11 strain, the ATR1 *A. thaliana* NADPH-P450 reductase gene is inserted in the chromosome under the control of the galactose-inducible and glucose-repressed yeast hybrid promoter *GAL10-CYC1* (Pompon *et al.*, 1996). pYeDP60 is a multicopy expression vector with an expression cassette under control of the same *GAL10-CYC1* promoter. Construction of the expression vectors of *CYP71D51*, *CYP76B1*, *CYP72A224*, *CYP73A92*, *CYP98A23/A27* and *CYP706A3* were previously described in Gavira *et al.*, 2013, Robineau *et al.*, 1998, Miettinen *et al.*, 2014, Renault *et al.*, 2017, Alber *et al.*, 2019, and Boachon *et al.*, 2019, respectively. Construction of the plasmids for the expression of *CYP706C55* and *CYP706M1* have been described in (Hansen *et al.*, 2018) and (Cankar *et al.*, 2014), respectively. Yeast transformation with the expression vectors was previously described (Ginglinger *et al.*, 2013).

Transformed yeast colonies were inoculated into 30 mL SGI medium (0.7% (w/v) yeast extract, 0.1% (w/v) bacto casamino acids, 0.002% (v/v) tryptophan, 2% (w/v) glucose) and grown at 28°C for 24 h with shaking (180 rpm) to reach an optical density of 1 at 600 nm. The overnight culture was diluted into 200 mL of YPGE medium (1% (w/v) yeast extract, 1% (w/v) peptone, 3% (v/v) ethanol, 0.5% (w/v) glucose), and cells were grown at 28°C with shaking (180 rpm) until cell density reached OD₆₀₀ of 0.7 to 0.9. Ten

mL of 200 g.L⁻¹ galactose were then added for induction of P450 expression, and cells were then further grown at 20°C with shaking at 180 rpm overnight. The yeast cells were harvested by centrifugation (15 min, 4,500 rpm, 4°C), washed in 30 mL of TEK buffer (50 mM Tris HCl pH 7.5, 1 mM EDTA, 100 mM KCl), centrifuged at 7,000 rpm for 10 min at 4°C, and resuspended in 1 mL of cold TES buffer (50 mM Tris HCl pH 7.5, 1 mM EDTA, 600 mM sorbitol). Cells were broken by vigorous shaking with glass beads (250 to 500 µM diameter) five times for a total of 5 min. The crude extract was recovered, and the beads were washed twice with 20 mL of cold TES. The homogenate was centrifuged for 20 min at 7,000 rpm and 4°C, and the resulting supernatant was centrifuged for 1h at 30,000 rpm and 4°C. The resulting pellets were then resuspended in 2 mL of TEG (50 mM Tris HCl pH 7.5, 0.5 mM EDTA, and 30% (v/v) glycerol) and stored at -30°C (Liu et al., 2016).

Quantification of P450 expression

Microsomal suspensions were diluted in TEG buffer to record CO-bound reduced versus reduced differential absorption spectra using a Cary 300 UV-Visible spectrophotometer. To this end, each sample was reduced with N₂S₂O₄ and dispatched between the two cuvettes for setting a baseline between 380 and 500 nm, before bubbling carbon monoxide in the assay cuvette for about 30 seconds. The absorbance spectrum of the CO-bound ferrous P450 was then recorded and used for the calculation of the P450 concentration according to Omura and Sato (1964).

Assays of herbicide conversion with yeast microsomes

The screening for herbicide conversion was carried out in a final volume of 100 µL containing 80 µL of Na phosphate buffer 20 mM pH 7.4, containing 100 µM of herbicide in the presence of 300 µM of NADPH and 10 µL of yeast microsomal membranes. The incubation was carried out at 25°C for 20 min and stopped by adding 200 µL of acetonitrile/HCl (99:1, v/v). The mixture was then centrifuged at 13,000 rpm for 5 min to remove precipitated proteins. The supernatant was transferred to 250 µL HPLC vials and analyzed on an Alliance 2695 Waters HPLC apparatus set with a C18 column (5 µm, 100 Å, 150 mm, 4.6 mm, Kinetex) using a binary gradient system of solvents A (water containing 0.1% (v/v) formic acid) and B (100% HPLC-grade acetonitrile containing 0.1% (v/v) formic acid) as follows: 0 to 5 min 10% to 50% B, then, 5 to 15 min 50% to 95% B,

hold for 2 min, followed by 95% to 10% for 1 min, hold for 1 min. Flow rate was 1 mL.min⁻¹ and column temperature 35°C. The formation of products was monitored with a diode array absorbance detector from 220 to 400 nm. All solvents were HPLC grade and filtered and degassed before use. All assays were conducted in triplicate.

Herbicide conversion in whole yeast

Yeast colonies were inoculated into 30 mL SGI medium and grown at 28°C for 24 h with shaking (180 rpm). The overnight culture was diluted into 200 mL of YPGE, and cells were grown at 28°C with shaking at 180 rpm until the cell density reached an OD₆₀₀ of 0.7 to 0.9. Ten mL of 200 g.L⁻¹ galactose were then added for induction of P450 expression at room temperature with shaking at 180 rpm for 24 hours. To test herbicide conversion by living P450-expressing yeasts, 5 mL of 200 µM herbicide were added to the culture medium, which was further incubated overnight at room temperature with shaking at 180 rpm. The yeast cells were then harvested by centrifugation (15 min at 4,500 rpm and 4°C), and the supernatant was collected. The pelleted yeast cells were resuspended in 500 µL of methanol (99:1, v/v), then vortexed and left 30 for minutes at room temperature. After 10 min centrifugation at 13,000 rpm, the supernatant was recovered and analyzed by high performance liquid chromatography (HPLC). Fifty mL of culture medium were extracted and concentrated using solid-phase extraction (SPE). The SPE cartridges (Oasis HLB 3 cc, 60 mg; Waters) were conditioned with 5 mL of methanol, then 5 mL of water. The filtration of the samples through the cartridges was carried out at a flow-rate of 7 mL.min⁻¹. The compounds retained on the column were eluted with 2 mL of methanol. 200 µL of the eluates were transferred to HPLC vials and analyzed on an Alliance 2695 Waters HPLC apparatus, as described in the herbicide *in vitro* conversion section. In some cases, when handling of a large number of samples was required, the culture medium was directly analyzed by HPLC without prior concentration.

Tests of herbicide tolerance

Seeds of *A. thaliana* Col-0 ecotype and of the CYP706A3 T-DNA insertion and overexpression lines were sterilized in ethanol 70% (v/v), SDS 0.05% (w/v) for 20 min. Sterilized seeds were sown on solid medium containing 8 g.L⁻¹ agar and 2.45 g.L⁻¹ Murashige and Skoog including vitamins (Duchefa-Biochemie), adjusted to pH 5.8. Plants were grown in growth chambers with a light intensity of 70 to 90 mmol m⁻².s⁻¹ at 22°C

during the 16 h day period and at 20°C during the 8 h night period. After germination, plantlets were transferred to a new plate of the same medium with 0, 0.05, 0.1, 0.2, 0.5, 1, 2, 3, 4, 6, 8, 10, 12 μ M of herbicides. Plants were placed in the growth chamber for 15 days.

Leaf disc assay

For transient expression of the genes of interest in *Nicotiana benthamiana* leaves, the plant expression constructs (pCAMBIA3300u, 35S:CYP706A3, empty vector) (Boachon *et al.*, 2019) were introduced into the *Agrobacterium tumefaciens* strain GV3101 (van der Fits *et al.*, 2000) by electroporation as described by Weigel and Glazebrook (2006). The *Agrobacterium* cells carrying the expression vectors were then grown in 5 mL Luria broth (LB) medium overnight in a shaker operated at 180 rpm and 30 °C with appropriate antibiotic selection (gentamycin, kanamycin, and rifampicin). Bacteria were pelleted by centrifugation for 20 min at 4,500 rpm, washed twice with water, and resuspended in tap-water to OD₆₀₀ = 0.5. Young, fully expanded leaves of 6-week-old *N. benthamiana* plants, cultivated in a growth chamber at 20° C with a photoperiod of 16/8 h light/dark cycle, were infiltrated with the bacterial mix on the abaxial side using a needleless syringe. After 5 days, 14 mm diameter discs were excised from the infiltrated leaves with a cork borer. Leaf discs (20 per sample) were placed in 10 mL of 20 mM pH 7.4 Na phosphate citrate buffer containing 200 μ M of herbicides in a Petri dish, exposed to vacuum twice, and placed in a growth chamber at 20° C with a photoperiod of 16/8 h light/dark for 24 h. The leaf discs were directly ground in 4 mL methanol with a mortar and pestle. The extracts were centrifuged 5 min at 12,000 rpm, and 200 μ L of the supernatants were transferred to HPLC vials and analyzed on an Alliance 2695 Waters HPLC system as described above. Incubation media of the leaf discs were separately analyzed by HPLC after centrifugation for 1 min at 2,000 rpm. All assays were conducted in triplicate.

Thin-layer and silica column chromatography

Thin-layer chromatography (TLC) was performed using Merck-TLC Silica gel 60 F₂₅₄ aluminum plates. The plates were developed in a mobile phase containing petroleum ether and ethyl acetate in ratio of 70:30. After drying, plates were revealed either with sulfuric vanillin, with a KMnO₄ solution, or with a mixture of phosphomolybdic acid-cerium sulfate followed by heating using a heat gun, and read under UV light. Preparative thin-

layer chromatography was performed using 20 X 20 cm silica gel 60 F254 Merck-glass plates, 0.5 mm thick. Merck Geduran® 40-63 µm silica gel was used for column chromatography. The crude material was purified by column chromatography using a step gradient of EtOAc in petroleum ether (0 to 10%, v/v) to afford hydroxylated pendimethalin compounds.

LC-Q-TOF acquisition

Extracts were analyzed using liquid chromatography (LC) coupled to high resolution mass spectrometry (HRMS) on a Dionex Ultimate 3000 (Thermo) coupled to a Q-TOF Impact II (Bruker). Chromatographic separation was achieved using an Acquity UPLC BEH C18 column (100 x 2.1 mm, 1.7 µm; Waters) and pre-column. The mobile phase consisted of (A) water and (B) methanol, both containing 0.1 % formic acid. The run started by 2 min of 95% A, then a linear gradient was applied to reach 100% B at 10 min, followed by isocratic run using B during 3min. Return to initial conditions was achieved in 1 min, with a total runtime of 15 min. The column was operated at 35°C with a flow-rate of 0.30mL min⁻¹.

The spectrometer was used in positive ion mode, with a spectra rate of 2 Hz on a mass range from 20 to 1000 Da. The capillary voltage was set at 2500 V, the nebulizer at 2 Bars and the dry gas at 8 L min⁻¹, with a dry temperature of 200 °C. Fragments were obtained via auto-MS/MS with a MS/MS collision energy ramping from 18 to 45 eV depending on the mass of the parent ion.

Nuclear magnetic resonance (NMR)

NMR spectra were recorded using a Bruker AV-300, AV-400, or AV-500 spectrometer with the solvent residual peak as internal standard. Splitting patterns were reported as s, singlet; d, doublet; t, triplet; q, quartet; m, multiplet and br, broad singlet.

Homology modeling of CYP706A3

Homology modeling and preparation of CYP706A3 structure for docking studies were performed according to the protocol described in Boachon *et al.* (2019), modified with the following adjustments. The multiple sequence alignment of the three templates CYP2R1 (pdb 3czh), CYP17A1 (pdb 5irq), and CYP1A2 (pdb 2hi4) used for Modeller 9v18 was that calculated solely by Promals3D (Pei *et al.*, 2008), to which was added a new template

corresponding to a single heme compound with the geometry and charges calculated by DFT by Shahrokh *et al.* (2012). The resulting alignment with the heme parametrized was then submitted to Modeller, and a python script was subsequently applied to the best model for assigning to the heme the electrostatic charges of Shahrokh *et al.* (2012), in the Fe(III) ground or compound I states. The model selected was the best compromise between the Dope score of Modeller and the QMEANDisco score (0.68) calculated by Swissmodel (Studer *et al.*, 2020).

Docking of herbicide

Molecular docking experiments with herbicide molecules into the CYP706A3 active site were performed using AutoDock 4 (release 4.2.6) in the semi-flexible mode, and prepared with AutoDock Tools (Morris *et al.*, 2009). Ligand molecules were built using ChemDraw molecular sketcher, and optimized and parameterized under the UCSF Chimera molecular modeling suite using AM1-BCC charges model, and the structure files saved under MOL2 format as input files for AutoDock. The MOL2 format files, created by Chimera for the receptor (charges generated with AMBER ff14) and the ligands, were converted into the PDBQT format file by AutoDockTools (ADT), without using the charge calculation provided by ADT. For ligand structures, partial charges were finally assigned using MMF94 force field under Avogadro software after different tests based on the pendimethalin known metabolism. In all docking runs, the receptor was kept rigid, and the ligand fully flexible. The docking box, in which grid maps were computed using program AutoGrid4, included the active site with the iron-protoporphyrin group on one edge, and the whole distal moiety of the enzyme, including access channels and protein surface, to allow a large sampling of potential poses. The grid built by AutoGrid included 60, 60 and 60 points in x, y and z directions, with a grid spacing of 0.37 Å. For each herbicide conformer, 100 independent runs were performed using the Lamarckian genetic algorithm (Fuhrmann *et al.*, 2010). The default settings were applied for all other parameters (maximum number of evaluations set to 2500000). The resulting poses were assigned a score calculated by Autodock that can be considered as an estimated free energy of ligand binding (indicative of binding affinity), then clustered as a function of the closeness of their positions and conformations with Root Mean Square Deviation (RMSD) set between 2.0 Å or 2.5 Å, and finally ranked by their binding score (for the best pose in the cluster).

Results

Screening for herbicide P450-dependent herbicide metabolism

We first tested herbicide metabolism using the microsomal membranes purified from yeasts transformed with the genes encoding the different candidates, to be able to check for successful enzyme expression. After galactose induction of the gene expression, yeast microsomal membranes were isolated by differential centrifugation. The production of the respective P450 enzymes was then checked and quantified by UV-Vis differential spectrophotometry (Omura and Sato, 1964). All the investigated P450 enzymes were successfully detected and quantified in yeast membranes (**Figure 1A-E; Supplemental Table 2**).

To determine the capacity of the candidates to catalyze herbicide oxidation, microsomal membranes were then incubated with NADPH and herbicides representative of the major classes of active compounds (**Supplemental Table 1**). Membranes isolated from yeast transformed with an empty vector was used as a control. After termination of the reaction, each sample was analyzed by high performance liquid chromatography with diode-array detection (HPLC-DAD) to reveal potential oxidation products. This initial screening confirmed the already reported activity of the *Helianthus tuberosus* CYP76B1 (used as a positive control) with regard to phenylurea herbicides (Robineau *et al.*, 1998; Didierjean *et al.*, 2002), and revealed a novel oxidative activity of *Arabidopsis thaliana* CYP706A3 on pendimethalin (**Table 2; Figure 2**). However, the amounts of herbicide conversion products obtained under these conditions were not sufficient for the full characterization of the products.

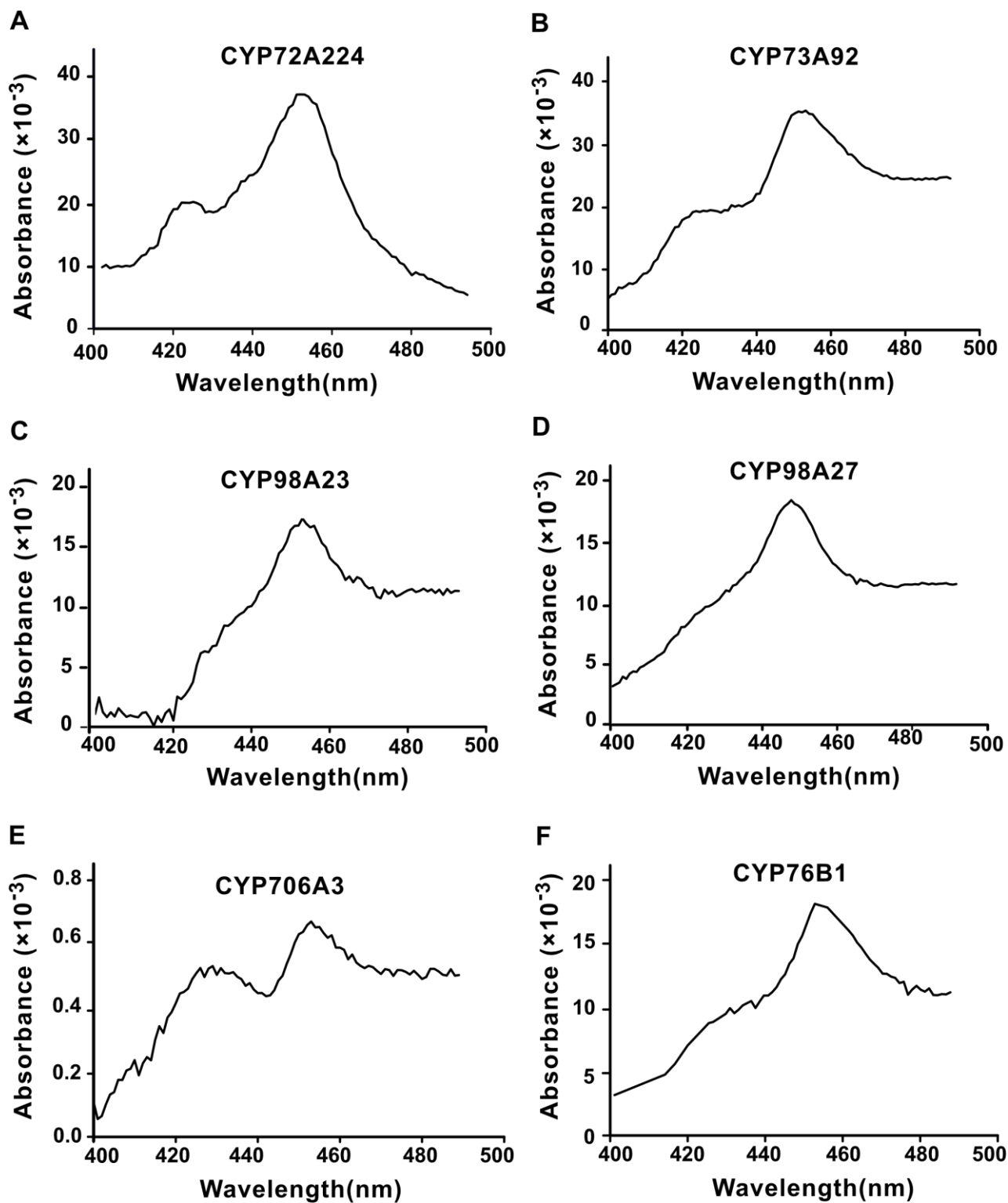


Figure 1. Carbon monoxide-reduced versus reduced difference spectra of recombinant P450 investigated.

200 mL microsomal membranes were diluted 10-fold in TEG buffer for recording the absorbance of the reduced-CO bound enzyme as described in the Methods section.

Absorbance at 450 nm indicates the presence of functional P450. Absorbance at 420 nm is indicative of the presence of inactive enzyme (disrupted heme-cysteine bond).

Table 2. Screening for CYP-dependent herbicide oxidation.

Microsomal membranes from yeasts transformed with P450 expression vectors were incubated with herbicides (100 μ M) for 20 min in the presence of NADPH (300 μ M). (+) Herbicide was converted; (-) herbicide was not converted. Yeast transformed with an empty vector was used as a negative control.

Family	Herbicide	Conversion					
		CYP98A23	CYP98A27	CYP706A3	CYP73A98	CYP72A224	CYP76B1
Dinitroaniline	Pendimethalin	-	-	+	-	-	-
Triazines	Atrazine	-	-	-	-	-	-
	Terbutryn	-	-	-	-	-	-
	Simazine	-	-	-	-	-	-
Imidazolinones	Imazethapyr	-	-	-	-	-	-
Sulfonylureas	Nicosulfuron	-	-	-	-	-	-
	Rimsulfuron	-	-	-	-	-	-
Phenylureas	Chlorbromuron	-	-	-	-	-	+
	Metobromuron	-	-	-	-	-	+
	Chlortoluron	-	-	-	-	-	+
Benzoic acids	Chloramben	-	-	-	-	-	-
	Dicamba	-	-	-	-	-	-
Nitriles	Bromoxynil	-	-	-	-	-	-
Aryloxyphenoxy propionates	Haloxypop-methyl	-	-	-	-	-	-
	Fenoxaprop- <i>p</i> -ethyl	-	-	-	-	-	-
Pridazinone	Norflurazon	-	-	-	-	-	-
Benzothia diazinone	Bentazon	-	-	-	-	-	-
Chlorinated anilide	Propanil	-	-	-	-	-	-
Diphenyl ethers	Bifenox	-	-	-	-	-	-
Phenoxy-carboxylic-acids	2,4-D	-	-	-	-	-	-

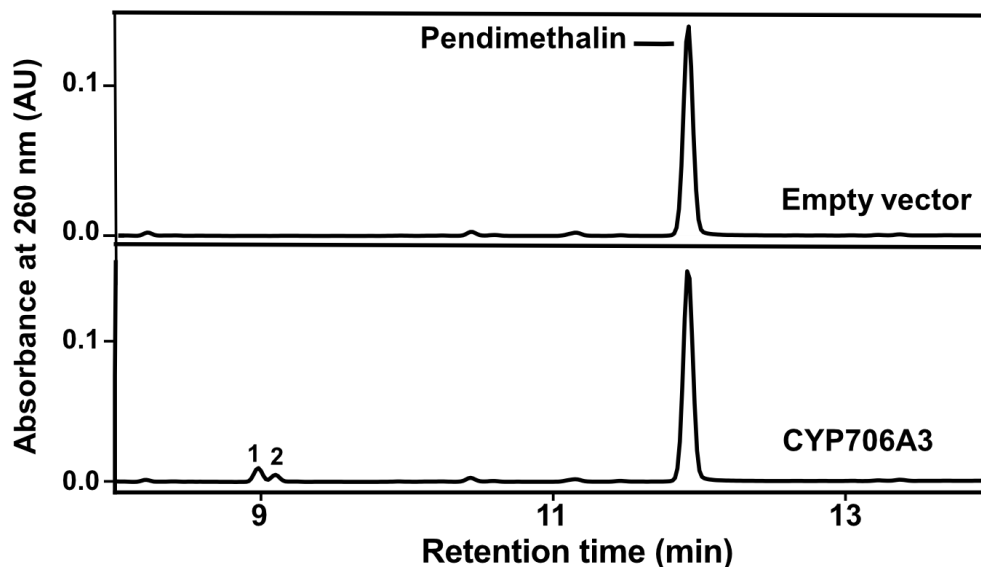


Figure 2. Conversion of pendimethalin by CYP706A3 in recombinant yeast microsomes.

HPLC-DAD chromatogram of the reaction mixture resulting from the incubation of 100 μ M pendimethalin with microsomes of yeast transformed with an empty vector (upper panel) or with a vector harboring *CYP706A3* (lower panel) for 20 min in the presence of NADPH (10 μ g of P450 in the assay). Based on retention times, peaks **1** and **2** were identified as potential products. AU: absorbance units.

Pendimethalin is converted by CYP706A3 in whole yeast and *Nicotiana benthamiana*

For confirmation the activity of CYP706A3 and generation of oxidation products in amounts sufficient for structural characterization, pendimethalin conversion was further assayed using whole transgenic yeast cultures and transient *CYP706A3* expression in *N. benthamiana*.

For the whole yeast conversion assays, transformed cells were grown to an OD of 0.8 before induction of the protein expression with galactose, before addition of herbicide to the culture medium. Pendimethalin and conversion products were extracted after 24 hours of incubation, separated from the yeast cells or from the culture medium. From the yeast cell extract, pendimethalin conversion products were recovered, but in small amounts (**Supplemental Figure 1**). Conversely, in the extract of the culture medium, no residual pendimethalin was detected, but large amounts of two conversion products showing

absorption and retention times identical to those previously obtained with the yeast membranes were observed (**Figure 3A-B; Supplemental Figure 2**).

CYP706A3 was also transiently expressed by infiltration of transformed *Agrobacterium* in the leaves of *N. benthamiana*. Leaf discs were excised 5 days post-agroinfiltration, vacuum-infiltrated with Na-phosphate buffer containing 100 μ M of pendimethalin, and further incubated in the same buffer for 24 hours. Products were methanol-extracted from the leaf discs and incubation buffers for analysis by HPLC-DAD. Only low amounts of herbicide conversion products were detected in the leaf disc extracts (**Figure 3C**). Still, analysis of the extracts from the incubation buffer confirmed the *CYP706A3*-dependent conversion of pendimethalin (**Figure 3D**), with the detection of the same two products as in yeast assays, but in lower amounts.

Therefore, whole yeast conversion was upscaled to generate metabolites in sufficient amounts for structural identification.

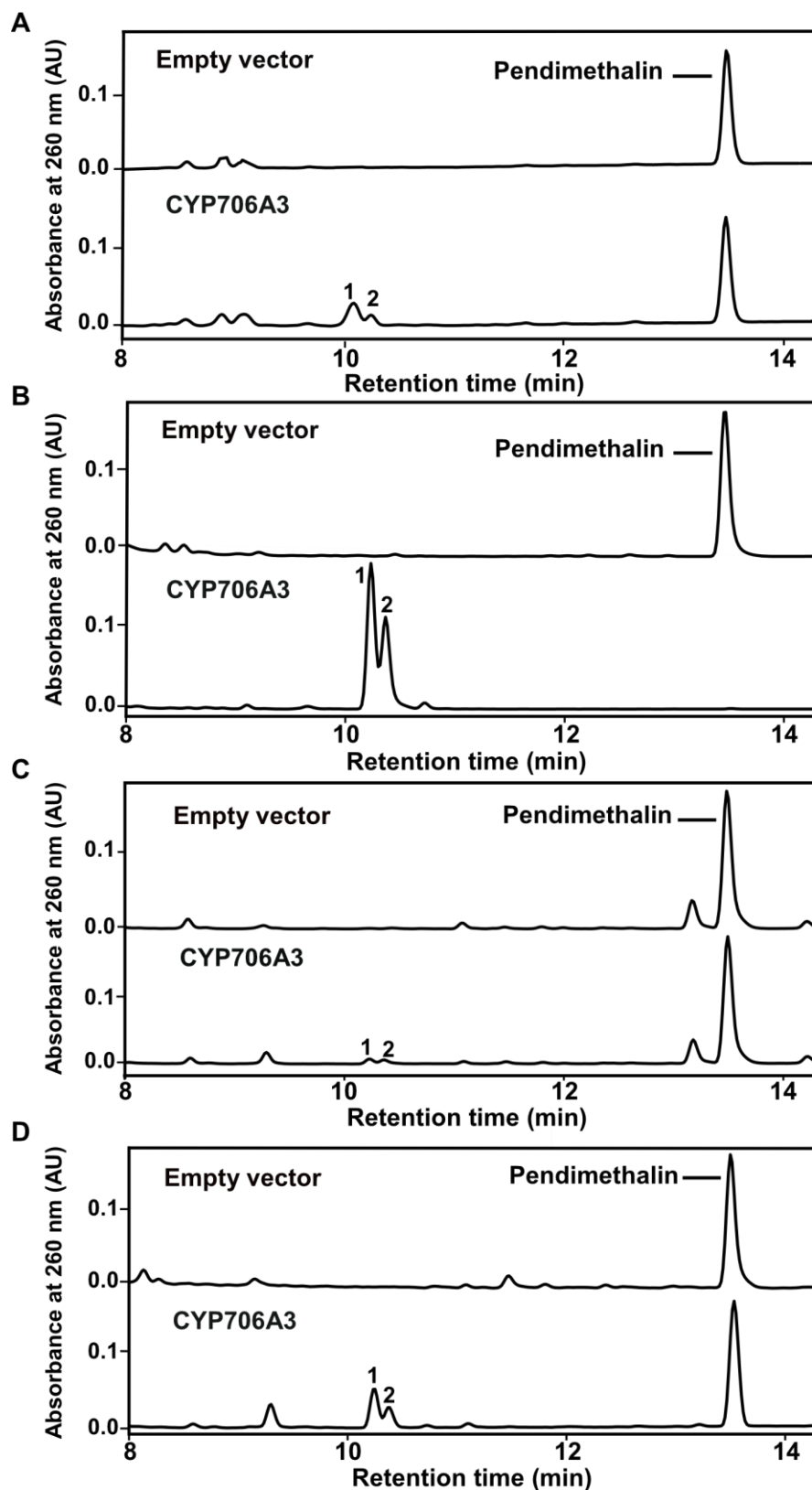


Figure 3. Pendimethalin conversion by CYP706A3 in whole yeast and *N. benthamiana* leaf discs.

A. and **B.** Whole yeast, transformed with *CYP706A3*-harbouring or empty expression vector (empty-control), was grown and *CYP706A3* expression was induced as described in the Methods section. After overnight galactose induction of *CYP706A3* expression, 200 μ M of pendimethalin were added to the medium. Conversion products were extracted after 24 hours further incubation at room temperature, separately from yeast cell and growth medium, and analyzed by HPLC-DAD. Upper panel: empty vector Lower panel: *CYP706A3* + pendimethalin. Peaks **1** and **2** correspond to the products detected in Figure 2. **A.** Yeast cell extract. **B.** Growth medium extract.

C. and **D.** *N. benthamiana* leaf discs, transiently expressing *CYP706A3* or the empty pCAMBIA330035Su plant expression vector (EV control), were incubated in 20 mM Na-phosphate buffer (pH 7.4) containing 200 μ M pendimethalin at 20°C under light for 24 h. Methanol-extracts from the leaf-discs or incubation media were separately analyzed by HPLC-DAD. **C.** Extracts of the agroinfiltrated leaf discs. **D.** Extracts of the leaf disc incubation media.

Products of *CYP706A3*-mediated pendimethalin conversion are two diastereoisomers

In a first step to product characterization, liquid chromatography coupled to mass spectrometry (LC-MS) analysis was carried out. It suggested that the two peaks resulting from the *CYP706A3*-mediated pendimethalin conversion were oxygenated products with the same mass and fragmentation patterns (**Figure 4; Supplemental Figure 3**), hydroxylated on the side chain in the terminal or penultimate position.

Unambiguous product identification required nuclear magnetic resonance (NMR) characterization, and thus larger amounts of pure compounds. Pooled methanol extracts of whole yeast conversion were analyzed by thin-layer chromatography (TLC). Two major and two minor products more hydrophilic than pendimethalin were detected (**Figure 5A**). The two major products, with close R_f values, were then separated by preparative TLC, eluted, and submitted to NMR analysis. Both ^1H -NMR and ^{13}C -NMR spectra of the purified compounds were consistent with the prior LC-MS results, indicating that pendimethalin was hydroxylated by *CYP706A3* on the penultimate carbon of the side-chain. Hydroxylation resulted in the formation of two stereocenters. The two products are thus most likely diastereoisomers (**Figure 5B and C; Supplemental Figure 4**).

For a final check if the two TLC-purified products were those identified as products via LC, they were injected separately and simultaneously on LC-DAD and compared to the elution profile of a whole yeast incubation (**Supplemental Figure 4**). This experiment

confirmed that the major TLC-purified products corresponded to the peaks **1** and **2** detected via LC. This allowed us to determine the catalytic parameters of the CYP706A3-mediated pendimethalin 4-hydroxylation using the yeast microsome assay. The reaction proceeded with a K_m of 436 (\pm 140) μ M and a k_{cat} of 2.34 (\pm 0.44) min^{-1} for pendimethalin (Supplemental Figure 5).

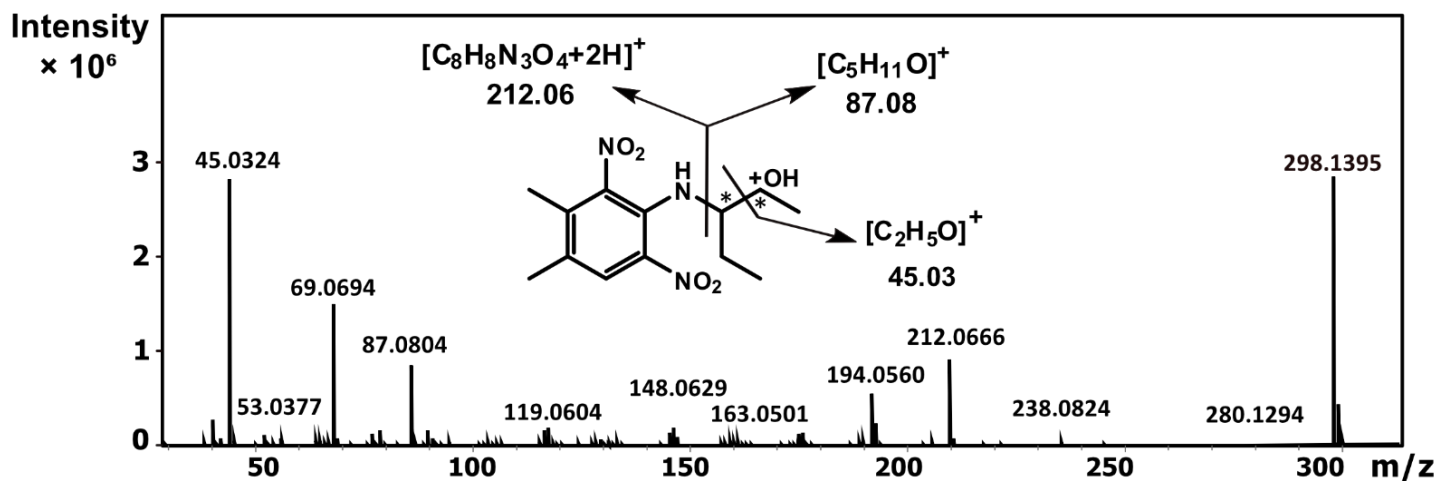


Figure 4. LC-MC characterization of the pendimethalin oxidation products.

Fragmentation patterns of the products of CYP706A3-mediated conversion of pendimethalin detected upon LC-MS analysis. The fragmentation patterns of products **1** and **2** were identical.

Note that pendimethalin hydroxylation on the side-chain generates two chiral carbons.

a.

Pendimethalin	Two products
----------------------	---------------------

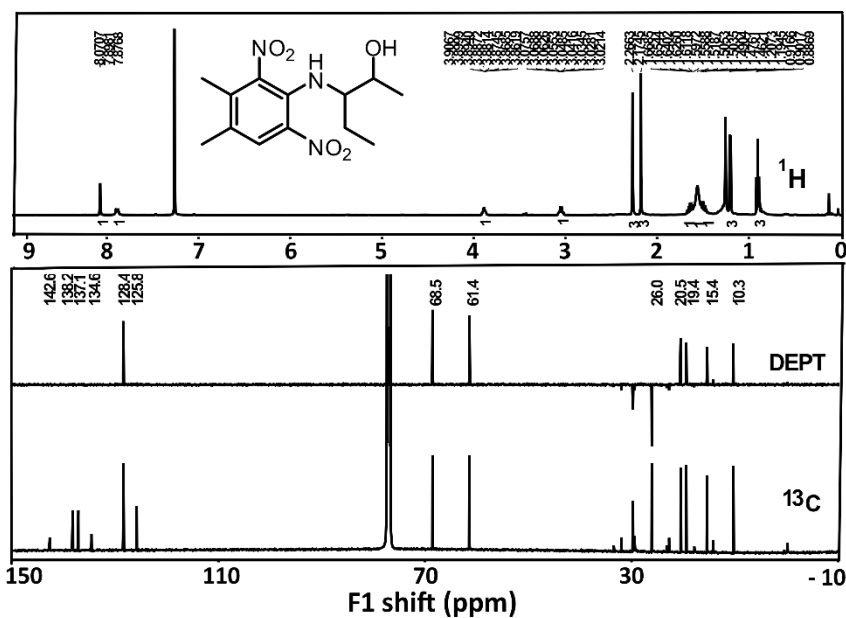
b.

Pendimethalin

Two products

Empty vector

B



C

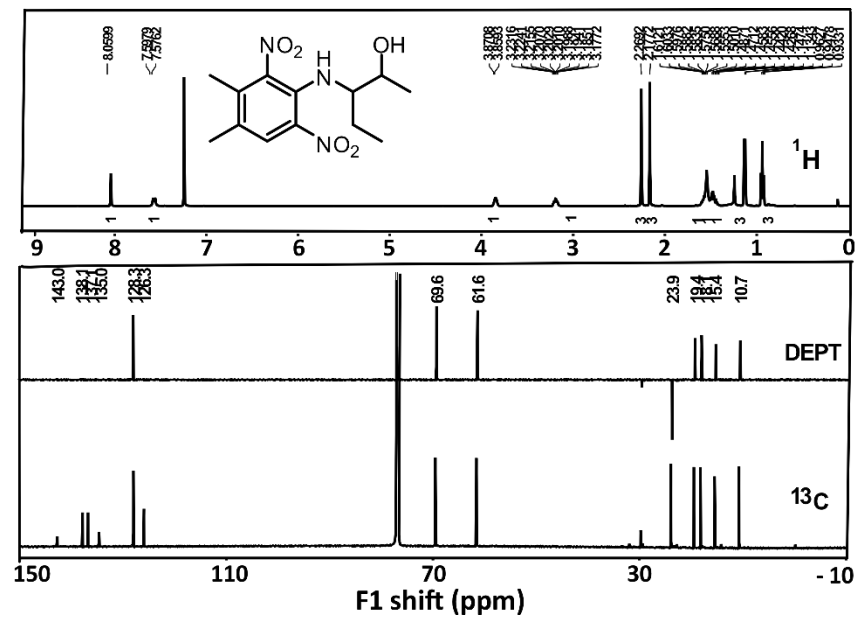


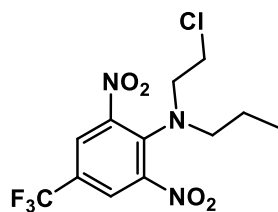
Figure 5. NMR characterization of the pendimethalin oxidation products.

- A. TLC separation and purification of the pendimethalin metabolites. Plates were developed and revealed as described in the Methods section.
 - B. ^1H -NMR and ^{13}C -NMR spectra of diastereoisomer1.
 - C. ^1H -NMR and ^{13}C -NMR spectra of diastereoisomer2.
- NMR determination is provided in Supplemental information.

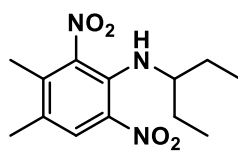
CYP706A3 oxidizes most herbicides belonging to the class of dinitroanilines

CYP706A3 was previously shown to oxidize a broad spectrum of terpenoids, including both sesqui- and mono-terpenes (Boachon *et al*, 2019). We thus set out to determine whether CYP706A3 was also able to convert a range of dinitroaniline herbicides. To this end, we tested the metabolism of ethalfluralin, fluchloralin, trifluralin, benefin and oryzalin (**Figure 6**) using a 24 h whole yeast conversion experiment. Methanol extract HPLC-DAD profiles of the yeast incubation media obtained with *CYP706A3*- and empty vector-transformed yeasts were compared. Expression of *CYP706A3* resulted in a decrease in the active compound and the concomitant formation of more polar products for ethalfluralin, fluchloralin, trifluralin and benefin, but not for oryzalin (**Figure 7**). For several dinitroanilines (e.g. fluchloralin, benefin and ethalfluralin), the formation of more than one potential polar product was detected (**Figure 7**). LC-MS/MS search for potential conversion products indicated that those were essentially mono- and di-oxygenated products (**Supplemental Figure 6**).

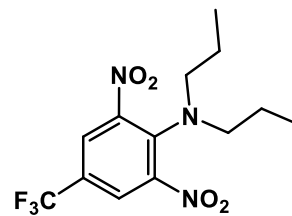
The whole yeast assays were clearly more effective to detect CYP706A3-mediated herbicide conversion than tests using purified microsomal membranes. A screening to detect the metabolism of compounds in Table 2 was thus performed a second time using the whole yeast assay. It did not detect conversion of any further active compound.



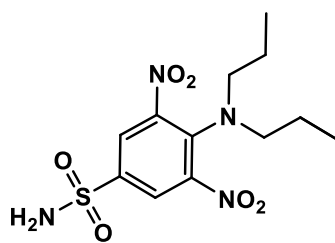
Fluchloralin



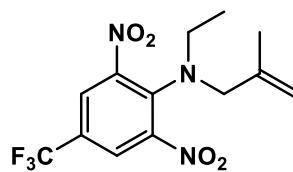
Pendimethalin



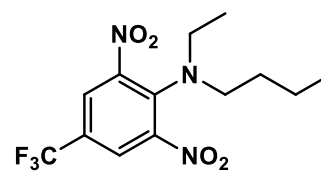
Trifluralin



Oryzalin



Ethalfluralin



Benefin

Figure 6. Dinitroaniline herbicides tested as substrates of CYP706A3.

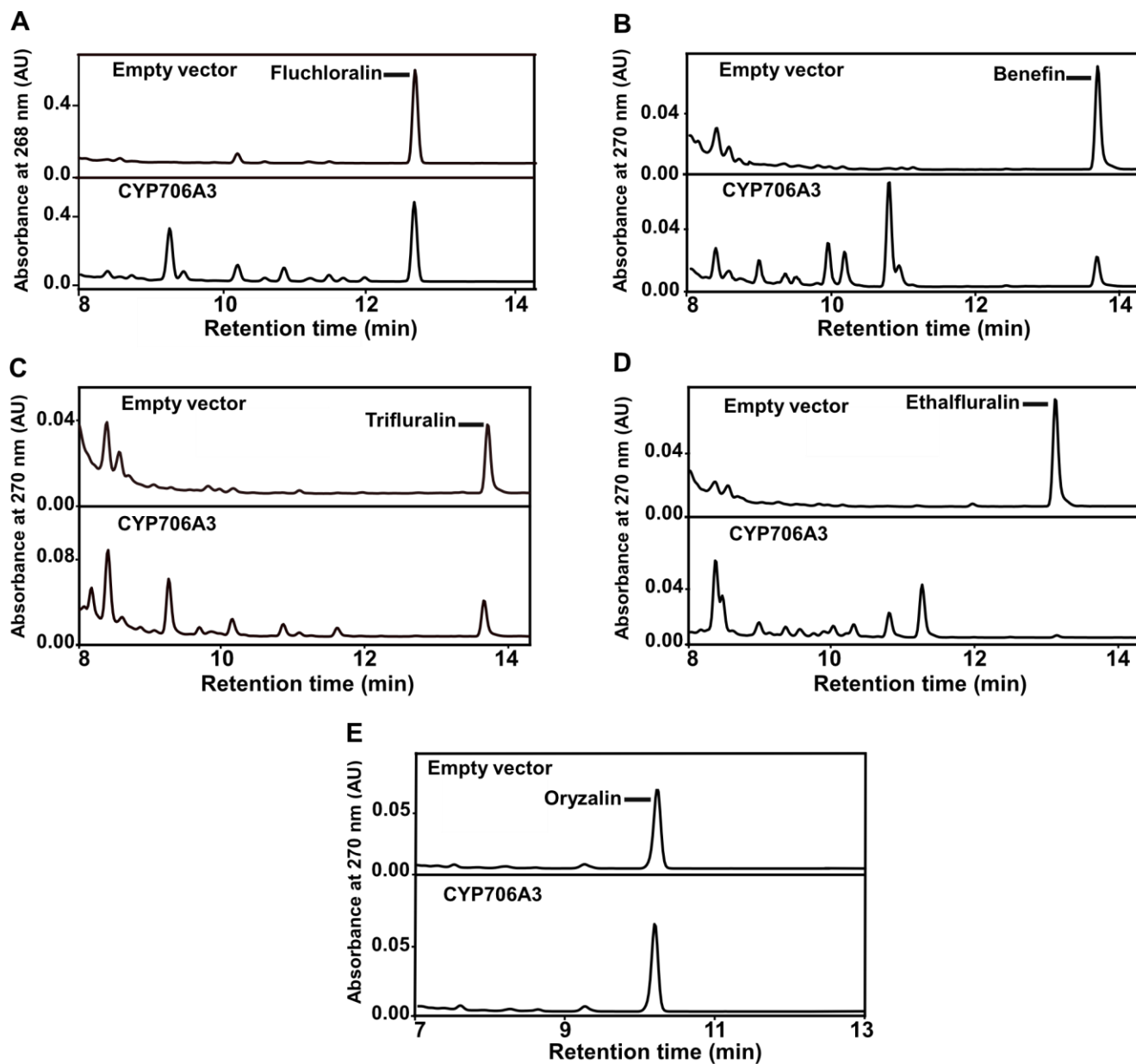


Figure 7. CYP706A3-mediated dinitroaniline conversion in whole yeast assay.

CYP706A3- or empty vector-transformed whole yeast cultures were incubated with 200 μ M of herbicide for 24 hours at 20°C. **A.** Fluchloralin; **B.** Benefin; **C.** Trifluralin; **D.** Ethalfluralin; **E.** Oryzalin.

CYP706A3 ectopic expression increases dinitroaniline tolerance in *A. thaliana*

CYP706A3 expression is restricted to developing and mature inflorescences (Boachon *et al.*, 2019) in wild-type *A. thaliana*. Ectopic overexpression of phenylurea-oxidizing P450 enzymes has been previously reported to increase herbicide tolerance in

tobacco and *Arabidopsis* (Didierjean *et al.*, 2002; Höfer *et al.*, 2014). To determine whether CYP706A3-dependent metabolism of dinitroanilines incurs herbicide detoxification and to increased herbicide resistance in the plant, a genetically engineered *Arabidopsis* line expressing CYP706A3 in most plant tissues (Boachon *et al.*, 2019) was thus tested for dinitroaniline tolerance. As shown in **Figure 8**, a concentration of 1 μ M of pendimethalin, ethalfluralin, fluchloralin, trifluralin or benefin, which resulted in almost total inhibition of the growth of wild-type *Arabidopsis* seedlings, did not affect 35S:CYP706A3 transformed plants. Conversely, in the case of oryzalin, no significant difference between wild-type and 35S:CYP706A3 plants was observed.

To determine the overall gain in herbicide tolerance conferred by CYP703A6 ectopic expression, we compared the effect of a stepwise increase herbicide concentration on wild-type and transformed plant growth (**Figure 9A-F**). Tolerance factors calculated from this experiment indicated an increase in tolerance of about 50-fold to pendimethalin, 11-fold to trifluralin and fluchloralin and 8-fold to ethalfluralin and benefin for 35S:CYP706A3 seedlings compared to wild type (**Supplemental Table 3**). Conversely, no increase in herbicide tolerance was detected for oryzalin.

To confirm herbicide conversion, methanol extracts of pendimethalin-treated *Arabidopsis* seedling were analyzed by HPLC-DAD. No residual herbicide was detected in the plants, nor primary metabolites previously identified after yeast and conversion, indicating further herbicide metabolism in the transformed plants.

CYP706A3 ectopic overexpression thus results in a significant gain in herbicide tolerance. This gain in herbicide resistance well correlates with CYP706A3-dependent herbicide metabolism detected in transformed yeast.

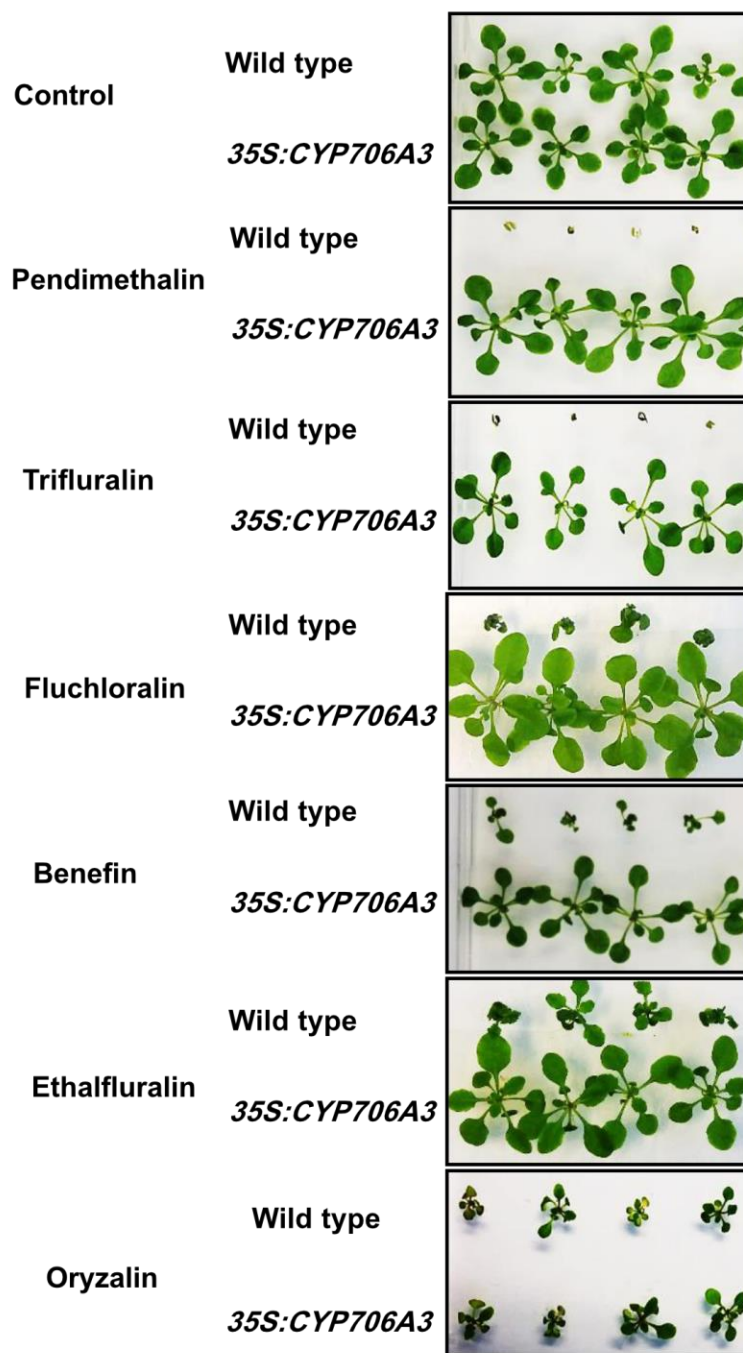


Figure 8. *A. thaliana* ectopically expressing *CYP706A3* is tolerant to dinitroaniline herbicides.

Plants were grown for 15 days in the presence or absence of 1 μ M of dinitroanilines.

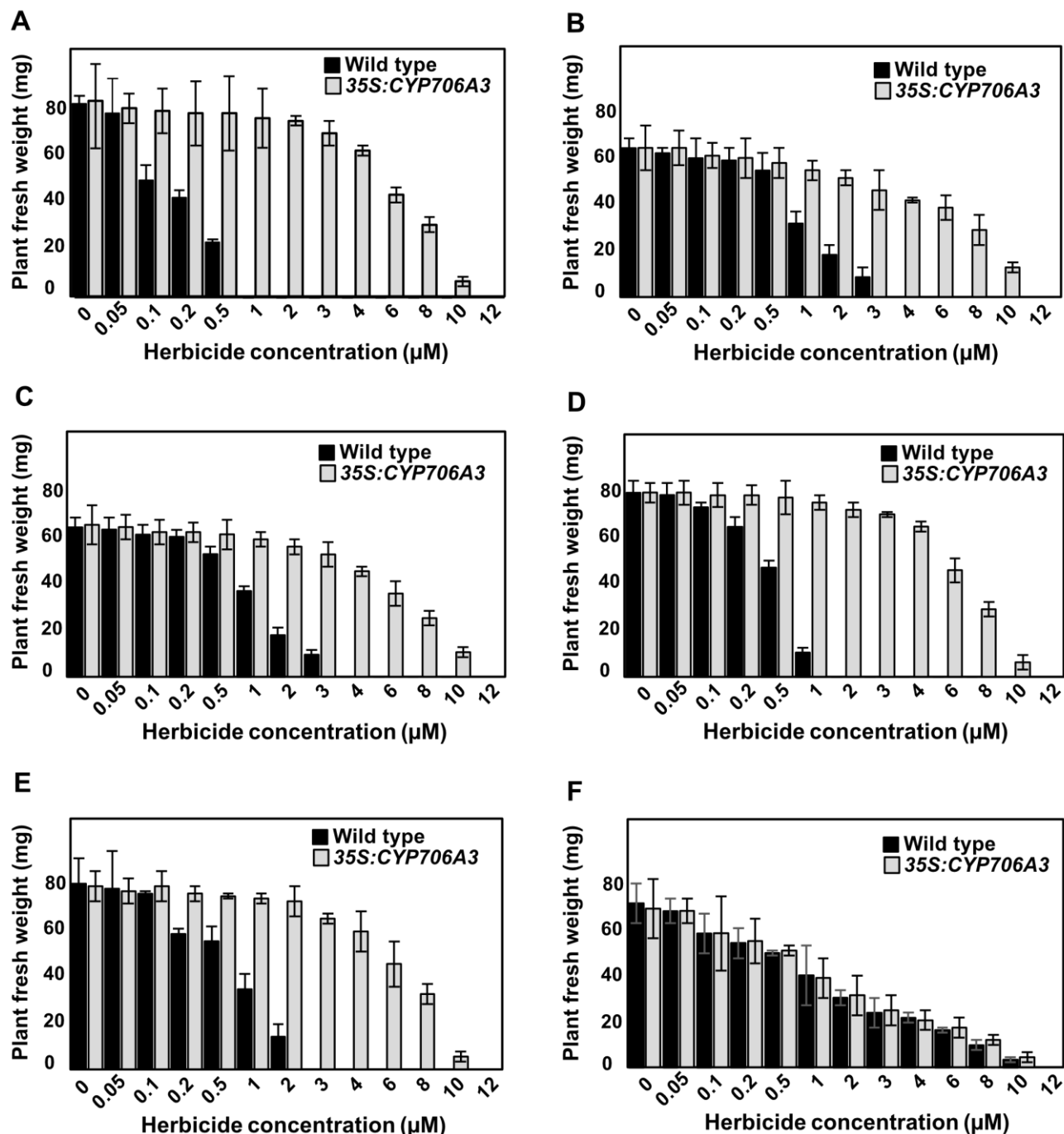


Figure 9. Evaluation of the gain in herbicide resistance conferred by the ectopic overexpression of *CYP706A3* in *A. thaliana*.

Tolerance of the *A. thaliana* 35S:CYP706A3 overexpressing line (35S:CYP706A3) to increased concentrations of pendimethalin (A), benfen (B), ethalfluralin (C), trifluralin (D), fluchloralin (E), and oryzalin (F) was compared to that of a wild type (WT) control. Plants were grown during 15 days on MS medium either without or with different concentrations of herbicides at 22°C during the 16 h day period and at 20°C during the 8 h night period. Data are average weight of three plants.

Structural basis for herbicide metabolism by CYP706A3

The results of Autodock 4 docking experiments of six dinitroanilines into the active site cavity of the rebuilt 3D of CYP706A3 are displayed **Figure 10** and **Supplemental Figure 7**. Altogether, they indicate a rather good affinity of the active site for all the compounds investigated. The empirical affinity score given by Autodock, expressed in kcal.mol^{-1} , normalized on well-characterized protein complexes, can be considered as an estimated free energy of ligand binding, and the energy values in a homogeneous family of molecules can be compared. The docking of all compounds resulted in similar overall binding affinity for lowest energy and most populated clusters of poses, and for clusters involving hydroxylation of hydrocarbons. Pendimethalin and oryzalin exhibited the best affinities (respectively -8.75 and $-8.52 \text{ kcal.mol}^{-1}$ of energy score), while the 4 other dinitroanilines displayed homogeneous affinities ranging from -7.3 to $-7.9 \text{ kcal.mol}^{-1}$. For productive poses, i.e. yielding to a metabolism on a CH site, the most predominant poses for all molecules oriented the alkyl chains towards the heme iron in the active site. In some cases (pendimethalin, oryzalin), the lowest energy and most populated clusters corresponded to poses where the subterminal CH_2 and terminal CH_3 groups were distant from the heme iron at about 3 \AA , highly favorable for oxidative attack. The equidistance indicates that the metabolism can occur either on the two carbon sites with the same probability, and when the subterminal group CH_2 is closer, the hydroxylation introduces a chirality on the oxidized carbon and can lead to two diastereoisomers. For other molecules, the same positions of metabolism were found in lowest energy clusters involving CH proximity, with an additional possible metabolism on the antepenultimate position in benefin molecule (CH_2 group, third pose, **Supplemental Figure 7**). It must be mentioned that the preparation of all ligands (conformational and partial charges optimization) involved the neutral form (no global charge) of the molecules. The docking process could have considered the positive isomer for oryzalin, of which the sulfonamide group is likely to be ionized at physiological pH. This docking has not been considered due to the high hydrophobicity of access channels characterized in the model protein (Boachon *et al.*, 2019). In its neutral form, after the docking results, oryzalin exhibited a good binding affinity, with prevalent oxidation on the two terminal carbons of the alkyl chain. Compared to other molecules, oryzalin was the only one to be bound through an ionic and electrostatic interaction of the opposite moiety (which bears the sulfonamide

group) with hydrophilic Asn 122 and Asp128 residues located at the top of the active site cavity, that can explain its improved affinity compared to the majority of other dinitroanilines (**Supplemental Figure 8**).

Based on docking experiments we would thus expect an efficient metabolism of oryzalin by CYP706A3. In an attempt to understand the absence of oryzalin conversion observed experimentally, we compared the relative water solubilities, LogPs, and dissociation constants (*pKa*) of the set of dinitroanilines investigated. As shown in **Table 3**, the water solubility of oryzalin is significantly higher than those of the other dinitroanilines investigated. Its *pKa* is 9.8 instead of the negative range for the metabolized compounds. Its topological polar surface area is 163 Å² versus 104 Å² for pendimethalin. Interestingly, a comparison of the properties of CYP706A3 and CYP76 enzymes (**Table 3**) shows that they form very distinct classes of compounds.

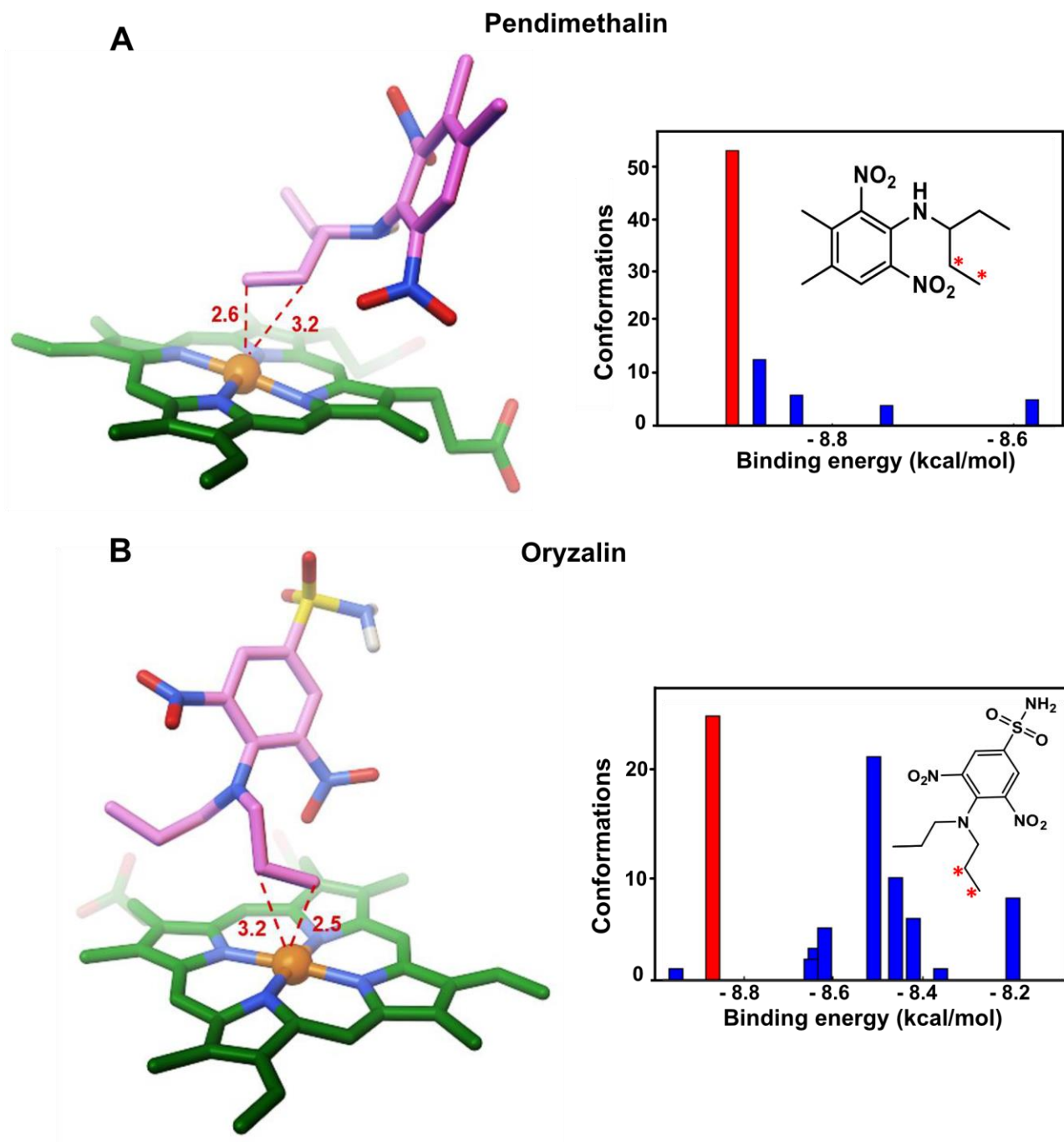


Figure 10. Binding mode of dinitroanilines pendimethalin and oryzalin in *CYP706A3* active site.

Docking experiments were performed with Autodock 4.2.6 on the rebuilt 3D model of *CYP706A3*. Each run contains 100 poses computed. The histograms of the docking scores (in kcal/mol) have been generated with RMSD tolerance of 2 Å (pendimethalin) and 2.5 Å (oryzalin) for clustering. The distribution of poses revealed predominant clusters at lowest energy, indicating the most probable binding positions. Heme cofactor is represented in green sticks with iron atom sphere in orange, and ligands are represented in sticks in atom color mode. Distances of the substrate carbon atoms to the heme iron are indicated in Angstroms. The cluster bar corresponding to the docking pose is

highlighted in red. In each predominant cluster the distances between CH₂/CH₃ groups and Fe can vary but keep equivalent proportions

A. Predominant docking pose of pendimethalin, with binding energy of $-8.75 \text{ kcal.mol}^{-1}$.

B. Predominant docking pose of oryzalin with binding energy of $-8.52 \text{ kcal.mol}^{-1}$.

Table 3. Physical properties of dinitroaniline herbicides and natural substrates of CYP706A3 and CYP76 enzymes.

Herbicide	Water solubility (mg/L)	LogP	pKa	References
Substrates of CYP706A3				
Pendimethalin	0.3	5.2	-2.24	Pubchem Chemicalbook
Trifluralin	0.2	5.34	-1.45	Pubchem Chemicalbook
Ethalfuralin	0.3	5.11	-1.76	Pubchem Chemicalbook
Oryzalin	2.5	3.73	9.4	Pubchem Chemicalbook
Benefin	1	5.29	-0.59	Pubchem Chemicalbook
Fluchloralin	0.9	4.63	-1.91	Pubchem Chemicalbook
Thujopsene	Insoluble	4.56	NA	Chemeo
Barbatene	Insoluble	4.56	NA	Chemeo
Substrates of CYP76 enzymes				
Linalool	1590	2.97	14.5	Pubchem Chemicalbook
Geraniol	100	3.56	14.4	Pubchem Chemicalbook
Chlorotoluron	70	2.41	14.43	Pubchem Chemicalbook
Linuron	75	3.20	12.13	Pubchem Chemicalbook
Isoproturon	60	2.87	15.06	Pubchem Chemicalbook

Dinitroaniline conversion capacity is present in other sesquiterpene metabolizing P450 enzymes

Structural data suggest that dinitroaniline oxidation by CYP706A3 might be associated with the size and hydrophobicity of its active site, and possibly also with the size and hydrophobicity of its access channels (Boachon *et al.*, 2019). Such properties are expected to be shared with other members of the CYP706 family and/or other sesquiterpenoid metabolizing P450 enzymes. To test this hypothesis, we assayed the capacity of other P450 enzymes, belonging to the CYP706 and CYP71 families, isolated from different plant species and previously reported to oxidize sesquiterpenoids (CYP706M1 from Alaska cedar, Cankar *et al.*, 2014 ; CYP71D51 from *A. thaliana*, Gavira *et al.*, 2013) or other small volatile compounds (CYP706C55 catalyzing phenylacetaldoxime dehydration in *Eucalyptus cladocalyx*; Hansen *et al.*, 2018) to convert dinitroanilines. They were expressed in yeast, and dinitroaniline conversion was evaluated in the incubation medium using the whole yeast assay, primarily based on the decrease in active compound by comparison with yeast transformed with an empty vector. As show in **Figure 11**, all the tested enzymes, but more notably the two members of the CYP706 family from cedar and eucalyptus, were able to metabolize dinitroanilines, although with higher selectivity with regard to the different members of the class of herbicides than CYP706A3. The reaction was then upscaled to compare the reaction products via HPLC-DAD and LC-MS (**Supplemental Figure 6 and 9**). This experiment confirmed divergent substrate and regiospecificities of the four enzymes, also revealing that they formed different oxidation products. CYP706M1 from Alaska cedar was the most active for trifluralin conversion, while CYP706AC55 from eucalyptus was the most active on benefin. The latter was the only one with weak activity on oryzalin.

The capacity to metabolize dintroanilines thus seems a common feature conserved in different members of the CYP706 family (including subfamilies from distant taxa such Rosidae and Gymnospems).

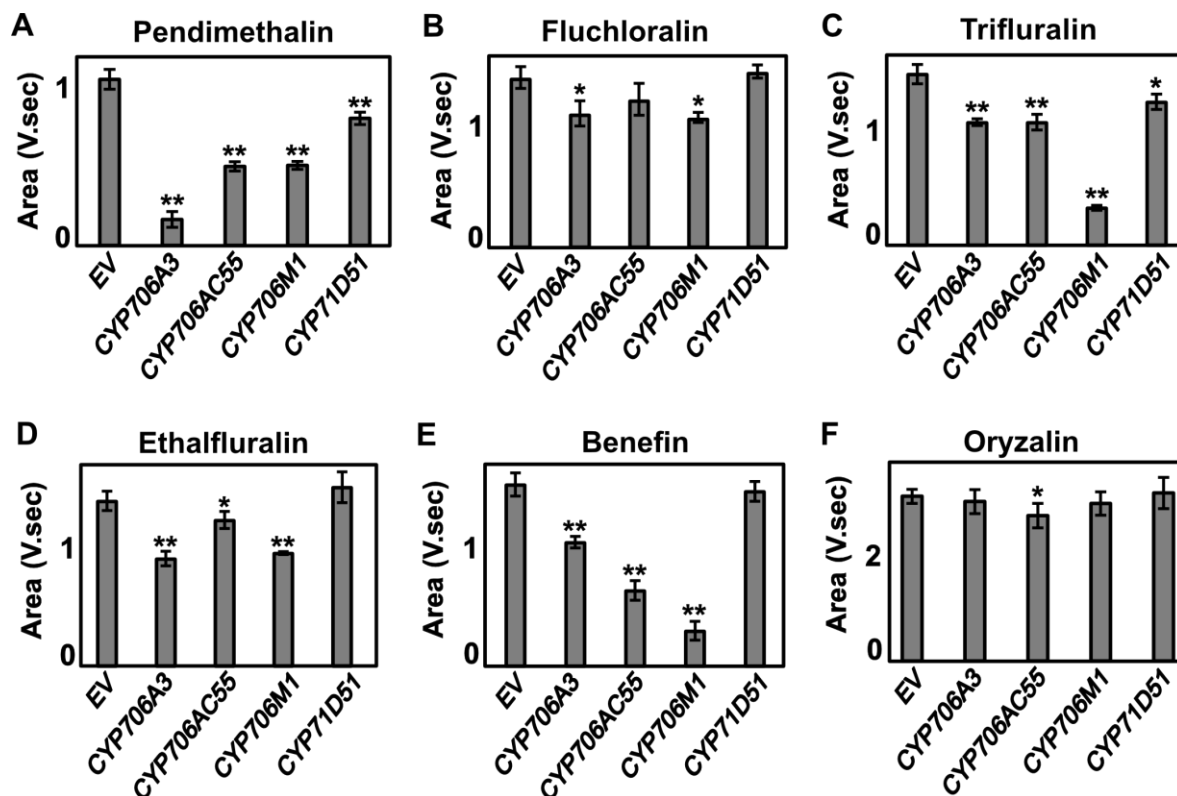


Figure 11. Dinitroaniline conversion by other sesquiterpene-metabolizing enzymes.

Five ml cultures of empty vector- or P450-transformed yeasts were incubated in 20 ml tubes with 200 μ M of herbicide for 24 hours at 20°C with shaking at 180 rpm. Culture supernatant was collected after centrifugation at 4,500 rpm for 15 min and directly injected for high performance chromatography with diode array detection. Residual herbicide was evaluated from the herbicide peak area. Data shown are means \pm SD of three replicates. Statistically significant differences between empty vector control and P450-transformed yeasts are indicated by stars (Student's t-test: * $p < 0.05$; ** $p < 0.01$).

Discussion

Evolution of P450-mediated herbicide resistance in weeds is still poorly understood. It is well established that resistance most often results from the selection pressure exerted by repeated herbicide treatments, but the molecular mechanisms leading to this resistance are rarely and only superficially documented. The mechanisms proposed include nucleotide mutation/polymorphism within P450 genes, gene duplication or changes in gene regulation (resulting from increased expression or modification of expression pattern). It is still unclear if herbicide metabolism is principally associated with specific families/classes of P450 enzymes showing unusual promiscuity, with P450 gene

families present in high copy in the plant genomes, or with accumulation of weak resistance alleles in the same plant. Another pending question is whether the metabolism of specific herbicide chemistries can be related to the metabolism of particular endogenous compounds because of structural similarities.

In this study, our aim was to test the hypothesis that the propensity of P450 enzymes to convert herbicides might be related to their intrinsic promiscuity with regard to natural compounds. Only a limited number of plant P450 enzymes have been investigated for their capacity to metabolize a significant set of substrate analogs or innate plant metabolites. We thus set out to screen for metabolism of herbicides with different chemistries, focusing on six of them, among the best documented concerning their substrate specificity or promiscuity. This approach reveals the capacity of P450 enzymes to convert and detoxify the active compounds belonging to the class of dinitroanilines.

Dinitroanilines are pre-emergence, soil-incorporated microtubule assembly inhibitors used to control annual grass and certain dicot weeds in several major crops, especially wheat, soybean and cotton. Dinitroaniline-resistant populations have been reported in weeds as diverse as *Alopecurus myosuroides* (James *et al.*, 1995), *Lolium rigidum* (McAlister *et al.*, 1995; Broster *et al.*, 2013; Owens *et al.*, 2014; Chen *et al.*, 2018a,b, 2019, 2020), *Eleusine indica* (Mudge *et al.*, 1994), *Setaria viridis* (Morrison *et al.*, 1994), *Amaranthus palmeri* (Gossett *et al.*, 1992), *Poa annua* (Lowe *et al.*, 2001) and *Alopecurus aequalis* (Hashim *et al.*, 2012). In many cases, this resistance was shown to result from mutations in the gene encoding the target-site, α -tubulin (Hashim *et al.*, 2012; Anthony *et al.*, 1998; Yamamoto *et al.*, 1998; Délye *et al.*, 2004; Chen *et al.*, 2018, 2020; Chu *et al.*, 2018; Chen *et al.*, 2020). Still, more recent investigations on Australian trifluralin resistant populations of *L. rigidum* point to metabolism as the most frequent cause of the resistance in this weed (Chen *et al.*, 2018b), a synergy between trifluralin and the insecticide phorate in addition suggesting P450-mediated metabolism in several multi-resistant populations (Busi *et al.*, 2017). Still, no P450 enzyme was so far associated with dinitroaniline metabolism.

Here we show that CYP706A3 hydroxylates pendimethalin when expressed in yeast and in *N. benthamiana*, forming two products resolved by both LC and TLC. Their MS and NMR structure characterizations concur to indicate an attack on the penultimate position

of the side-chain for both of them, and thus suggest that they are diastereoisomers (**Figures 4 and 5**). This is supported by docking experiments in the 3D model of the enzyme indicating that the most favorable pose of pendimethalin can lead to attack of the penultimate carbons of both branches of the side chain (**Figure 10**). We show in addition that CYP706A3 also metabolizes the other herbicides belonging to the chemical class of dinitroanilines (apart from oryzalin), including ethalfluralin, benefin, fluchloralin, trifluralin, and in most cases generating several products (**Figure 7**). Moreover, we demonstrate that the CYP706A3-dependent metabolism of dinitroanilines results in herbicide detoxification, as indicated by the increase in herbicide tolerance observed in *Arabidopsis* seedlings when *CYP706A3* is expressed under the control of a *CaMV35S* promoter (**Figure 8**). The increase in herbicide resistance achieved by CYP706A3 ectopic expression ranges from 8-fold for benefin and ethalfluralin to 50-fold in the case of pendimethalin (**Figure 9**), comparable to resistances reported in weeds as a result of target-site mutation (Chen *et al.*, 2018a, 2020). This is achieved despite a rather modest catalytic efficiency for the hydroxylation of pendimethalin. Notably, the ectopic expression experiment also provides evidence that the modification and increase in native gene expression that extends the enzyme production from the flower tissues (in the wild-type) to the vegetative parts of the plant is sufficient to confer herbicide tolerance.

CYP706A3 is the most promiscuous P450 enzyme among those investigated in our screening. It was recently reported to oxidize an unusually broad set of natural sesquiterpenes and monoterpenes in *Arabidopsis* flowers to generate terpene oxides, which have a protective role against florivores (Boachon *et al.*, 2019). This innate enzyme promiscuity regarding volatile C10 and C15 terpenes olefins most likely explains the CYP706A3-mediated metabolism of dinitroanilines. It suggests that mono-/sesquiterpenes and dinitroanilines share common structural or biophysical properties, well suited for proper access to and docking in the active site of the enzyme. Molecular docking experiments of all dinitroanilines molecules revealed low energy docking positions in the CYP706A3 active site at distances allowing oxidative attack, in agreement with metabolism detected experimentally. In particular, the modelling experiments revealed that the alkyl chain is always the moiety of the molecule oriented towards the heme iron in lowest energy clusters of poses, with the subterminal position of the alkyl chain being potentially oxidized (**Figure 10; Supplemental Figure 5**). Unexpected, therefore, was the

absence of CYP706A3-mediated conversion of oryzalin, for which we obtained low energy docking poses in the active site of the enzyme (**Figure 10**). A plausible explanation for this apparent conflict is possibly provided by the physical properties of oryzalin and of the substrate access channels of CYP706A3. Modelling of the CYP706A3 3D structure has previously identified two access channels to the active site. Both were narrow and essentially lined with hydrophobic residues, hence adapted for specific access of small and hydrophobic molecules. They were, in addition, oriented to the membrane or the membrane surface (Boachon *et al.*, 2019). Trifluralin is very hydrophobic and was reported to be very volatile (Chen *et al.*, 2018), a property shared by all the CYP706A3 natural substrates. Most dinitroanilines are very hydrophobic compounds as well, with very low water solubilities and unlikely to dissociate. An exception is oryzalin, which is expected to be protonated at physiological pH (**Table 3**). It can thus be hypothesized that the hydrophilicity and charge of oryzalin prevents its access to the active site and effective processing by CYP706A3.

The structural properties of the active site and access channels of CYP706A3, including size, hydrophobicity, and their associated enzyme promiscuity, can be assumed to be shared by other CYP706s or P450 enzymes metabolizing sesquiterpenes or small hydrophobic compounds. We thus postulated that other sesquiterpene-metabolizing P450s might be able to convert dinitroanilines. This assumption seems to be correct. CYP706M1 and CYP71D51 are sesquiterpene-metabolizing enzymes previously isolated from Alaska cedar (Cankar *et al.*, 2014) and Arabidopsis (Gavira *et al.*, 2013), respectively, and CYP706C55 from eucalyptus is reported to dehydrate phenylacetaldoxime (Hansen *et al.*, 2018). We show here that all of them metabolize dinitroanilines (**Figure 11**). This suggests that a large number of P450s from very diverse plant species, especially when belonging to the CYP706 family, can potentially contribute to the evolution of dinitroaniline resistance. It is interesting to note that the P450 enzymes investigated, with distinct substrate preferences for terpene olefins, also show contrasting preferences for dinitroaniline herbicides and generate different conversion products (**Figure 11**; **Supplemental Figure 9**).

We previously showed that several members of the CYP76 family from different plant sources, having as natural function the oxidation of monoterpenols, were metabolizing the herbicides belonging to the chemical group of phenylurea (Robineau *et al.*, 1998;

Didierjean *et al.*, 2002; Höfer *et al.*, 2014). In this study, we demonstrate that P450 enzymes oxidizing mono- and sesqui-terpenes as natural substrates and belonging to the CYP706 and CYP71 families hold the potential to metabolize and detoxify dinitroanilines. In both cases, P450 families showing high taxa-specific gene duplications in plant genomes (so-called blooms) and clear promiscuity with regard to their natural substrates are involved. In both cases also, the currently emerging picture is that a compatibility between the properties of the active sites/substrate access channels and the respective chemistries of natural and herbicide substrates is required for effective metabolism. Currently available data seem to indicate that common size and physicochemical properties shared by natural and xenobiotic substrates might prevail over structural analogies to favor metabolism. At first sight, the recent characterization of CYP81As from *Echinochloa phyllopogon* as multifunctional herbicide-metabolizing enzymes might seem to contradict this picture. Some of the members of the CYP81A subfamily from *E. phyllopogon* were shown to be able to metabolize up to 18 herbicides belonging to 13 distinct chemical groups (including compounds with different sizes and chemical properties) and to confer the most remarkable metabolism-related cross-resistance reported so far (Iwakami *et al.*, 2014; Iwakami *et al.*, 2019; Guo *et al.*, 2019; Dimaano *et al.*, 2020). Nevertheless, the very large substrate scope of CYP81s from Poaceae does not include dinitroanilines, nor phenylurea and more than 50% of the herbicides investigated (Dimaano *et al.*, 2020). Moreover, CYP81As display a clear preference for the metabolism of one chemical class of herbicides, sulfonylureas (Dimaano *et al.*, 2020). It seems thus very likely that CYP81As, if doubtless unusually promiscuous, principally process a specific type of plant natural metabolites. Interestingly, like CYP76s, CYP71s and CYP706s, CYP81s belong to a cytochrome P450 family showing repeated blooms along plant evolution, indicative of a role in plant adaptation to ecological niches (Nelson and Werck-Reichhart, 2011). This raises the intriguing question of the natural substrates and ecological roles of CYP81As in Poaceae.

Altogether, our recent data start to reveal the correlations existing between herbicide metabolism and P450 ecological functions, such as plant defense against insects and control of microbial communities (Höfer *et al.*, 2014; Boachon *et al.*, 2015; Boachon *et al.*, 2019). These studies should help to anticipate negative side-effects of herbicide treatments on natural plant defense and associated fitness costs. Beyond providing a

description of enzymes potentially responsible for metabolic resistance, structural models for the educated design of synergists, and a phylogenetic/genomic background for understanding of the mechanisms of evolution of herbicide tolerance, this work, bridging herbicide metabolism with innate ecological functions, will thus permit better herbicide management.

Acknowledgments: We are grateful to Drs. J. Beekwilder and E.H.J. Neilson, respectively, for kindly providing the CYP706M1 and CYP706C55 yeast expression vectors. Fa.A. thanks University of Mohaghegh Ardabili for PhD funding and University of Strasbourg for support to international mobility.

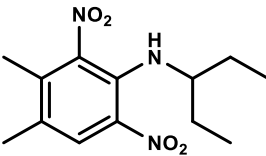
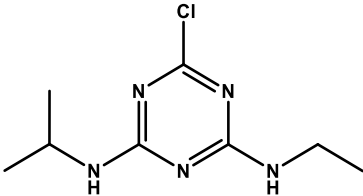
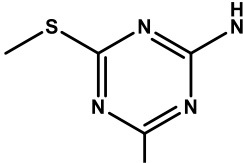
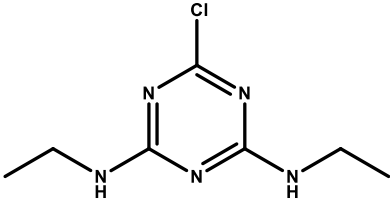
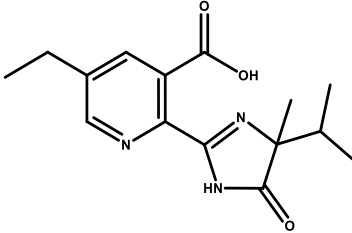
Author contribution: DW-R, NN, LM, FrA designed and supervised the research; FaA, CN, EL, CV, FrA performed experiments; FaA, CV, LM analyzed the data; MTA, provided financial support; FaA, FrA, DW-R wrote the paper.

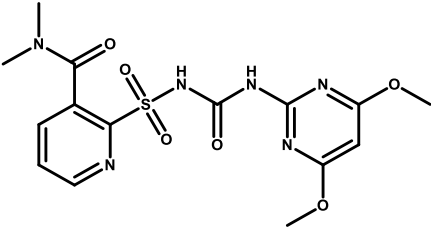
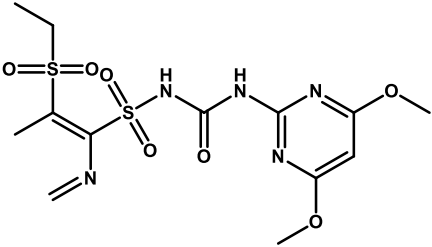
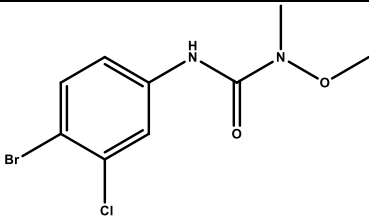
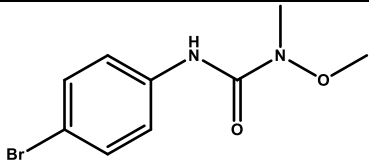
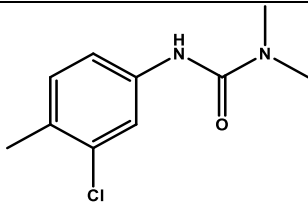
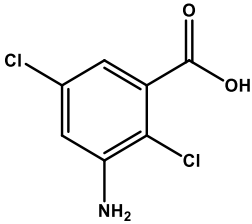
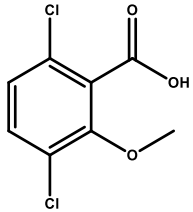
ORCID

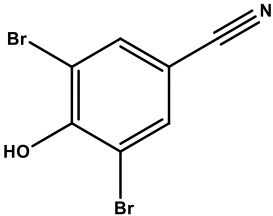
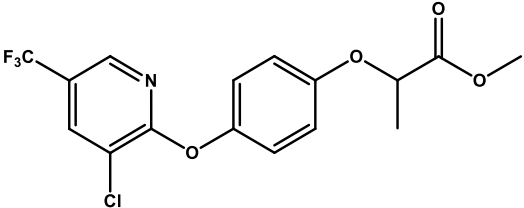
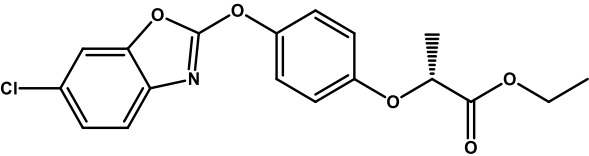
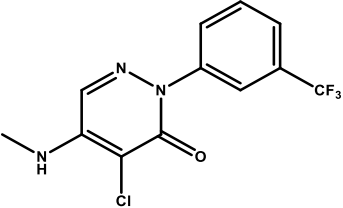
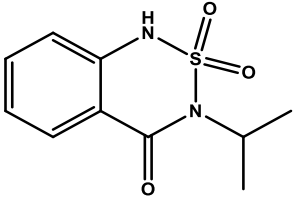
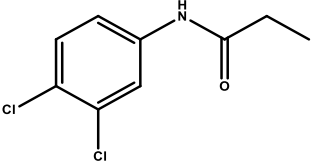
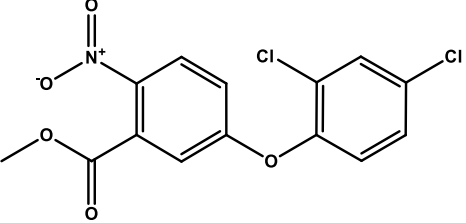
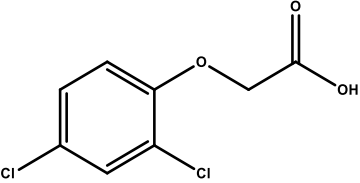
Fatemeh Abdollahi 0000-0002-6653-4289
Mohammad Taghi Alebrahim 0000-0002-6032-6470
Chheng Ngov 0000-0003-2839-1624
Etienne Lallemand 0000-0003-2013-9766
Claire Villette 0000-0003-2564-5529
Julie Zumsteg 0000-0001-8772-1182
Danièle Werck-Reichhart 0000-0003-2869-4262
François André 0000-0003-1742-2800
Nicolas Navrot 0000-0002-2141-1808
Laurence Miesch 0000-0002-0369-9908

Supplemental material

Supplemental Table 1. Herbicides tested as substrates of the plant P450 enzyme

Chemical Family	Active Ingredients	MW (g/mol)	Structure
Dinitroanilines	Pendimethalin	281.3	
Triazines	Atrazine	215.6	
	Terbutryn	241.3	
	Simazine	201.6	
Imidazolinones	Imazethapyr	289.3	

Sulfonylureas	Nicosulfuron	410.4	
	Rimsulfuron	431.4	
Phenylureas	Chlorbromuron	293.5	
	Metobromuron	259.1	
	Chlortoluron	212.7	
Benzoic acids	Chloramben	206.1	
	Dicamba	221.1	

Nitriles	Bromoxynil	276.9	
Aryloxyphenoxy propionates	Haloxypop-methyl	375.7	
	Fenoxaprop- <i>p</i> -ethyl	361.8	
Pridazinone	Norflurazon	303.6	
Benzothia diazinone	Bentazon	240.3	
Chlorinated anilide	Propanil	218.1	
Diphenyl ethers	Bifenox	342.2	
Phenoxy-carboxylic-acids	2,4-D	221.1	

Supplemental Table 2 Quantification of P450 expression in yeast.

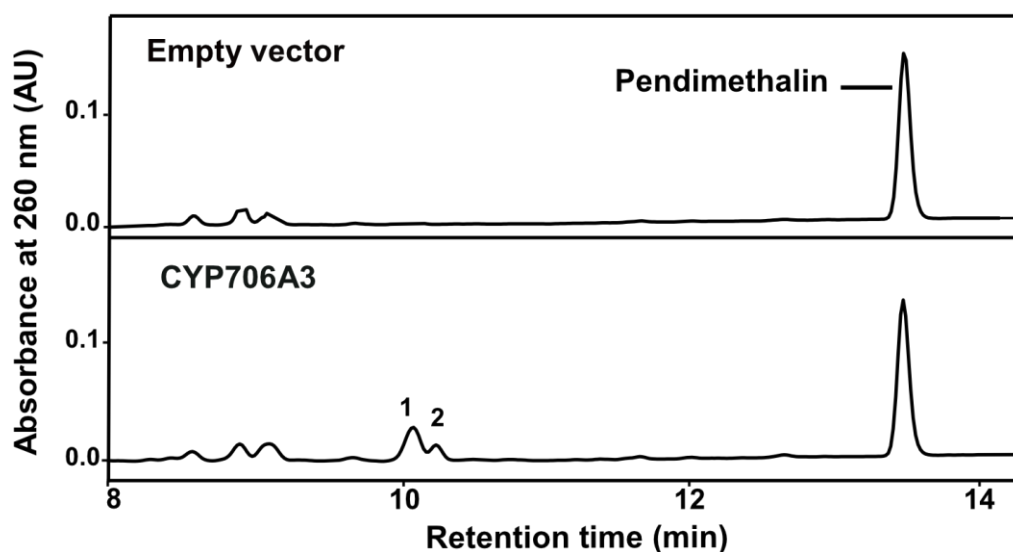
P450 was quantified in recombinant yeast microsomal fractions by differential spectrophotometry as described in the method section.

P450 enzyme	P450 concentration (μM)
CYP72A224	1.63
CYP73A92	1.32
CYP98A23	0.71
CYP98A27	0.67
CYP706A3	0.23
CYP76B1	0.72
CYP706C55	1.9
CYP706M1	0.12
CYP71D51	0.21

Supplemental Table 3. Estimated gain in herbicide tolerance of the CaMV 35S:CYP706A3 transformed Arabidopsis plant versus wild-type (WT).

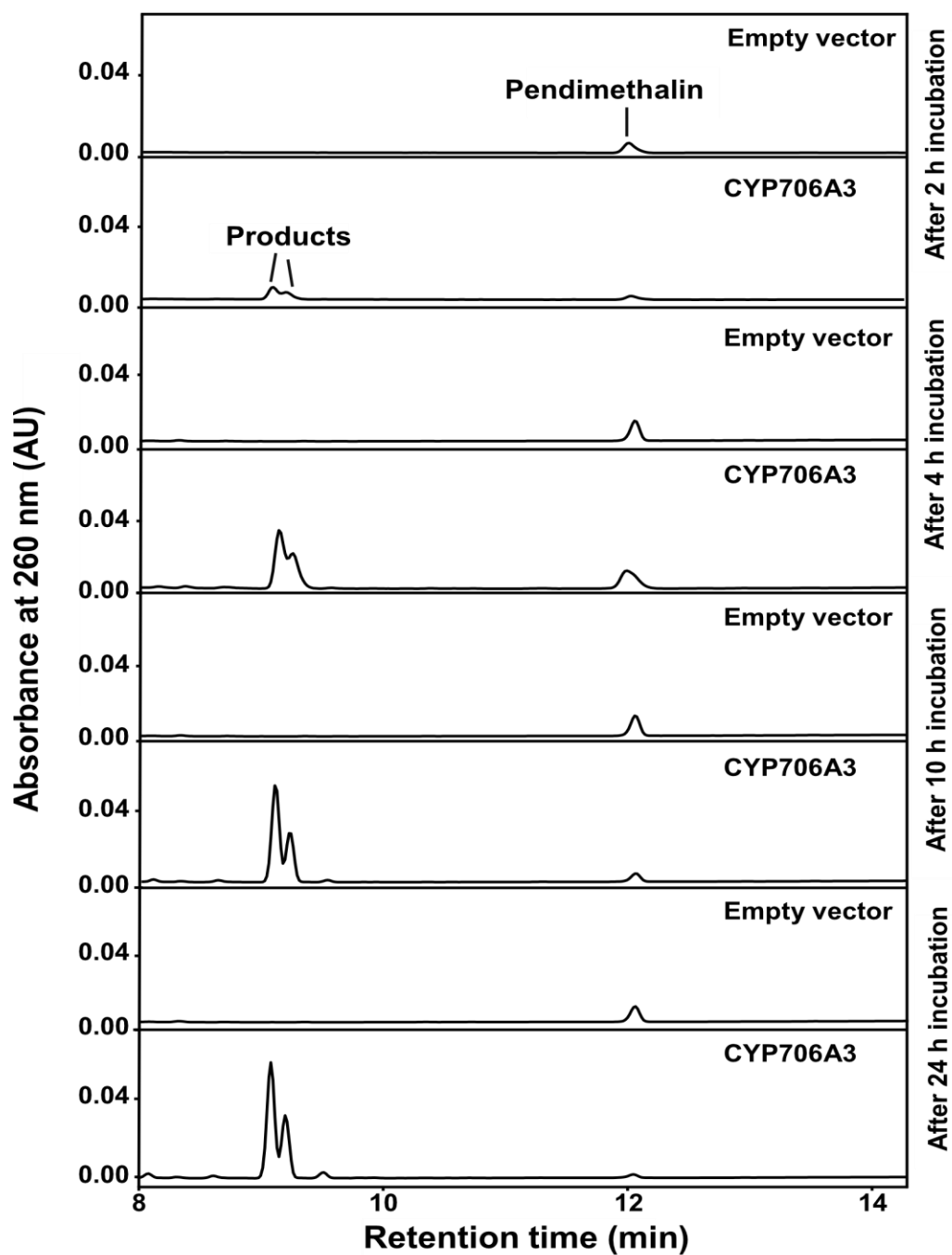
I_{50} and tolerance factors (I_{50} CYP706A3/ I_{50} WT) were calculated from data in Figure 9.

Herbicide	I_{50} (μM)		Tolerance factor
	Wild Type	CYP706A3	
Pendimethalin	0.19	10	52
Trifluralin	0.84	9.6	11
Fluchloralin	0.78	9.2	12
Ethalfuralin	1.19	9.6	8
Benefin	1.16	9	7.7



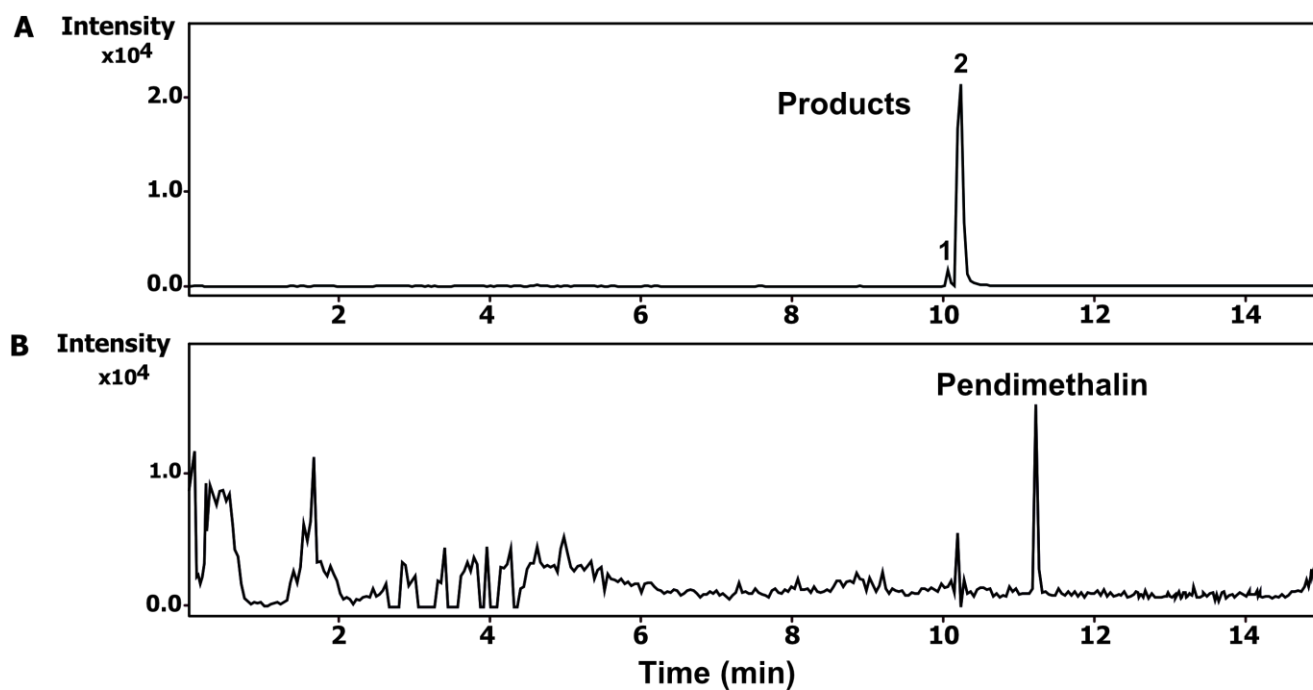
Supplemental Figure 1. *CYP706A3*-mediated pendimethalin conversion products detected in cell yeast extract.

CYP706A3- or empty vector-transformed whole yeast cultures were incubated with 200 μ M of herbicide for 24 hours at 20°C. The yeast cells were resuspended in 500 μ L methanol (99:1 v/v), and centrifuged. The supernatant was recovered and analyzed by high performance liquid chromatography (HPLC). Empty vector-transformed (upper panel). *CYP706A3*-transformed (lower panel). Peaks **1** and **2** correspond to the products.



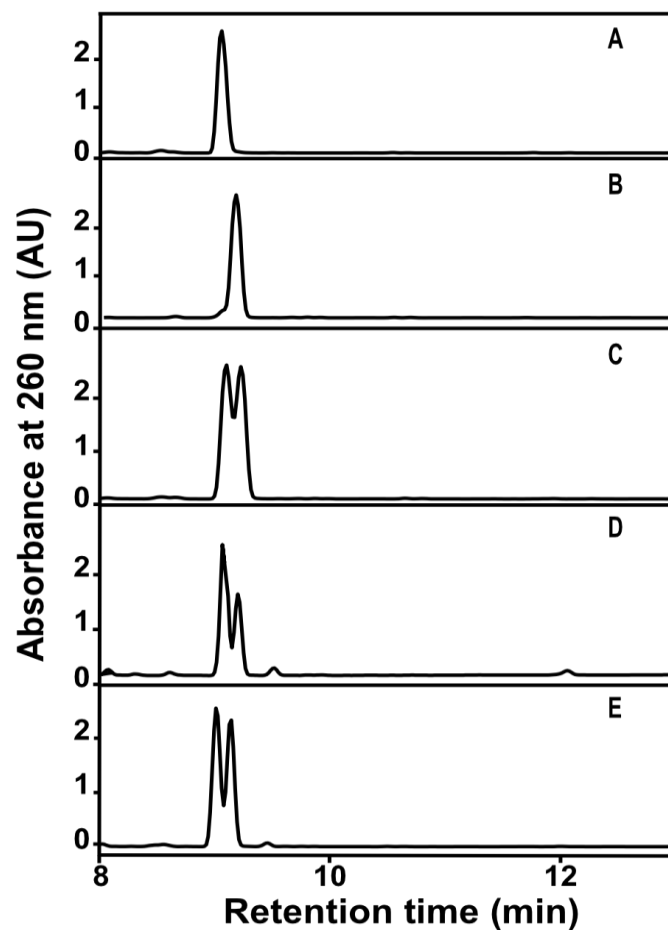
Supplemental Figure 2. Optimization of the incubation time for the production of CYP706A3 oxidation products in the whole yeast culture.

Yeasts expressing *CYP706A3* or the empty expression vector (empty-control) were incubated with 200 μ M of pendimethalin for 2 to 24 hours at room temperature. Pendimethalin conversion was evaluated by HPLC-DAD.



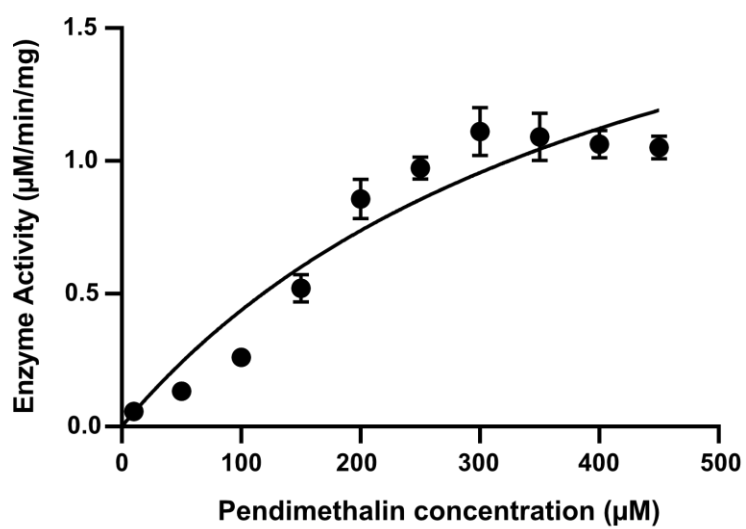
Supplemental Figure 3. LC-MS profiling of the pendimethalin conversion products of CYP706A3.

- A.** Extracted ion chromatogram of products ($C_{13}H_{19}N_3O_5$, $[M+H]^+$)
- B.** Extracted ion chromatogram of pendimethalin ($C_{13}H_{19}N_3O_4$, $[M+H]^+$)



Supplemental Figure 4. The TLC-purified products correspond to the peak 1 and 2 detected by HPLC-DAD and LC-MS.

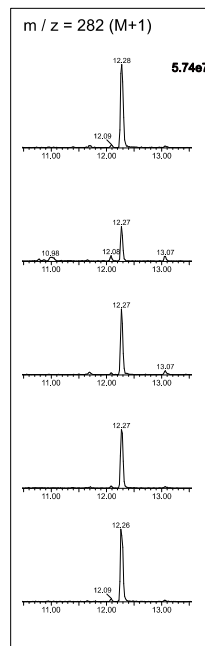
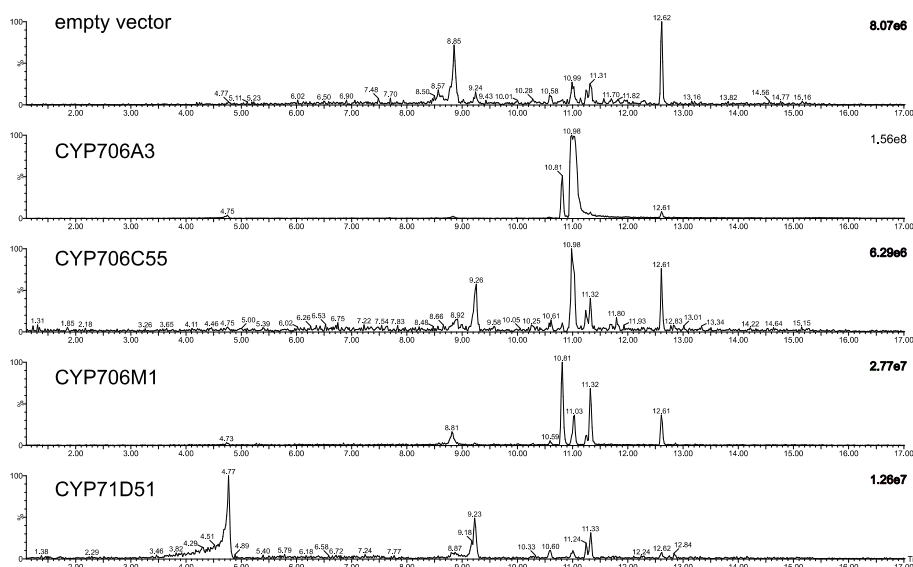
The two TLC-purified products were injected separately (**A** and **B**) and as a mix (**C**) on HPLC-DAD, and compared to the extract of a whole yeast culture (**D**). E. Mix of whole yeast culture and purified products.



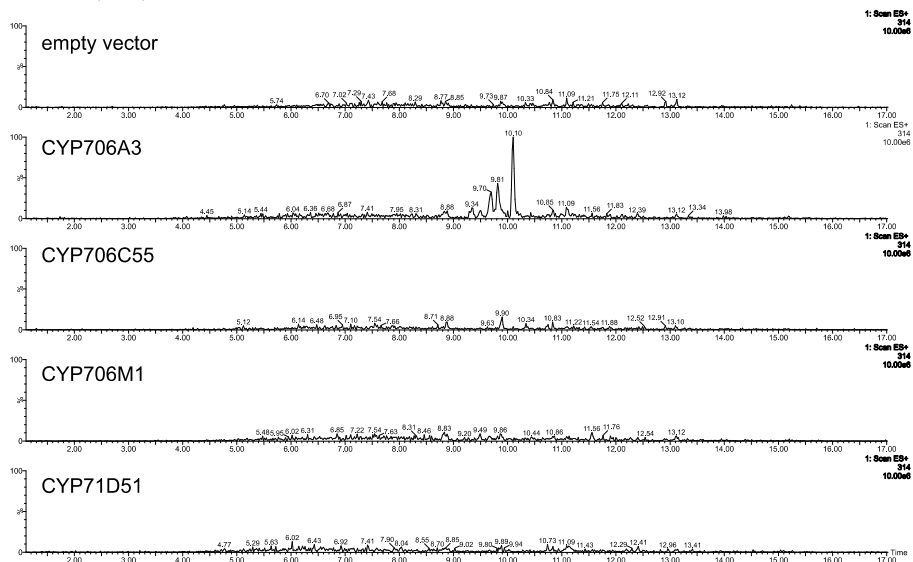
Supplemental Figure 5. Saturation curve based on Michaelis-Menten non-linear regression used to calculate affinity constant and turnover of CYP706A3 with pendimethalin.

A Pendimethalin

m / z = 298 (M+16)

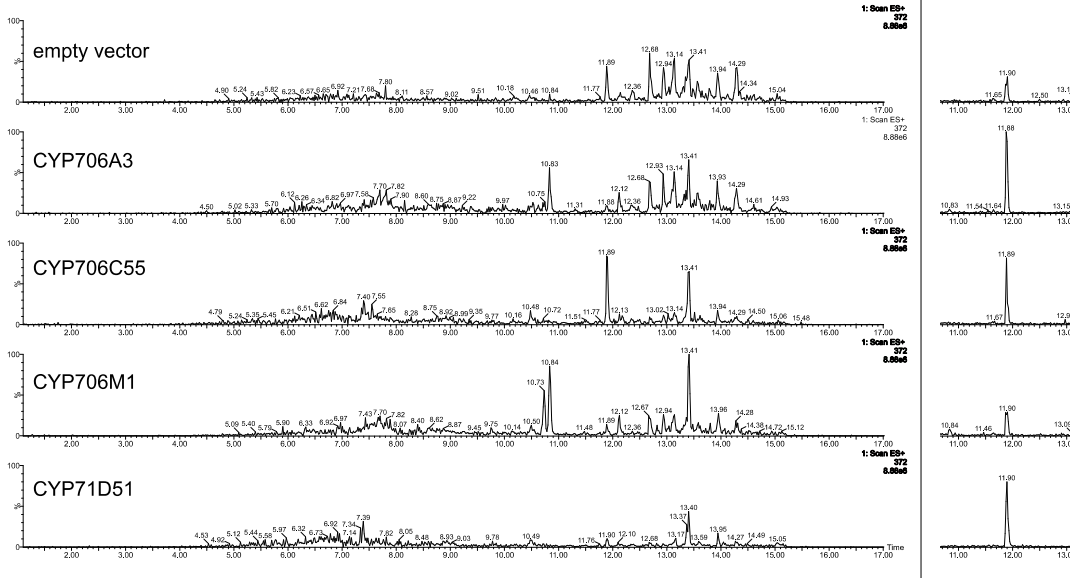


m / z = 314 (M+32)

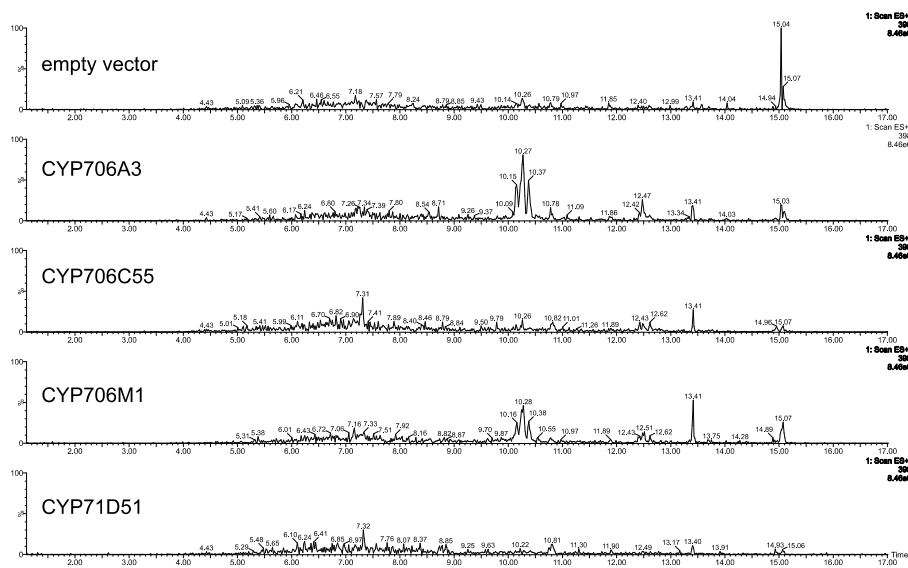


B Fluchloralin

m / z = 372 (M+16)



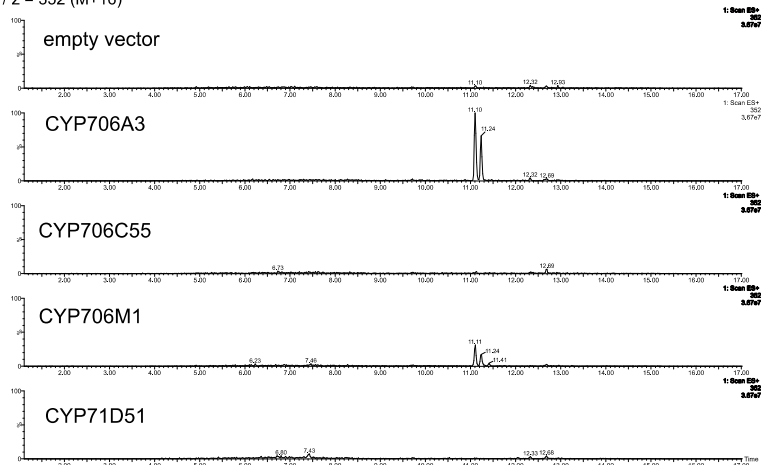
m / z = 398 (M+32)



C

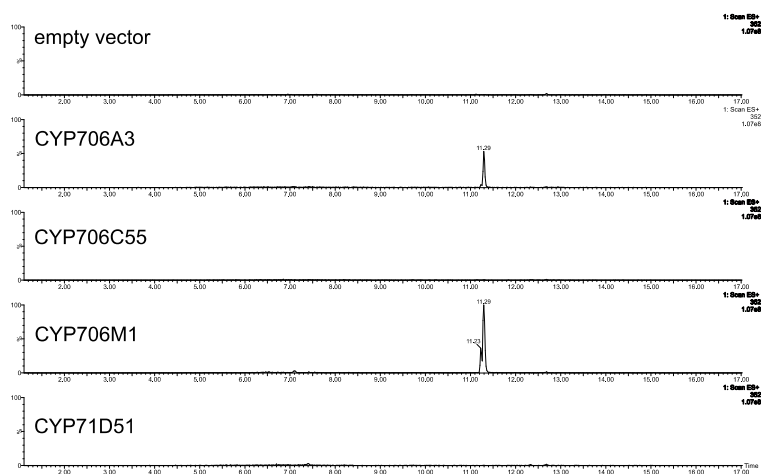
Benefin

m / z = 352 (M+16)



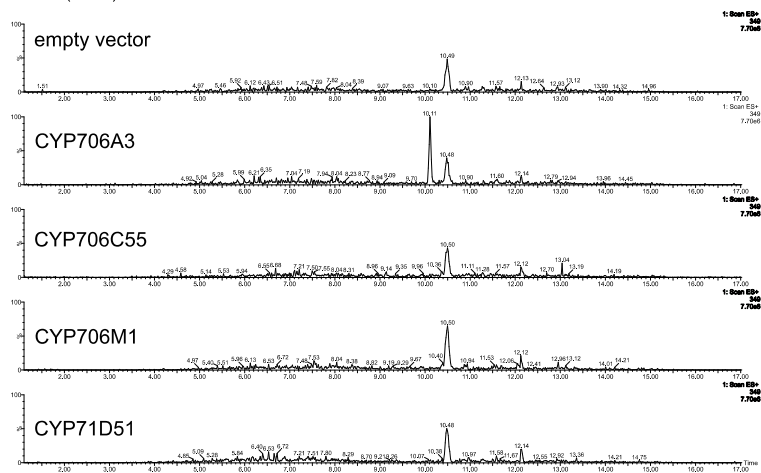
Trifluralin

m / z = 352 (M+16)



Ethalfuralin

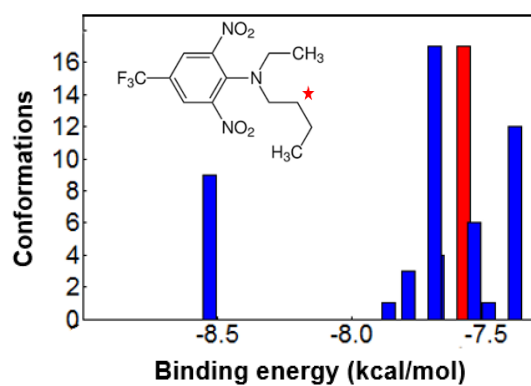
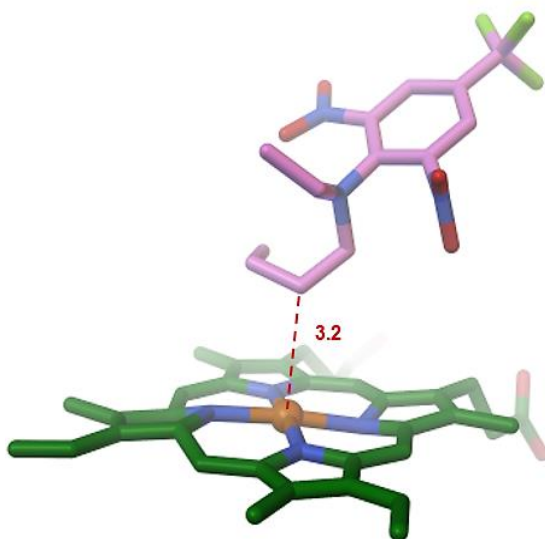
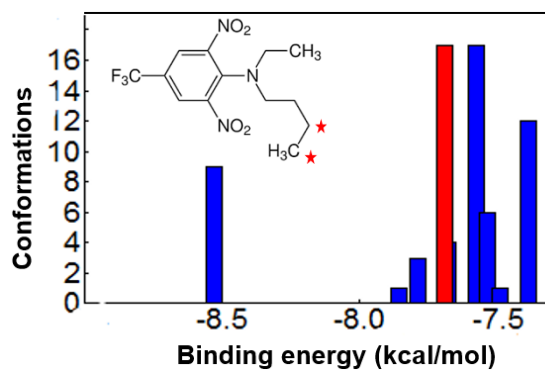
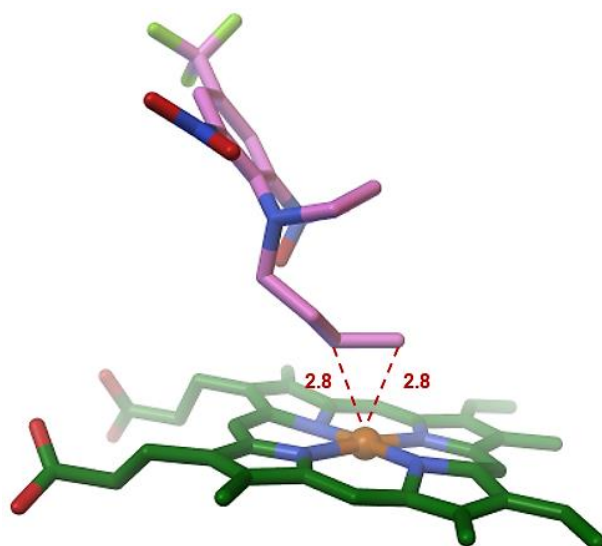
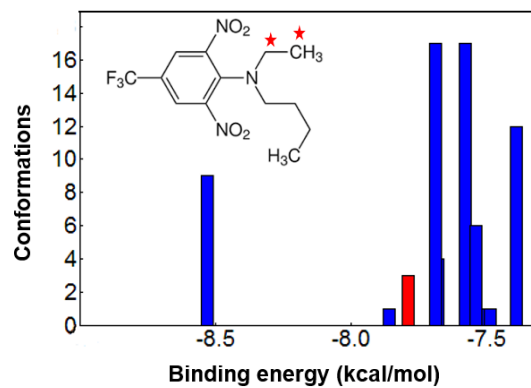
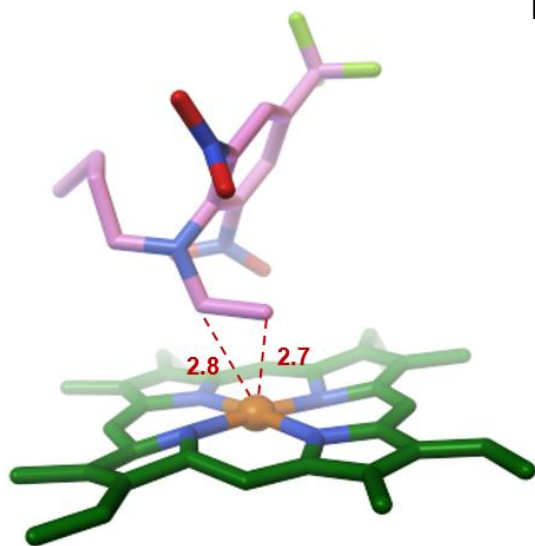
m / z = 349 (M+16)



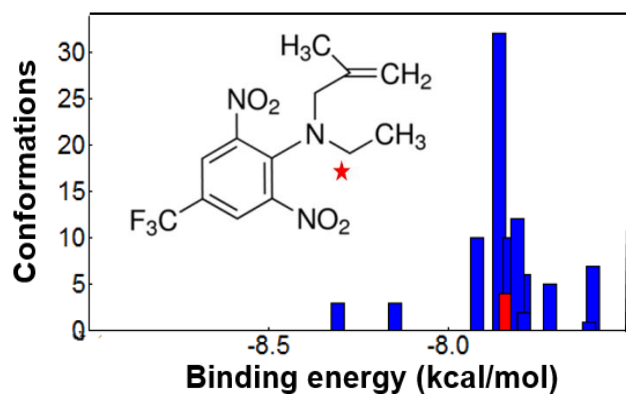
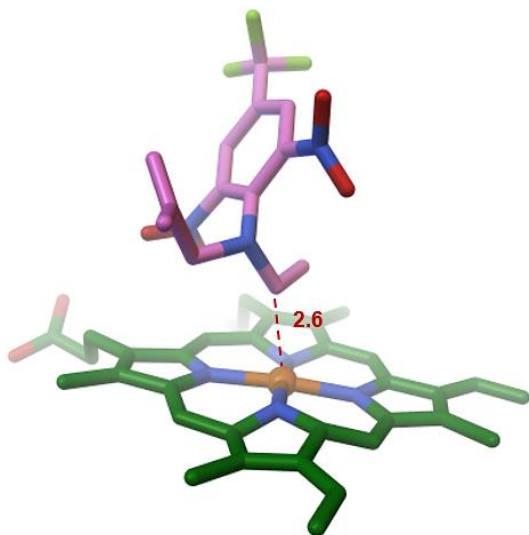
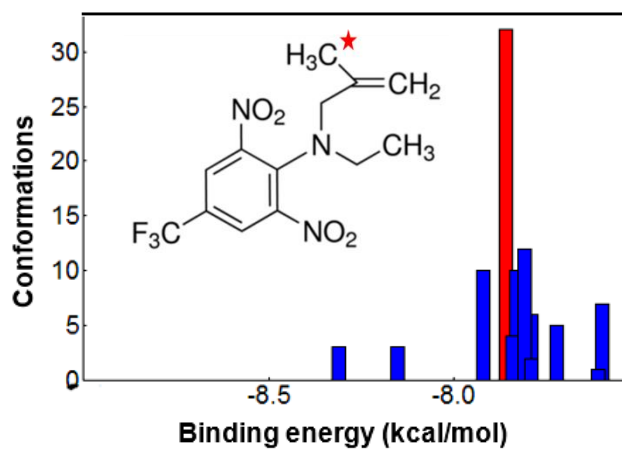
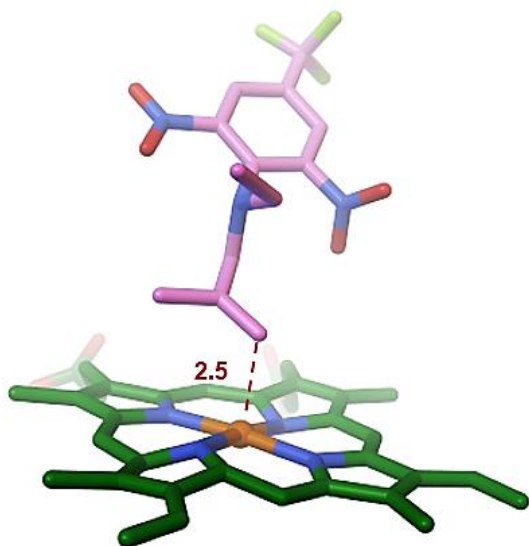
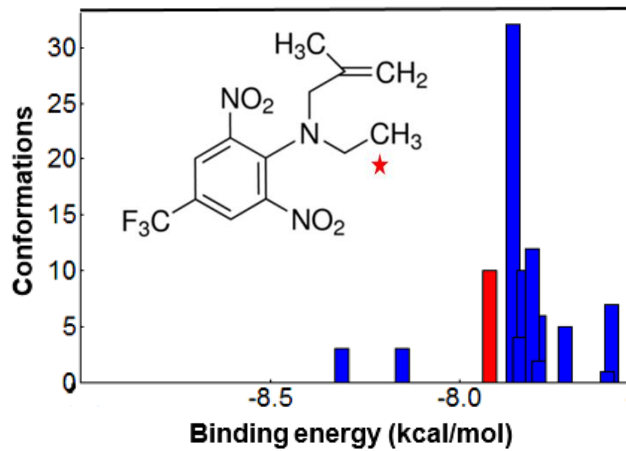
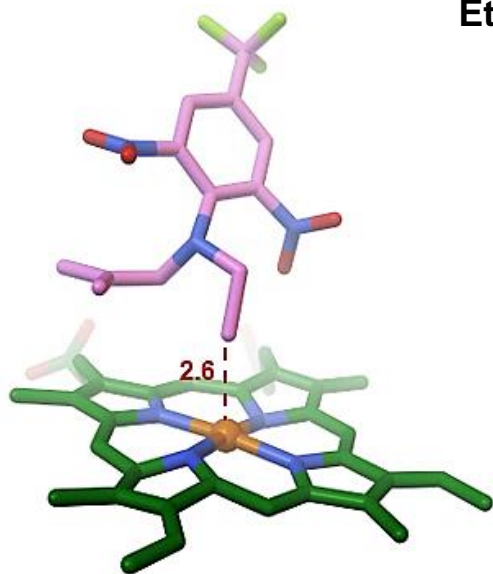
Supplemental Figure 6. Extracted ion chromatograms corresponding to m/z of dinitroaniline active ingredients (M+1) (when detectable) and oxygenated conversion products (M+16, M+32) resulting from tested P450-dependent conversion.

A. Pendimethalin (m/z=182), oxidized (m/z=298) and twice oxidized (m/z=314). **B.** Fluchloralin (m/z=356), oxidized (m/z=372) and twice oxidized (m/z=398). **C.** Benefin, trifluralin and ethalfluralin. Only single-oxidized derivatives (M+16) were detected, with m/z corresponding to 352, 352 and 349, respectively for benefin, trifluralin and ethalfluralin. Data were acquired using Acquity UPLC system (Waters) coupled to a Quattro Premier XE mass spectrometer (Waters) equipped with an electrospray ionization source and an Acquity UPLC BEH C18 (100 Å 2.1 mm, 1.7 µm; Waters) column and precolumn. The mobile phase consisted of (A) water and (B) methanol, both containing 0.1% formic acid. The run began with 2 min of 95% A. Then a linear gradient was applied to reach 100% B at 12 min, followed by an isocratic run using 100% B for 1 min. Return to initial conditions was achieved in 2 min, with a total run time of 17 min. The column was operated at 35°C with a flow rate of 0.35 ml/min, injecting 0.05 ml samples. Nitrogen was used as the drying and nebulizing gas. The nebulizer gas flow was set to 50 l/h and the desolvation gas flow to 900 l/h. The interface temperature was set at 400°C and the source temperature at 135°C. The capillary voltage was set to 3.4 kV and the cone voltage to 25 V; the ionization was in positive mode. For qualitative analysis and mass spectra determination, samples were analyzed with full scan in positive mode, with an energy cone of +25 V on a range of 100 to 600 m/z and with a 0.4-s scan time. Data acquisition and analyses were performed with MassLynx and QuanLynx software version 4.1 (Waters).

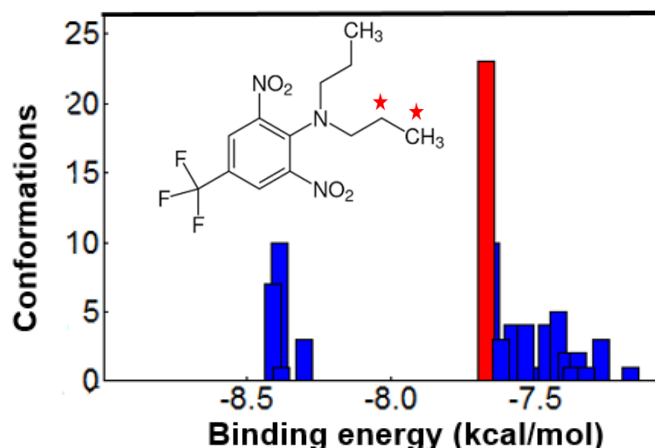
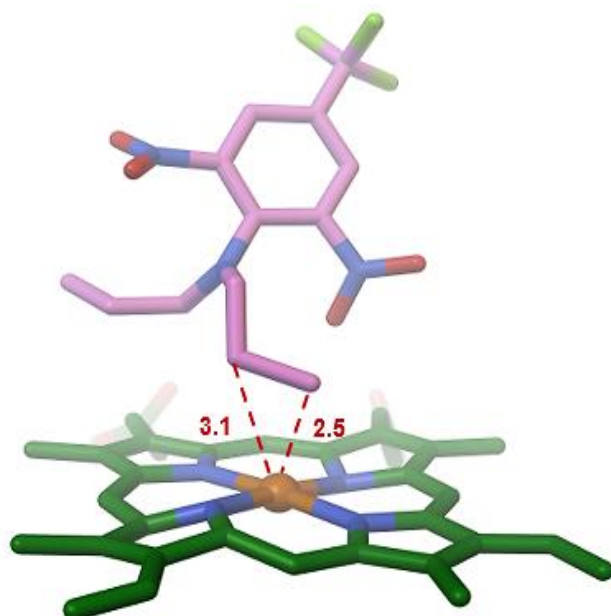
Benefin



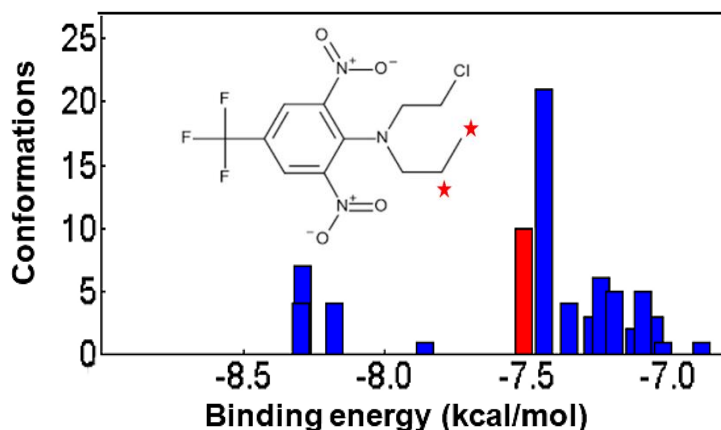
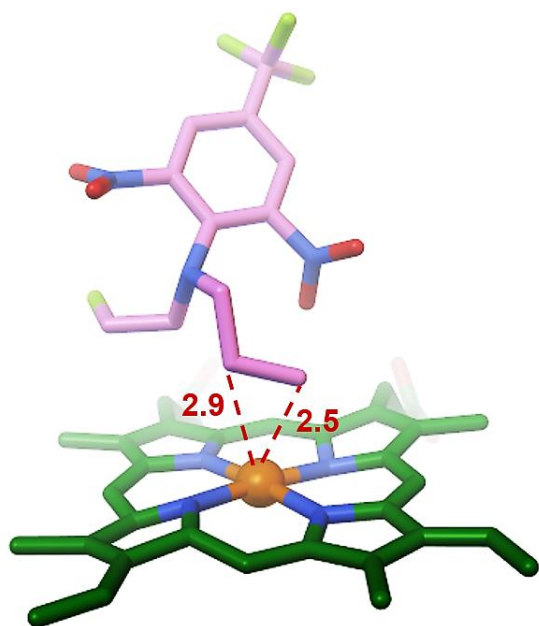
Ethalfuralin



Trifluralin



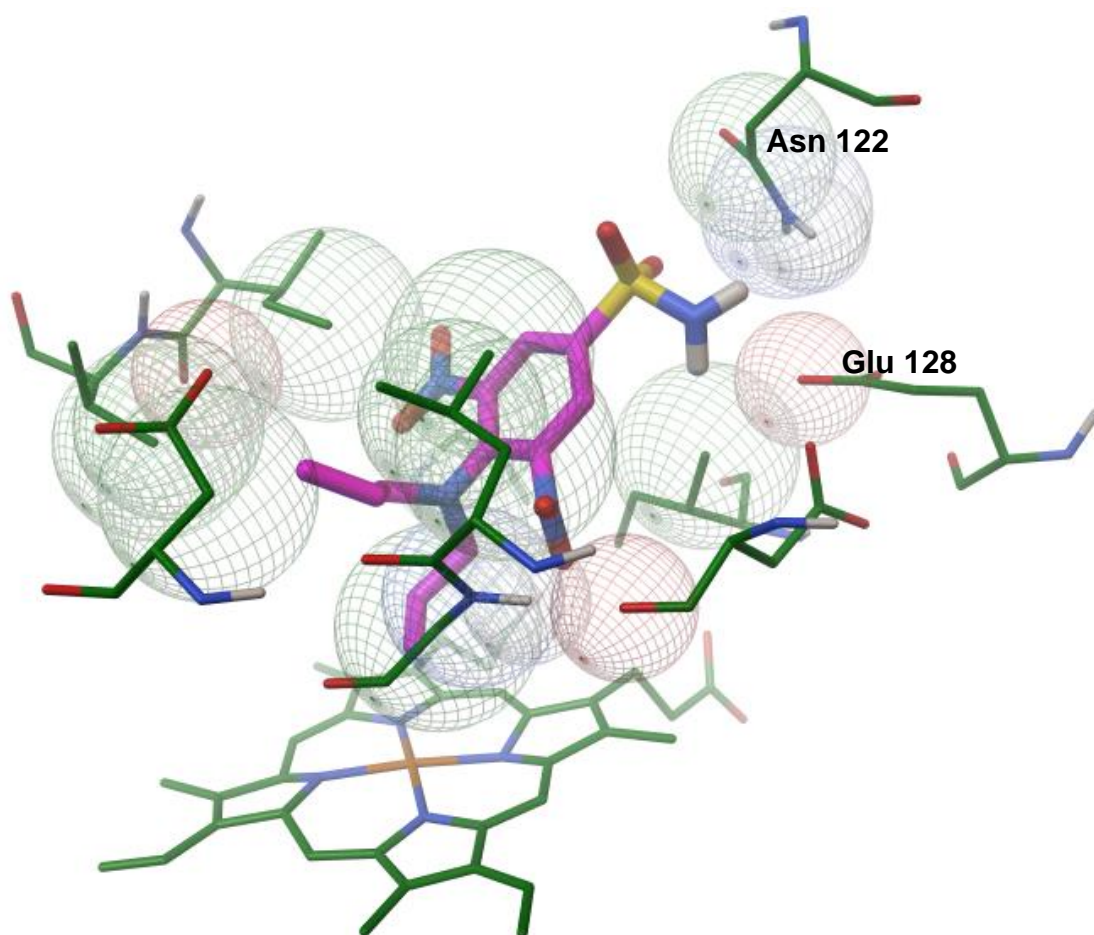
Fluchloralin



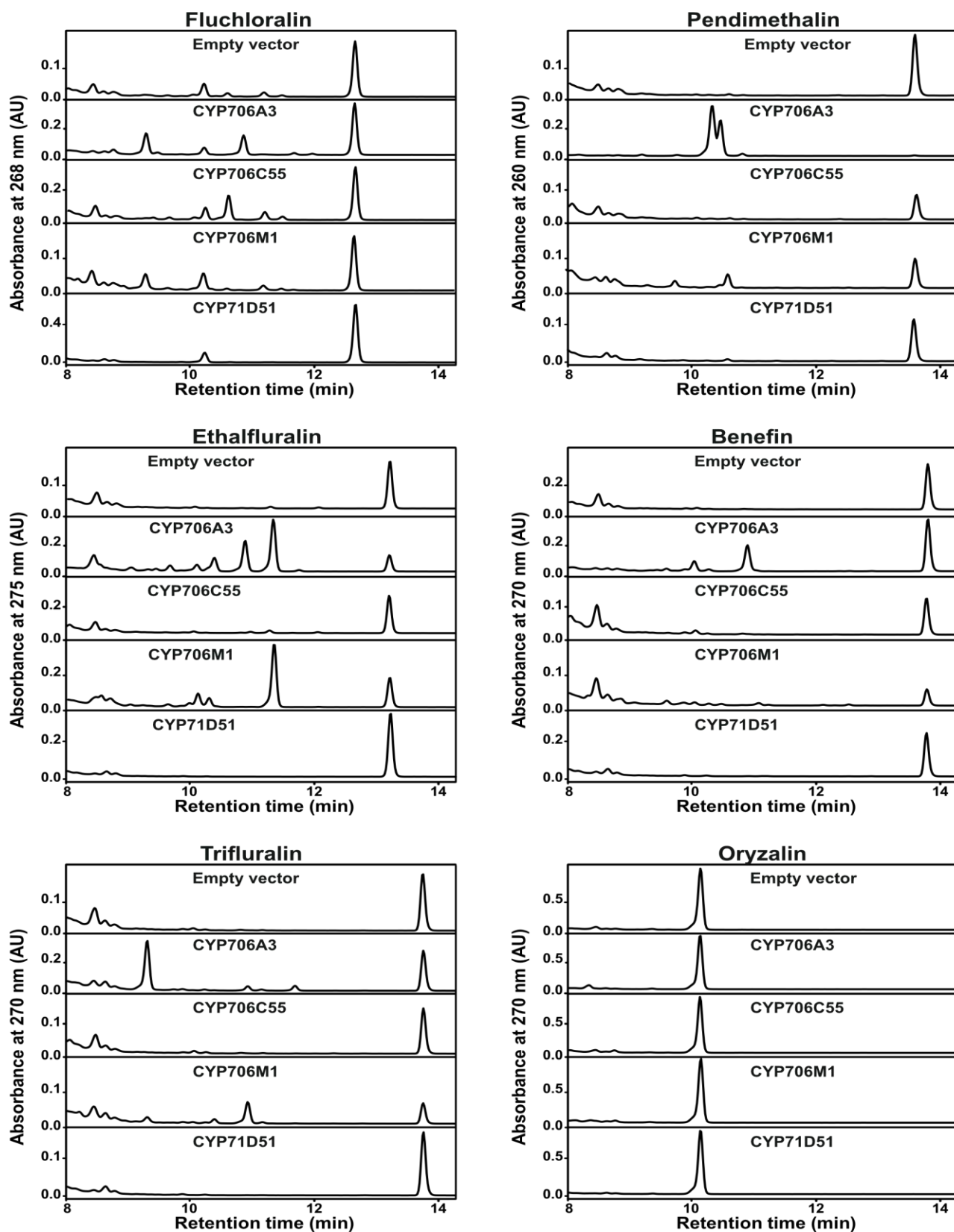
Supplemental Figure 7. Binding mode of other dinitroanilines in CYP706A3 active site.

Docking experiments were performed with Autodock 4.2.6 on the rebuilt 3D model of CYP706A3. Computational details can be found in Figure 10 legend. All histograms of the docking scores (in kcal/mol) were generated with RMSD tolerance of 2 Å for clustering. In all cases the distribution of poses revealed lowest energy clusters corresponding to NO₂ group (or Cl for Fluchloralin) closest to the iron atom. The lowest energy clusters corresponding to hydrocarbon oxidation site are displayed (left panel), and the cluster bar corresponding to the docking pose is highlighted in red in the histograms (right panel). When binding scores were very similar and not discriminating, several poses are displayed

(Benefin and Ethalfluralin), that can be considered as equiprobable binding positions leading to different metabolites. Distances of the substrate carbon atoms to the heme iron are indicated in Angstroms. All other representation details are as in legend of Figure 10. The binding energies of all displayed docking poses are summarized in appendix table 2.



Supplemental Figure 8. View of the best affinity score pose of Oryzalin in model AtCYP706A3 active site showing the H-bonding interactions between sulfonamide group and Asn 122 and Glu 128 residues on the top of the active site.

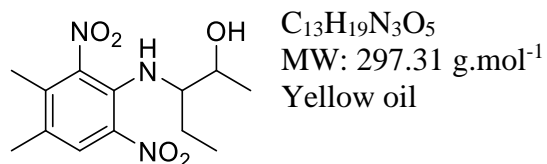


Supplemental Figure 9. Dinitroaniline conversion by other sesquiterpene-metabolizing enzymes.

Fifty mL cultures of empty vector- or P450-transformed yeasts were incubated in 100 mL Erlenmeyer flasks with 200 μ M of herbicide for 24 hours at 20°C and with shaking at 180 rpm. Culture supernatants were collected after centrifugation at 4,500 rpm for 10 min and were extracted and concentrated using SPE cartridges, injected on HPLC-DAD. Note that better culture aeration of the culture as compared to Figure 11 improves P450-mediated herbicide conversion.

Supplemental information : NMR determination

3-((3,4-dimethyl-2,6-dinitrophenyl)amino)pentan-2-ol



Diastereoisomer 1:

¹H NMR (CDCl₃, 500 MHz): δ = 8.07 (s, 1H), 7.89 (d, J = 10.7 Hz, 1H), 3.88 (qd, J = 6.3, 3.4 Hz, 1H), 3.05 (dtd, J = 10.1, 6.6, 3.4 Hz, 1H), 2.27 (s, 3H), 2.17 (s, 3H), 1.64 (dp, J = 14.4, 7.3 Hz, 1H), 1.56 (s, 1H), 1.52 – 1.45 (m, 1H), 1.20 (d, J = 6.4 Hz, 3H), 0.90 (t, J = 7.4 Hz, 3H) ppm.

¹³C NMR (CDCl₃, 125 MHz): δ = 142.6, 138.1, 137.1, 134.6, 128.4, 125.8, 68.5, 61.4, 26.0, 20.5, 19.4, 15.4, 10.3 ppm.

Diastereoisomer 2:

¹H NMR (CDCl₃, 500 MHz): δ = 8.06 (s, 1H), 7.59 (d, J = 10.8 Hz, 1H), 3.89 – 3.82 (m, 1H), 3.24 – 3.17 (m, 1H), 2.27 (s, 3H), 2.18 (s, 3H), 1.63 – 1.56 (m, 1H), 1.56 (s, 1H), 1.51 – 1.42 (m, 1H), 1.14 (d, J = 6.6 Hz, 3H), 0.98 – 0.92 (t, J = 7.4 Hz, 3H) ppm.

¹³C NMR (CDCl₃, 125 MHz): δ = 143.0, 138.1, 137.1, 135.0, 128.3, 126.3, 69.6, 61.6, 23.9, 19.4, 18.1, 15.4, 10.7 ppm.

Chapter 4

General Discussion and Conclusion

This study was pursued in order to understand the role of cytochrome P450 enzymes in the emergence of herbicide resistance, and to elucidate the molecular mechanisms endowing P450-mediated resistance to herbicides. A main question addressed was if promiscuous enzymes were providing a favorable background for the evolution of herbicide resistance. I only investigated a small sample of plant P450 enzymes, since only few of them have been previously tested with a range of different natural substrates to determine their innate promiscuity. However my data suggest that the proposed hypothesis was correct, since the most promiscuous of the P450s investigated, CYP706A3, revealed a novel capacity to metabolize dinitroanilines. Previous work had indicated that trifluralin tolerance of some resistant *L. rigidum* populations was likely to result from enhanced P450-mediated metabolism (Chen et al., 2018), but this is the first demonstration of the involvement of plant P450 enzymes in the metabolism of dinitroanilines. I tested six of the most commonly used dinitroanilines as substrates, and most of them (i.e. pendimethalin, ethalfluralin, benefin, trifluralin and fluchloralin), with the exception of oryzalin, were metabolized by CYP706A3. The metabolites of pendimethalin were characterized by LC/MS and NMR, and my results indicated that the hydroxylation of pendimethalin occurred at the subterminal position of the side chain, forming two diastereoisomers. The products resulting from the metabolism of the other dinitroanilines are currently under investigation via LC-MS. In most cases, several metabolites seem to be formed, but their full structural NMR characterization will not be possible, since they are generated in too low amounts.

Interestingly, the docking experiments of pendimethalin in a 3D model of CYP706A3 well match my experimental data and identify two low binding energy poses for pendimethalin that could favor an attack on each branch of the side chain. In the same way, several low energy docking poses can be obtained for most of the other dinitroanilines, which are all predicted to be oxidized on terminal and/or subterminal carbons of their side-chains.

Another point addressed by the homology modelling experiments was to determine the reason for the absence of oryzalin metabolism. We expected the hydrophilic sulfonamide side chain of oryzalin to prevent its docking in the active site of CYP706A3.

Very surprisingly though, my docking experiments show that this is not the case, and identify a low energy docking pose for oryzalin. The oryzalin recalcitrance to CYP706A3-mediated metabolism thus seems to result from the impossibility to pass through the very hydrophobic access channels of the enzyme, directed to the membrane or to membrane surface, while the compound is more water soluble and expected to be essentially protonated at physiological pH. This is an interesting new concept, and suggests that oryzalin might be active on weed populations resistant to most other dinitroanilines, such as Australian trifluralin-resistant *Lolium rigidum* populations.

CYP706A3 is exclusively expressed in the flower buds and open flowers in wild-type Arabidopsis plants. The availability in the lab of an Arabidopsis line ectopically overexpressing CYP706A3 allowed me to determine if extending CYP706A3 expression to vegetative tissues conferred an increase in dinitroaniline tolerance. My data demonstrate that this is definitely the case, since they show a 52-fold increase in tolerance for pendimethalin of the 35S:CYP706A3 line, and a 8 to 11-fold increase of tolerance for the other dinitroanilines, roughly reflecting the efficiencies of conversion of the different dinitroanilines by CYP706A3. As expected, CYP706A3 overexpression does not confer any increase in oryzalin tolerance. The efficiency of pendimethalin conversion is quite low, with a K_m 436 μ M and k_{cat} of 2.34 min^{-1} , and the efficiency of the conversion of the other dinitroanilines seems even lower. My data thus indicate that quite moderate herbicide conversion efficiency is sufficient to confer herbicide resistance.

No ortholog of CYP706A3 is present in most weeds or crop plant. I have thus tested the capacity of other plant P450s to metabolize dinitroanilines. Those include other members of the CYP706 family in phylogenetically distant plants such as cedar or eucalyptus, and an Arabidopsis sesquiterpene-metabolizing P450 of the CYP71 family available in the laboratory. More P450s were included in the first screening (Appendix Table 4.1), including paralogs of CYP706A3 and some representative of the CYP81 family from Arabidopsis (since CYP81As were identified as highly promiscuous multi-herbicide metabolizing enzymes in two weed species). This first screening could not validate recombinant P450 expression, nor repeatable herbicide conversion for the latter set. It was thus discarded in final experiments. The tests performed with well-expressed P450s however clearly demonstrated that CYP706M1 from Alaska cedar, CYP706C55 from

Eucalyptus cladocalyx and CYP71D51 from *A. thaliana* all have the capacity to oxidize dinitroanilines, to different extents, with different substrate preferences, and forming different products. However, none of them significantly metabolized oryzalin. CYP706A3, CYP706M1, CYP706C55 and CYP71D51 were all shown to metabolize mono- and/or sesquiterpenes or another small hydrophobic compound, phenylacetaldoxime. All this leads to two conclusions. The first is that a large number of P450 enzymes involved in the metabolism of small hydrophobic compounds such as small terpenes, in particular when belonging to the widespread CYP706 family, are likely to contribute to the evolution of resistance to dinitroanilines. The second is that oryzalin should be less prone to evolution of metabolism-based resistance than the other dinitroanilines.

This work provides a second example of P450s with physiological functions that can be associated with the metabolism of a specific class of herbicides. The first example was the members of the CYP76 subfamilies using monoterpenols that were shown capable of metabolizing phenylurea (Didierjean et al., 2002; Höfer et al., 2014; Boachon et al., 2015; Boachon et al., 2019). A more systematic investigation is thus required to obtain a general picture of the plant P450 catalytic functions and innate promiscuities, covering both physiological and agrochemical substrates. It would help to predict the evolution of herbicide resistance, to design strategies to fight emerging resistances, but also to understand the physiological impact of herbicide/pesticide treatments on plant (including crop) development, defense and adaptation. It would also help to understand the evolution of novel functions in P450 families, based on the intrinsic properties of their active sites and access channels.

CYP706-mediated dinitroaniline metabolism has been here confirmed with three enzymes representative of diverse plant lineages, but so far only from dicots and gymnosperms, and no major crops or resistant weeds. The demonstration that the CYP706 family can contribute to dinitroaniline metabolism in grass crops and resistant weed populations is still required. The characterization of the P450s involved in this resistance and in the dinitroaniline metabolism in crops, will permit to generate structural models for the educated design of inhibitors. Selective inhibitors that would lead to appropriate P450 inactivation, could then be used as dinitroaniline synergists on resistant weed populations. They may also help to reduce doses of herbicides used in the field in

order to circumvent or delay the emergence of herbicide resistance. As demonstrated by the recalcitrance of oryzalin to P450-mediated metabolism, the main interest of structural models (or crystal structures) of the dinitroaniline-metabolizing might however reside in the possibility to design new herbicides with no access to the relevant P450 active sites or modified side chains improper to oxidative attack. Overall, this knowledge is expected to support the management of herbicide resistance in the future.

References

- Alber AV, Renault H, Basilio-Lopes A, Bassard J, Liu Z, Ullmann P, Lesot A, Bihel F, Schmitt M, Werck-Reichhart D, Ehlting J. 2019.** Evolution of coumaroyl conjugate 3-hydroxylases in land plants: lignin biosynthesis and defense. *Plant J.* **99**: 924-936.
- Alder EF, Wright WL, Soper QF. 1960.** Control of seedling grasses in turf with diphenylacetone nitrile and a substituted dinitroaniline. *Proc. North. Cent. Weed Control Conf.* **17**: 23–24.
- Alebrahim MT, Zangoueinejad R, Tseng TM. 2017.** Herbicide Resistance in Weeds and Crops. *Intech Open*. London, UK.
- Anthony RG, Waldin TR, Ray JA, Bright SW and Hussey PJ. 1998.** Herbicide resistance caused by spontaneous mutation of the cytoskeletal protein tubulin. *Nature* **393**: 260–263.
- Bak S, Beisson F, Bishop G, Hamberger B, Höfer R, Paquette S, Werck-Reichhart D. 2011.** Cytochromes p450. *Arabidopsis Book*. **9**: e0144.
- Batard Y, LeRet M, Schalk M, Zimmerlin A, Durst F, Werck-Reichhart D. 1998.** Molecular cloning and functional expression in yeast of CYP76B1, a xenobiotic-inducible 7-ethoxycoumarin O-deethylase from *Helianthus tuberosus*. *Plant J.* **14**:111–120.
- Bibi Z. 2008.** Role of cytochrome P450 in drug interactions. *Nutr Metab.* **5**: 27-37.
- Boachon B, Burdloff Y, Ruan J, Rojo R, Junker R, Vincent B, Nicolè F, Bringel F, Lesot A, Henry L, Bassard JE, Mathieu S, Allouche F, Kaplan I, Dudareva N, Vuilleumier S, Miesch L, André F, Navrot N, Chen XY, Werck-Reichhart D. 2019.** A promiscuous CYP706A3 reduces terpene volatile emission from Arabidopsis flowers, affecting florivores and the floral microbiome. *Plant Cell.* **12**: 2947-2972.
- Boachon B, Junker RR, Miesch L, Bassard JE, Höfer R, Caillieaudeaux R, Seidel DE, Lesot A, Heinrich C, Ginglinger JF, Allouche L, Vincent B, Wahyuni DS, Paetz C, Beran F, Miesch M, Schneider B, Leiss K, Werck-Reichhart D.**

- 2015.** CYP76C1 (cytochrome P450)-mediated linalool metabolism and the formation of volatile and soluble linalool oxides in *Arabidopsis* flowers: a strategy for defense against floral antagonists. *Plant Cell*. **27**: 2972–2990.
- Brazier-Hicks M, Gershater M, Dixon D, Edwards R. 2018.** Substrate specificity and safener inducibility of the plant UDP-glucose-dependent family 1 glycosyltransferase super-family. *J. Plant Biotechnol.* **16**: 337–348.
- Brazier-Hicks M, Howell A, Cohn J, Hawkes T, Hall G, Mcindoe E, Edwards R. 2020.** Chemically induced herbicide tolerance in rice by the safener metcamifen is associated with a phased stress response, *J. Experimental Botany*. **71**: 411–421.
- Broster JC, Koetz EA, Wu H. 2013.** Herbicide resistance levels in annual ryegrass (*Lolium rigidum* Gaud.) and wild oat (*Avena* spp.) in southwestern New South Wales. *Plant Protect. Sci.* **28**: 126-142.
- Burnet MWM, Loveys BR, Holtum JA M, Powles SB. 1993.** A mechanism of chlorotoluron resistance in *Lolium rigidum*. *Planta*. **190**: 182–189.
- Busi R, Gaines TA, Powles S. 2017.** Phorate can reverse P450 metabolism-based herbicide resistance in *Lolium rigidum*. *Pest Manag. Sci.* **73**: 410–417.
- Busi R, Neve P, Powles S. 2013.** Evolved polygenic herbicide resistance in *Lolium rigidum* by low-dose herbicide selection within standing genetic variation. *Evol Appl.* **6**: 231–242.
- Cankar K, van Houwelingen A, Goedbloed M, Renirie R, de Jong R M, Bouwmeester H, Bosch B, Sonke T, Beekwilder J. 2014.** Valencene oxidase CYP706M1 from Alaska cedar (*Callitropsis nootkatensis*). *FEBS Lett.* **588**: 1001–1007.
- Chen J^b, Yu Q, Owen M, Han H, Powles SB. 2018.** Dinitroaniline herbicide resistance in a multiple-resistant *Lolium rigidum* population. *Pest Manag. Sci.* **74**: 925-932.
- Chen J, Chu Z, Han H, Goggin DE, Yu Q, Sayer C, Powles SB. 2020.** A Val-202-Phe α -tubulin mutation and enhanced metabolism confer dinitroaniline resistance in a single *Lolium rigidum* population. *Pest Manag. Sci.* **76**: 645-652.

- Chen J, Lu H, Han H, Yu Q, Sayer C, Powles S. 2019.** Genetic inheritance of dinitroaniline resistance in an annual ryegrass population. *Plant Sci.* **283**:189-194.
- Chen J^a, Goggin D, Han H, Busi R, Yu Q, Powles S. 2018.** Enhanced trifluralin metabolism can confer resistance in *Lolium rigidum*. *J. Agric. Food Chem.* **66**: 7589-7596.
- Chu Z, Chen J, Nyporko A, Han H, Yu Q, Powles S. 2018.** Novel α -tubulin mutations conferring resistance to dinitroaniline herbicides in *Lolium rigidum*. *Front. Plant Sci.* **9**: 97.
- Cobb AH, Reade RH. 2010.** Herbicides and Plant Physiology. *John Wiley and Sons. UK.*
- Collu G, Unver N, Peltenburg-Looman AMG, van der Heijden R, Verpoorte R, Memelink J. 2001.** Geraniol 10-hydroxylase, a cytochrome P450 enzyme involved in terpenoid indole alkaloid biosynthesis. *FEBS Lett.* **508**: 215–220.
- Coupland D. 1994.** Resistance to the auxin analog herbicides. In: Powles SB, Holtum JAM, eds. Herbicide resistance in plants. *Biol and biochem. Boca Raton, FL, USA: Lewis Publishers.* 171–214.
- Cummins I, Bryant D N, Edwards R. 2009.** Safener responsiveness and multiple herbicide resistance in the weed black-grass (*Alopecurus myosuroides*). *J. Plant Biotechnol.* **7**: 807–820.
- Cummins I, Wortley DJ, Sabbadin F, He Z, Coxon CR, Straker HE, Sellars JD, Knight K, Edwards L, Hughes D, Kaundun SS, Hutchings SJ, Steel PG, Edwards R. 2013.** Key role for a glutathione transferase in multiple-herbicide resistance in grass weeds. *Proc. Natl. Acad. Sci. USA.* **110**: 5812-5817.
- DeBoer GJ, Thornburgh S, Gilbert J, Gast RE. 2011.** The impact of uptake, translocation and metabolism on the differential selectivity between blackgrass and wheat for the herbicide pyroxsulam. *Pest Manag. Sci.* **67**: 279–286.
- Délye C, Jasieniuk M, Le Corre V. 2013.** Deciphering the evolution of herbicide resistance in weeds. *Trends Genet.* **29**: 649-658.

- Délye C, Menchari Y, Michel S, Darmency H. 2004.** Molecular bases for sensitivity to tubulin-binding herbicides in green foxtail. *Plant Physiol.* **136**: 3920–3932.
- Dempsey E, Prudêncio M, Fennell B, Gomes-Santos C, Barlow J, Bell A. 2013.** Antimitotic herbicides bind to an unidentified site on malarial parasite tubulin and block development of liver-stage Plasmodium parasites. *Mol. Biochem. Parasitol.* **188**: 116-127.
- Devine MD, Eberlein CV. 1997.** Physiological, biochemical and molecular aspects of herbicide resistance based on altered target sites. In: *Roe RM, Burton JD, Kuhr RJ, editors. Herbicide Activity: Toxicology, Biochemistry and Molecular Biology.* Amsterdam: IOS Press. 159-185.
- Didierjean L, Gondet L, Perkins R, Lau SC, Schaller H, O’Keefe DP, Werck-Reichhart D. 2002.** Engineering herbicide metabolism in tobacco and Arabidopsis with CYP76B1, a cytochrome P450 enzyme from *Jerusalem artichoke*. *Plant Physiol.* **130**:179–189.
- Dimaano NG, Yamaguchi T, Fukunishi K, Tominaga T, Iwakami S. 2020.** Functional characterization of cytochrome P450 CYP81A subfamily to disclose the pattern of cross-resistance in *Echinochloa phyllopogon*. *Plant Mol. Biol.* **102**: 403-416.
- Du H, Ran F, Dong HL, Wen J, Li JN, Liang Z. 2016.** Genome-Wide Analysis, Classification, Evolution, and Expression Analysis of the Cytochrome P450 93 Family in Land Plants. *PLoS One.* 11: e0165020.
- Duhoux A, Carrere S, Gouzy J, Bonin L, Delye C. 2015.** RNA-Seq analysis of rye-grass transcriptomic response to an herbicide inhibiting acetolactate-synthase identifies transcripts linked to non-target-site-based resistance. *Plant Mol. Biol.* **87**: 473–487.
- Duhoux A, Pernin F, Desserre D, Délye C. 2017.** Herbicide safeners decrease sensitivity to herbicides inhibiting acetolactate-synthase and likely activate non-target-site-based resistance pathways in the major grass weed *Lolium sp* (rye-grass). *Front Plant Sci.* **8**: 1310-1323.

- Epp J B, Schmitzer P R, Crouse G D. 2017.** Fifty years of herbicide research: Comparing the discovery of trifluralin and halauxifen-methyl. *Pest Manag. Sci.* **74**: 9-16.
- Feng YJ, Gao Y, Zhang Y, Dong LY, Li J. 2016.** Mechanisms of resistance to pyroxsulam and ACCase inhibitors in Japanese foxtail (*Alopecurus japonicus*). *Weed Sci.* **64**: 695–704.
- Fuhrmann J, Rurainski A, Lenhof HP, Neumann D. 2010.** A new Lamarckian genetic algorithm for flexible ligand-receptor docking. *Comput. Chem.* **31**: 1911–1918.
- Gaines TA, Lorentz L, Figge A, Herrmann J, Maiwald F, Ott MC, Han H, Busi R, Yu Q, Powles SB, Beffa R. 2014.** RNA-Seq transcriptome analysis to identify genes involved in metabolism-based diclofop resistance in *Lolium rigidum*. *Plant J.* **78**: 865–876.
- Gavira C, Höfer R, Lesot A, Lambert F, Zucca J, Werck-Reichhart D. 2013.** Challenges and pitfalls of P450-dependent (+)-valencene bioconversion by *Saccharomyces cerevisiae*. *Metab. Eng.* **18**: 25-35.
- Ginglinger JF, Boachon B, Höfer R, Paetz C, Köllner TG, Miesch L, Lugan R, Baltenweck R, Mutterer J, Ullmann P, Beran F, Claudel P, Verstappen F, Fischer MJ, Karst F, Bouwmeester H, Miesch M, Schneider B, Gershenzon J, Ehlting J, Werck-Reichhart D. 2013.** Gene coexpression analysis reveals complex metabolism of the monoterpene alcohol linalool in *Arabidopsis* flowers. *Plant Cell.* **25**: 4640–4657.
- Goodrich LV, Butts-Wilmsmeyer CJ, Bollero GB, Riechers DE. 2018.** Sequential pyroxsulfone applications with fluxofenim reduce sorghum injury and increase weed control. *J. Agron.* **110**: 1915–1924.
- Gossett BJ, Murdock EC, Toler JE. 1992.** Resistance of Palmer amaranth (*Amaranthus palmeri*) to the dinitroaniline herbicides. *Weed Technol.* **6**: 587–591.
- Gray HB, Winkler J R. 2010.** Electron flow through metalloproteins. *BbaBioenergetics* **1797**: 1563-1572.

- Grover R, Wolt JD, Cessna AJ, Schiefer HB. 1997.** Environmental fate of trifluralin. *Rev. Envir Conta. Toxicol.* **153**: 1-64.
- Groves J. 2015.** Cytochrome P450 enzymes: Understanding the biochemical hieroglyphs. *F1000.Rese.* **4** :178.
- Guo F, Iwakami S, Yamaguchi T, Uchino A, Sunohara Y, Matsumoto H. 2019.** Role of CYP81A cytochrome P450s in clomazone metabolism in *Echinochloa phyllopogon*. *Plant Sci.* **283**: 321-328.
- Han H, Yu Q, Cawthray GR, Powles SB. 2013.** Enhanced herbicide metabolism induced by 2,4-D in herbicide susceptible *Lolium rigidum* provides protection against diclofop-methyl. *Pest Manag. Sci.* **69**: 996–1000.
- Hannemann F, Bichet A, Ewen KM, Bernhardt R. 2007.** Cytochrome P450 systems - biological variations of electron transport chains. *Bba-Gen Subjects.* **1770**: 330-344.
- Hansen C, Sørensen M, Veiga T, Zibrandtsen J, Heskes A, Olsen C, Boughton B, Møller B, Neilson E. 2018.** Reconfigured cyanogenic glucoside biosynthesis in eucalyptus cladocalyx involves a cytochrome P450 CYP706C55. *Plant Physiol.* **178**: 1081–1095.
- Hashim S, Jan A, Sunohara Y, Hachinohe M, Ohdan H, Matsumoto H. 2012.** Mutation of alpha-tubulin genes in trifluralin-resistant water foxtail (*Alopecurus aequalis*). *Pest Manag. Sci.* **68**: 422–429.
- Hatzios KK, Burgos N. 2004.** Metabolism-based herbicide resistance: regulation by safeners. *Weed Sci.* **52**: 454–467.
- Heap I, Knight R. 1986.** The occurrence of herbicide cross-resistance in a population of annual ryegrass, *Lolium-rigidum*, resistant to diclofopmethyl. *Aust J Agric Res.* **37**: 149–156.
- Heap I. 2014.** Herbicide resistant weeds. In: Primentel D, Peshin R, editors. Integrated Pest Management. *Pesticide Problems.* **3**: 281-303.
- Höfer R, Boachon B, Renault H, Gavira C, Miesch L, Iglesias, J, Ginglinger JF, Allouche L, Miesch M, Grec S, Lariat R, Werck-Reichhart D. 2014.** Dual function

of the cytochrome P450 CYP76 family from *Arabidopsis thaliana* in the metabolism of monoterpenols and phenylurea herbicides. *Plant Physiol.* **166**: 1149–1161.

<http://www.weedscience.org>.

Ilc T, Halter D, Miesch L, Lauvoisard F, Kriegshauser L, Ilg A, Baltenweck R, Hugueney P, Werck-Reichhart D, Duchêne E, Navrot N. 2017. A grapevine cytochrome P450 generates the precursor of wine lactone, a key odorant in wine. *New Phytol.* **213**: 264-274.

Iwakami S, Endo M, Saika H, Okuno J, Nakamura N, Yokoyama M, Watanabe H, Toki Akira Uchino S, Inamura T. 2014. Cytochrome P450 CYP81A12 and CYP81A21 are associated with resistance to two acetolactate synthase inhibitors in *Echinochloa phyllopogon*. *Plant Physiol.* **165**: 618-629.

Iwakami S, Kamidate Y, Yamaguchi T, Ishizaka M, Endo M, Suda H, Nagai K, Sunohara Y, Toki S, Uchino A, Tominaga T, Matsumoto H. 2019. CYP81A P450s are involved in concomitant cross-resistance to acetolactate synthase and acetyl-CoA carboxylase herbicides in *Echinochloa phyllopogon*. *New Phytol.* **221**: 2112-2122.

James EH, Kemp MS, Moss SR. 1995. Phytotoxicity of trifluoromethyl- and methyl-substituted dinitroaniline herbicides on resistant and susceptible populations of black-grass (*Alopecurus myosuroides*). *Pest Manag. Sci.* **43**: 273-277.

Kleinman Z, Rubin B. 2017. Non-target-site glyphosate resistance in *Conyza bonariensis* is based on modified subcellular distribution of the herbicide. *Pest Manag. Sci.* **73**: 246–253.

Li R, Wang M, Wang Y, Schuman MC, Weinhold A, Schäfer M, Jiménez-Alemán GH, Barthel A, Baldwin IT. 2017. Flower-specific jasmonate signalling regulates constitutive floral defenses in wild tobacco. *Proc. Natl. Acad. Sci. U. S. A.* **114**: E7205–E7214.

Liu C, Liu S, Wang F, Wang Y, Liu K. 2012. Expression of a rice CYP81A6 gene confers tolerance to bentazon and sulfonylurea herbicides in both *Arabidopsis* and tobacco. *Plant Cell Tiss Org.* **109**: 419–28.

- Liu Z, Tavares R, Forsythe ES, André F, Lugan R, Jonasson G, Boutet-Mercey S, Tohge T, Beilstein MA, Werck-Reichhart D, Renault H. 2016.** Evolutionary interplay between sister cytochrome P450 genes shapes plasticity in plant metabolism. *Nat Commun.* **7**: 13026-13036.
- Lowe DB, Swire-Clark, McCarty LB, Whitwell T, Baird WV. 2001.** Biology and molecular analysis of dinitroaniline-resistant *Poa annua* L. *Int. Turfgrass Soc. Res. J.* **9**: 1019-1025.
- Ma B, Luo YW, Lin J, Qi XW, Zeng Q W, Xiang ZH, He N J. 2013.** Genome-wide identification and expression analyses of cytochrome P450 genes in mulberry (*Morus notabilis*). *J. Integrative Plant Biol.* **56**: 887–901.
- Manikandan P, Nagini S. 2018.** Cytochrome P450 Structure, Function and Clinical Significance: A Review. *Curr Drug Tar.* **19**: 38-54.
- Mansuy D. 1998.** The great diversity of reactions catalyzed by cytochrome P450. *Comp Biochem Physiol Part C.* **121**: 5-14.
- McAlister FM, Holtum JA, Powles SB. 1995.** Dinitroaniline herbicide resistance in rigid ryegrass (*Lolium rigidum*). *Weed Sci.* **43** :55–62.
- Miettinen K, Dong L, Navrot N, Schneider T, Burlat V, Pollier J, Woittiez L, van der Krol S, Lugan R, Ilc T, Verpoorte R, Oksman-Caldentey KM, Martinoia E, Bouwmeester H, Goossens A, Memelink J, Werck-Reichhart D. 2014.** The seco-iridoid pathway from *Catharanthus roseus*. *Nat. Commun.* **5**: 3606- 3618.
- Mizutani M, Ohta D. 2010.** Diversification of P450 genes during land plant evolution. *Annu Rev Plant Biol.* **61**: 291-315.
- Morris GM, Huey R, Lindstrom W, Sanner MF, Belew RK, Goodsell DS, Olson AJ. 2009.** AutoDock4 and AutoDockTools4: Automated docking with selective receptor flexibility. *Comput. Chem.* **30**: 2785–2791.
- Morrison IN, Todd BG, Nawolsky KM. 1989.** Confirmation of trifluralinresistant green foxtail (*Setaria viridis*) in Manitoba. *Weed Technol.* **3**:544–551.

- Moss SR, Cussans GW. 1985.** Variability in the susceptibility of *Alopecurus myosuroides* (black-grass) to chlortoluron and isoproturon. *Aspects Appl. Biol.* **9**: 91–98.
- Mudge LC, Gossett BJ, Murphy TR. 1984.** Resistance of goosegrass (*Eleusine indica*) to dinitroaniline herbicides. *Weed Sci.* **32**:591–594.
- Nakka S, Thompson CR, Peterson DE, Jugulam M. 2017.** Target site-based and non-target site based resistance to ALS inhibitors in Palmer amaranth (*Amaranthus palmeri*). *Weed Sci.* **65**: 681–689.
- Nelson D, Werck-Reichhart D. 2011.** A P450-centric view of plant evolution. *Plant J.* **66**:194–211.
- Nianiou-Obeidat I, Madesis P, Kissoudis C, Voulgari G, Chronopoulou E, Tsaftaris A, Labrou NE. 2017.** Plant glutathione transferase-mediated stress tolerance: functions and biotechnological applications. *Plant Cell Rep.* **36**: 791–805.
- O’Keefe DP, Tepperman JM, Dean C, Leto KJ, Erbes DL, Odell JT. 1994.** Plant expression of a bacterial cytochrome P450 that catalyzes activation of a sulfonylurea herbicide. *Plant Physiol.* **105**: 473–482.
- Oliveira MC, Gaines TA, Dayan FE, Patterson EL, Jhala AJ, Knezevic SZ. 2017.** Reversing resistance to tembotrione in an *Amaranthus tuberculatus* (var. *rudis*) population from Nebraska, USA with cytochrome P450 inhibitors. *Pest Manag. Sci.* **74**: 2296–2305.
- Omura T, Sato R. 1964.** The carbon monoxide-binding pigment of liver microsomes. *J. Biol. Chem.* **239**: 2370–2378.
- Owen MJ, Martinez NJ, Powles SB. 2014.** Multiple herbicide-resistant *Lolium rigidum* (annual ryegrass) now dominates across the Western Australian grain belt. *Weed Res.* **54**: 314–324.
- Pan G, Zhang X, Liu K, Zhang J, Wu X, Zhu J, Tu J. 2006.** Map-based cloning of a novel rice cytochrome P450 gene CYP81A6 that confers resistance to two different classes of herbicides. *Plant Mol. Biol.* **61**:933-943.

- Pei J, Kim B-H, Nick V. Grishin NV. 2008.** PROMALS3D: a tool for multiple sequence and structure alignment. *Nucleic Acids Res.* **36**: 2295-2300
- Perperopoulou F, Pouliou F, Labrou NE. 2017.** Recent advances in protein engineering and biotechnological applications of glutathione transferases. *Crit. Rev. Biotechnol.* **38**: 511–52.
- Pompon D, Louerat B, Bronine A, Urban P. 1996.** Yeast expression of animal and plant P450s in optimized redox environments. *Method Enzymol.* **272**: 51–64.
- Powles SB, Shaner DL. 2001.** Herbicide Resistance and World Grains. *Boca Raton/London/NewYork/Washington, DC: CRC Press.*
- Powles SB, Yu Q. 2010.** Evolution in action: plants resistant to herbicides. *Ann. Rev. Plant Biol.* **61**: 317–347.
- Renault H, De Marothy M, Jonasson G, Lara P, Nelson DR, Nilsson I, André F, von Heijne G, Werck-Reichhart D. 2017.** Gene Duplication Leads to Altered Membrane Topology of a Cytochrome P450 Enzyme in Seed Plants. *Mol. Biol. Evol.* **34**: 2041-2056.
- Riar DS, Norsworthy JK, Bond JA, Bararpour MT, Wilson MJ, Scott RC. 2012.** Resistance of barnyardgrass (*Echinochloa crus-galli*) populations to acetolactate synthase-inhibiting herbicides. *Int J Agron.*
- Riechers DE, Kreuz K, Zhang Q. 2010.** Detoxification without intoxication: herbicide safeners activate plant defense gene expression. *Plant Physiol.* **153**: 3–13.
- Robineau T, Batard Y, Nedelkina S, Cabello-Hurtado F, LeRet M, Sorokine O, Didierjean L, Werck-Reichhart D. 1998.** The chemically inducible plant cytochrome P450 CYP76B1 actively metabolizes phenylureas and other xenobiotics. *Plant Physiol.* **118**:1049-56.
- Rosenhauer M, Rosinger C, Petersen J. 2016.** Impact of the safener mefenpyr-diethyl on herbicide resistance evolution in *Alopecurus myosuroides* (Huds.) biotypes. *Julius-Kühn-Arch.* **452**: 50–56.

- Ryan GF. 1970.** Resistance of common groundsel to simazine and atrazine. *Weed Sci.* **18**: 614–16.
- Saika H, Horita J, Taguchi-Shiobara F, Nonaka S, Nishizawa-Yokoi A, Iwakami S, Hori K, Matsumoto T, Tanaka T, Itoh T, Yano M, Kaku K, Shimizu T, Toki S. 2014.** A novel rice cytochrome P450 gene, *CYP72A31*, confers tolerance to acetolactate synthase-inhibiting herbicides in rice and Arabidopsis. *Plant Physiol.* **166**: 1232-1240.
- Schuler MA, Werck-Reichhart D. 2003.** Functional genomics of P450s. *Annu. Rev. Plant Biol.* **54**: 629–67.
- Shahrokh K, Orendt A, Yost GS, Cheatham TE. 2012.** Quantum mechanically derived AMBER-compatible heme parameters for various states of the cytochrome P450 catalytic cycle. *Comput. Chem.* **33**: 119–133.
- Shergill LS, Bish MD, Jugulam M, Bradley KW. 2018.** Molecular and physiological characterization of six-way resistance in an *Amaranthus tuberculatus* var. rudis biotype from Missouri. *Pest. Manag. Sci.* **74**: 2688–2698.
- Siminszky B, Corbin FT, Ward ER, Fleischmann TJ, Dewey RE. 1999.** Expression of a soybean cytochrome P450 monooxygenase cDNA in yeast and tobacco enhances the metabolism of phenylurea herbicides. *Proc Natl Acad Sci USA.* **96**: 1750–1755.
- Studer G, Rempfer C, Waterhouse A., Gumienny G, Haas J, Schwede T. 2020.** QMEANDisCo - distance constraints applied on model quality estimation. *Bioinformatics.* **36**: 1765-1771.
- Switzer CM. 1957.** The existence of 2,4-D resistant strains of wild carrot. *11th. North-eastern Weed Control Conference.* **11**: 315-318.
- van der Fits L, Deakin EA, Hoge JHC, Memelink J. 2000.** The ternary transformation system: constitutive virG on a compatible plasmid dramatically increases Agrobacterium-mediated plant transformation. *Plant Mol. Biol.* **43**: 495–502.
- Vrbničanin S, Pavlovich A, Božić D. 2017.** Herbicide Resistance in Weeds and Crops. *Intech Open*. London, UK.

- Weigel D, Glazebrook J. 2006.** Transformation of *Agrobacterium* using electroporation. *CSH Prot.* 7.
- Werck-Reichhart D, Feyereisen R. 2000.** Cytochromes P450: a success story. *Genome Biol.* 6: 3003.1-3003.9.
- Werck-Reichhart D, Hehn A, Didierjean L. 2000.** Cytochromes P450 for engineering herbicide tolerance. *Trends Plant Sci.* 5:1360–1385.
- Whitehead CW, Switzer C M. 1963.** The differential response of strains of wild carrot to 2,4-d and related herbicides. *Plant Sci.* 43: 255-262.
- Xie F, Zhou X, Behr M, Fang C, Horii Y, Gu J, Kannan K, Ding X. 2010.** Mechanisms of olfactory toxicity of the herbicide 2,6-dichlorobenzonitrile: essential roles of CYP2A5 and target-tissue metabolic activation. *Toxicol Appl Pharmacol.* 249: 101-6.
- Yamamoto E, Zeng L, Baird WV. 1998.** α -Tubulin missense mutations correlate with antimicrotubule drug resistance in *Eleusine indica*. *Plant Cell.* 10: 297–308.
- Yang Q, Deng W, Li X, Yu Q, Bai L, Zheng M. 2016.** Target-site and non-target-site based resistance to the herbicide tribenuron-methyl in flaxweed (*Descurainia sophia* L.). *BMC Genomics.* 17: 551
- Yang Q, Li J, Shen J, Xu Y, Liu H, Deng W, Li X, Zheng M. 2018.** Metabolic Resistance to Ace Chlorophenololactate Synthase Inhibiting Herbicide Tribenuron-Methyl in *Descurainia sophia* L. Mediated by Cytochrome P450 Enzymes. *J. Agric. Food Chem.* 17: 4319-4327.
- Yu Q, Powles S. 2014.** Metabolism-based herbicide resistance and cross-resistance in crop weeds: a threat to herbicide sustainability and global crop production. *Plant Physiol.* 166:1106-1118.
- Yuan G, Liu W, Bi V, Du L, Guo W, Wang J. 2015.** Molecular basis for resistance to ACCase-inhibiting herbicides in *Pseudosclerochloa kengiana* populations. *Pesti Biochem. Physiol.* 119: 9-15.
- Yuan JS, Tranel PJ, Stewart CN Jr. 2007.** Non-target-site herbicide resistance: a family business. *Trends Plant Sci.* 12: 6–13.

- Zanger UM, Schwab M. 2013.** Cytochrome P450 enzymes in drugmetabolism: Regulation of gene expression, enzyme activities, and impact of genetic variation. *Pharmacol Ther.* **138**: 103-41.
- Zhang J, Xu Y, Wu X, Zhu L. 2002.** A bentazon and sulfonylurea sensitive mutant: breeding, genetics, and potential application in seed production of hybrid rice. *Theor Appl Genet.* **105**: 16–22.
- Zhang L, Lu Q, Chen HG, Pan G, Xiao S, Dai Y, Li Q, Zhang J, Wu X, Wu J, Tu J, Liu K. 2006.** Identification of a cytochrome P450 hydroxylase CYP81A6 as the candidate for the bentazon and sulfonylurea herbicide resistance gene, *Bel*, in rice. *Mol Breed.* **19**: 59–68.
- Zhang Q, Xu FX, Lambert KN, Riechers DE. 2007.** Safeners coordinately induce the expression of multiple proteins and MRP transcripts involved in herbicide metabolism and detoxification in *Triticum tauschii* seedling tissues. *Proteomics.* **7**: 1261–1278.
- Zhao N, Li Q, Guo WL, Zhang LL, Ge LA, Wang JX. 2018.** Effect of environmental factors on germination and emergence of shortawn foxtail (*Alopecurus aequalis*). *Weed Sci.* **66**: 47–56.
- Zhao N, Wang H, Zhang LL, Liu WT, Wang JX. 2019.** Resistance status of Japanese foxtail (*Alopecurus japonicus*) to fenoxaprop-*P*-ethyl in multiple wheat fields in Anhui Province and involved ACCase gene mutations. *Chin J Pestic Sci.* **21**: 35–42.

Appendix

Appendix Table 1. Investigated P450 enzymes.

CYP	Plant	In plant	Promiscuity	Reference
CYP73A92	<i>Brachypodium distachyon</i>	<i>Phenolics</i>	-	(Renault et al., 2017)
CYP98A23	<i>Populus trichocarpa</i>	<i>Phenolics</i>	-	(Alber et al., 2019)
CYP72A224	<i>Catharanthus roseus</i>	<i>Iridoids</i>	-	(Miettinen et al., 2014)
CYP98A27	<i>Populus trichocarpa</i>	<i>Phenolics</i>	+/-	(Alber et al, 2019)
CYP76B1	<i>Helianthus tuberosus</i>	<i>Alkoxycoumarins, Alkoxyresorufins, Phenylurea</i>	++	(Batard et al., 1998; Robineau et al., 1998)
CYP706A3	<i>Arabidopsis thaliana</i>	<i>Terpenoids</i>	+++	(Boachon et al., 2019)
CYP706A1	<i>Arabidopsis thaliana</i>	unknown		
CYP706A2	<i>Arabidopsis thaliana</i>	unknown		
CYP706A7	<i>Arabidopsis thaliana</i>	unknown		
CYP706M1	<i>Alaska cedar</i>	<i>Sesquiterpenes</i>		(Cankar et al, 2014)
CYP706C55	<i>Eucalyptus cladocalyx</i>	<i>Phenylacetaldoxime</i>		(Hansen et al, 2018)
CYP71D51	<i>Arabidopsis thaliana</i>	<i>Sesquiterpene</i>		(Gavira et al., 2013)
CYP81D11	<i>Arabidopsis thaliana</i>	unknown		
CYP81F1	<i>Arabidopsis thaliana</i>	unknown		
CYP81F2	<i>Arabidopsis thaliana</i>	unknown		
CYP81F4	<i>Arabidopsis thaliana</i>	unknown		
CYP81H1	<i>Arabidopsis thaliana</i>	unknown		

Appendix Table 2. Summary of docking poses found by Autodock 4.2.6 experiments performed on other dinitroanilines.

The poses were assigned a score calculated by Autodock that can be considered as an estimated free energy of ligand binding (indicative of binding affinity). The first ranked clusters involving CH groups closest to the iron atom are reported here and colored in red in the histograms displayed in supplemental figure 5. The other first clusters of better binding affinity corresponded in each histogram to non-productive poses, essentially due to overrated electrostatic attraction of NO₂ and Cl functional groups for iron atom using the scoring function of Autodock. For two molecules, Benefin and Ethalfluralin, three clusters that were found very close in binding energy score are reported, corresponding to three different docking poses. CH₂ and CH₃ refer to the terminal methylene and methyl groups of alkyl chain, except for Benefin where a position of metabolism was found on the antepenultimate carbon (* indicated). The distances found between closest CH(n) groups and the iron atom are fully consistent with the catalytic reaction.

Ligand Name	Distance (Å)		Rank of Cluster	Energy Binding (kcal/mol)
	CH ₂ -Fe	CH ₃ -Fe		
Trifluralin	3.1	2.5	5	-7.67
Fluchloralin	2.9	2.5	4	-7.31
Benefin	2.8	2.7	2	-7.79
	2.8	2.8	3	-7.58
	3.2 *	-	5	-7.54
Ethalfluralin	-	2.6	3	-7.92
	-	2.5	4	-7.86
	2.6	-	5	-7.84

Résumé en français

Introduction

Le principal problème causé par les mauvaises herbes est une réduction du rendement des cultures en raison d'une compétition pour la lumière ainsi que pour l'espace, les nutriments et l'eau. Les techniques de contrôle des mauvaises herbes ciblent pour cette raison une réduction de la capacité de compétition des adventices dans une culture et la prévention des problèmes qu'elles sont susceptibles de causer dans une future récolte. Les technologies de contrôle des mauvaises herbes ont évolué d'un ramassage à la main, à la houe primitive (6000 B.C.), aux outils à propulsion mécaniques (1920 A.D.), aux contrôles biologiques (1930 A.D.), puis chimiques (herbicides : 1947 A.D.).

Certaines de ces approches ont été abandonnées, alors que d'autres sont toujours en usage. L'application d'herbicides est l'une des approches les plus efficaces et durables. Elle est jusqu'ici la méthode la plus fiable et la moins chère permettant de limiter la propagation des mauvaises herbes, et celle qui a permis la production durable d'une nourriture abondante pour faire face à l'augmentation de la population mondiale. L'efficacité et le faible coût des herbicides a conduit à une forte dépendance à leur égard dans le monde développé. Cependant, ils sont la source de problèmes qui peuvent être réels ou perçus comme tels (Powles and Yu, 2010; Iwakami *et al*, 2014; Alebrahim *et al*, 2017).

Au cours des dernières années ont émergé des préoccupations concernant les résidus de pesticides ainsi que les problèmes de sécurité alimentaire qui y sont associés, leur impact sur l'environnement, et l'apparition de résistances aux herbicides. L'évolution de résistances des mauvaises herbes aux herbicides est un problème mondial de plus en plus incontrôlable qui affecte le rendement des récoltes. Les mécanismes de résistance aux herbicides sont généralement groupés en deux catégories : les résistances des cibles des herbicides ou les résistances indépendantes de leurs cibles (NTRS). Le plus souvent, une résistance indépendante de la cible est causée par une métabolisation accrue de l'herbicide, soit par un cytochrome P450 (P450), soit par une glutathion S-transférase (GST). Du point de vue du contrôle des mauvaises herbes, la résistance indépendante des cibles est une plus grande menace pour les récoltes, car elle implique souvent une

résistance à de multiples herbicides appartenant à différentes classes chimiques et qui présentent des modes d'action différents. Une meilleure compréhension des mécanismes à l'origine des résistances est importante pour pouvoir mettre en place des recommandations concernant de meilleures stratégies de gestion des mauvaises herbes (Powles and Yu, 2010; Iwakami *et al*, 2014; Heap, 2014; Délye *et al*, 2015; Yang *et al*, 2016; Vrbničanin *et al*, 2017; Alebrahim *et al*, 2017). Des études récentes mettent en avant la diversité des mécanismes de NTSR impliquant des cytochromes P450, ainsi que la difficulté à prédire l'émergence des résistances.

L'objectif général de ce projet est de tenter de mieux comprendre les mécanismes moléculaires et l'évolution des résistances aux herbicides P450-dépendantes. En particulier, notre objectif était de déterminer si le métabolisme des herbicides par les P450 végétaux pouvait être associé à une promiscuité intrinsèque de certaines de ces enzymes. Pour répondre à cette question, nous avons testé la capacité à métaboliser des herbicides représentatifs des principales familles chimiques de six cytochromes P450 de plantes dont les activités catalytiques vis à vis de substrats physiologiques sont bien documentées. Ces P450s candidats ont été sélectionnés de manière à représenter des enzymes décrites comme présentant différents degrés (de très faible à forte) de promiscuité vis à vis de leurs substrats physiologiques.

Résultats et discussion

Afin de tester leur activité catalytique, les P450s candidats ont été exprimés dans la levure. Pour ce faire, la souche de levure WAT11 et le plasmide d'expression pYeDP60 ont été utilisés. La souche WAT11 porte un gène de NADPH-P450 réductase d'*Arabidopsis* (ATR1) inséré dans le chromosome. pYeDP60 est un plasmide d'expression multicopie à partir duquel l'expression des P450s est contrôlée par le promoteur hybride inductible par le galactose et réprimé par le glucose *GAL10-CYC1*. Après induction des cultures de levure par le galactose, les membranes microsomales porteuses des cytochromes P450 exprimés ont été isolées par centrifugation différentielle. L'expression des P450s a été vérifiée et quantifiée par spectroscopie UV-Vis différentielle sur les fractions membranaires réduites par le Na₂S₂O₄ en présence ou en absence de monoxyde de carbone.

Afin de déterminer si le P450 candidat était capable de catalyser une oxydation des herbicides, les membranes de levures transformées (avec les gènes de P450s candidats ou un vecteur vide comme contrôle) ont été incubées en présence de différents herbicides représentatifs des principales classes de composés actifs et de NADPH. A la fin de la réaction, chaque échantillon a été analysé par HPLC-DAD (chromatographie liquide avec détection par barrette de diodes) afin de révéler les produits d'oxydation potentiels. Ce premier criblage a confirmé l'activité déjà décrite du CYP76B1 d'*Helianthus tuberosus* (utilisé comme contrôle positif) sur les phénylurées et a révélé une nouvelle activité du CYP706A3 d'*Arabidopsis thaliana* sur les dinitroanilines: en particulier sur la pendiméthaline, mais aussi sur la fluchloraline, la bénométhol, l'éthéfluraline et la trifluraline, mais pas sur l'oryzaline (**Table1**). Cependant, une faible conversion des herbicides a été observée lors de ces essais *in vitro* qui ont généré des quantités de produits insuffisantes pour permettre leur complète caractérisation.

Table 1. Le métabolisme CYP-dépendant des herbicides criblé par HPLC des essais in vitro

Famille	Herbicide	Oxydation					
		CYP98A23	CYP98A27	CYP706A3	CYP73A98	CYP72A224	CYP76B1
Dinitroanilines	Pendimethalin	-	-	+	-	-	-
	Fluchloralin	-	-	+	-	-	-
	Oryzalin	-	-	-	-	-	-
	Trifluralin	-	-	+	-	-	-
	Benefin	-	-	+	-	-	-
	Ethalfuralin	-	-	+	-	-	-
Triazines	Atrazine	-	-	-	-	-	-
	Terbutryn	-	-	-	-	-	-
	Simazine	-	-	-	-	-	-
Imidazolinones	Imazethapyr	-	-	-	-	-	-
Sulfonylureas	Nicosulfuron	-	-	-	-	-	-
	Rimsulfuron	-	-	-	-	-	-
Phenylureas	Chlorbromuron	-	-	-	-	-	+
	Metobromuron	-	-	-	-	-	+
	Chlortoluron	-	-	-	-	-	+
Benzoic acids	Chloramben	-	-	-	-	-	-
	Dicamba	-	-	-	-	-	-
Nitriles	Bromoxynil	-	-	-	-	-	-
Aryloxyphenoxy propionates	Haloxypop-methyl	-	-	-	-	-	-
	Fenoxaprop-p-ethyl	-	-	-	-	-	-
Pridazinone	Norflurazon	-	-	-	-	-	-
Benzothia diazinone	Bentazon	-	-	-	-	-	-
Chlorinated anilide	Propanil	-	-	-	-	-	-
Diphenyl ethers	Bifenox	-	-	-	-	-	-
Phenoxy-carboxylic-acids	2,4-D	-	-	-	-	-	-
(+) converti, (-) non converti							

Pour confirmer les activités enzymatiques et générer des quantités de produits suffisantes pour leur caractérisation structurale, la conversion de pendiméthaline a, dans un second temps, été testée en utilisant des cultures de levures intactes et *in planta*. Pour les essais de conversion en levure entière, les produits générés ont été isolés à partir du milieu de culture. Les résultats de cette expérience sont en bonne cohérence avec les produits de métabolisation de la pendiméthaline détectés *in vitro*, et des taux de conversions élevés ont pu être obtenus. **(Figure1)**. CYP706A3 a également été exprimé de manière transitoire par infiltration d'agrobactéries transformées dans des feuilles de *Nicotiana benthamiana*. Des disques de feuilles transformées ont été excisés 5 jours après l'infiltration, avant d'être incubés dans un tampon contenant l'herbicide à tester. Les produits formés ont été extraits au méthanol, à partir des disques de feuilles, ainsi qu'à partir du milieu d'incubation, avant d'être analysés par HPLC. De faibles quantités de produits ont pu être isolées à partir des disques foliaires. En revanche, l'analyse des produits extraits à partir du milieu d'incubation a permis de confirmer une conversion CYP706A3-dépendante de la pendiméthaline, avec génération des même produits que lors des essais en levure, mais en quantité moindre. Des conversions en levure intacte ont donc été mises en œuvre à plus grande échelle afin de générer des produits en quantité suffisante pour leur caractérisation structurale.

Dans un premier temps, une analyse par LC-MS (en chromatographie liquide avec détection par spectrométrie de masse) a été entreprise. Cette dernière a suggéré que les deux pics de produits obtenus à partir de la pendiméthaline sont des produits d'oxygénation de même masse et montrant des spectres de fragmentation identiques **(Figure 2)**, probablement hydroxylé sur la chaîne latérale isopentyle.

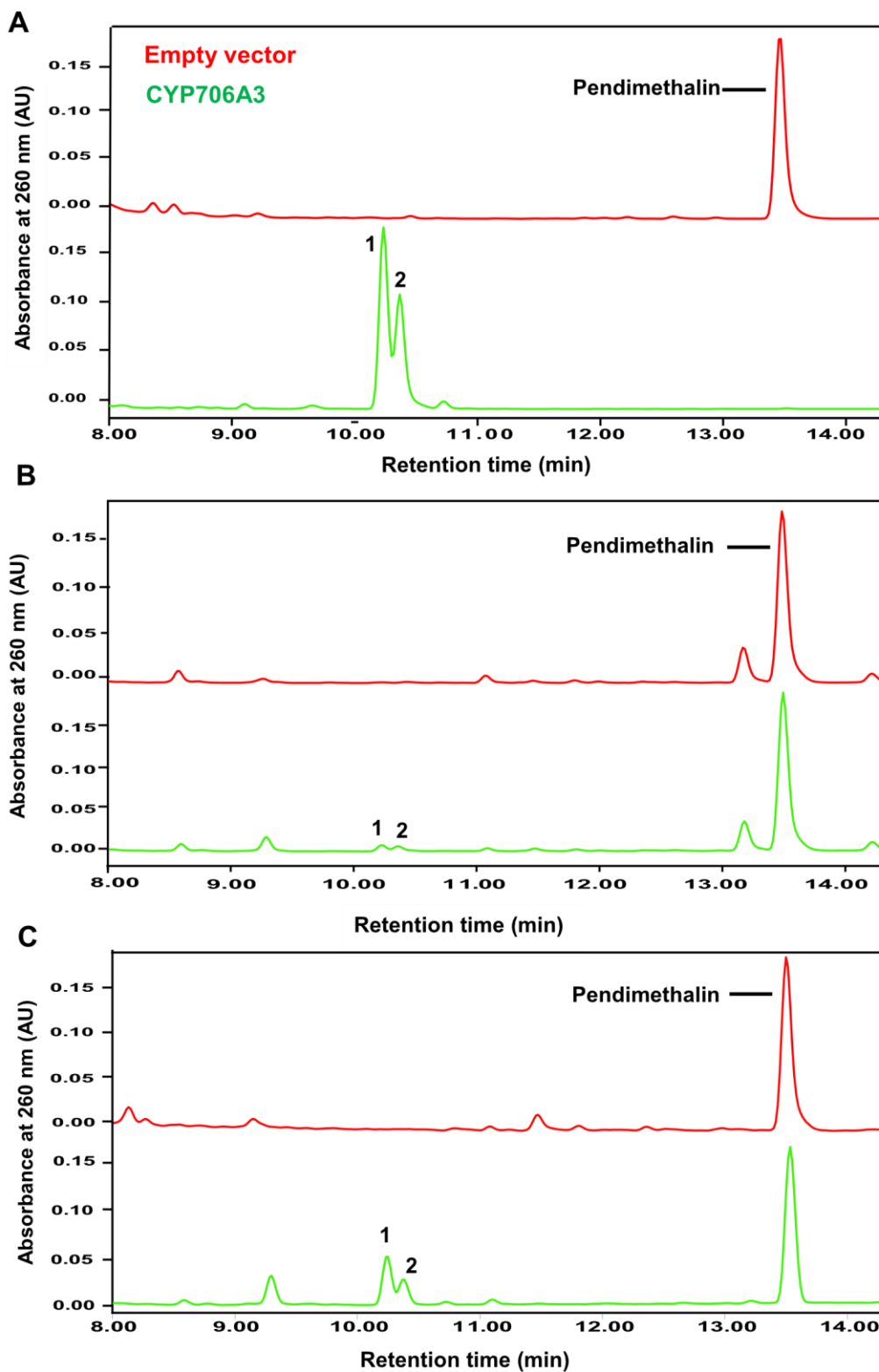


Figure 1. Profil HPLC-DAD montrant la conversion de la pendiméthaline par CYP706A3 exprimé en levure entière ou dans des disques de feuilles de *N. benthamiana*.

A, Des cultures de levures entières exprimant *CYP706A3* ou le vecteur vide (empty-control) ont été incubées en présence de 50 μ M de substrat pendant 24 heures à température ambiante. *CYP706A3* + pendiméthaline (vert) et vecteur vide (rouge). Les pics 1 et 2 correspondent aux produits.

B and C, Conversion de la pendiméthaline détectée dans des extraits méthanoliques de disques de feuilles ou de milieu d'incubation des disques de feuilles exprimant *CYP706A3* ou un vecteur d'expression pCAMBIA330035Su vide (EV control). Les disques de feuilles ont été incubés dans un tampon Na phosphate (pH 7.4) contenant 200 mM de pendiméthaline et placés dans une chambre de culture pendant 24 h.

Pour une identification sans ambiguïté par RMN (résonance magnétique nucléaire), une plus grande quantité des produits était cependant nécessaire. L'extrait méthanolique des cultures de levures a donc été purifié par chromatographie préparative en couche mince (TLC) sur des plaques de 0.5 mm de gel de silice 60 F₂₅₄ en verre (Eluant : éther de pétrole/ acétate d'éthyle 70:30 v/v. Deux produits avec des valeurs de R_f très proches ont ainsi pu être séparés (**Figure 3**).

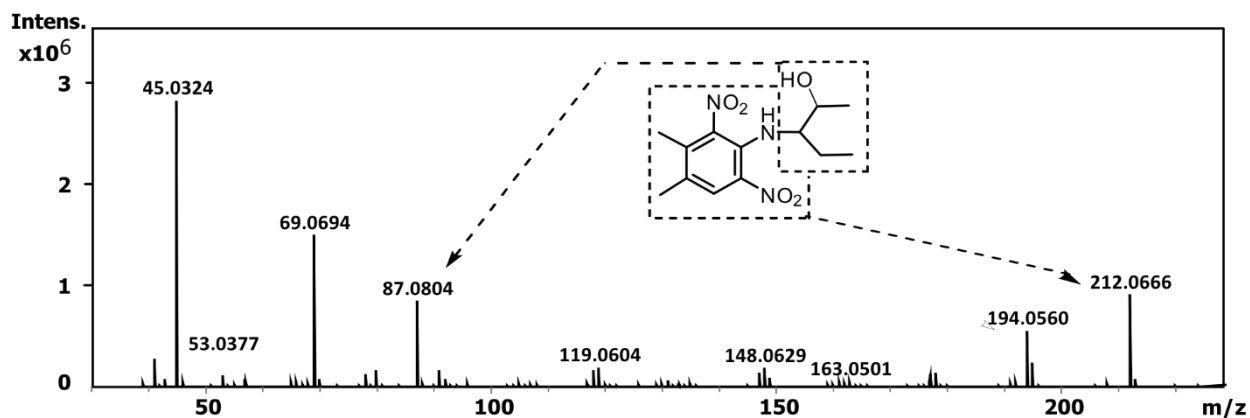


Figure 2. Caractérisation en LC-MS des produits résultant de la conversion de la pendiméthaline par *CYP706A3*.

Les spectres $^1\text{H-NMR}$ réalisés sur les deux produits purifiés sont en bon accord avec les analyse en LC-MS et indiquent que la pendiméthaline 1 a été hydroxylée en 2 sous forme de deux diastéréoisomères (ratio 1/1) (**Schéma 1**).

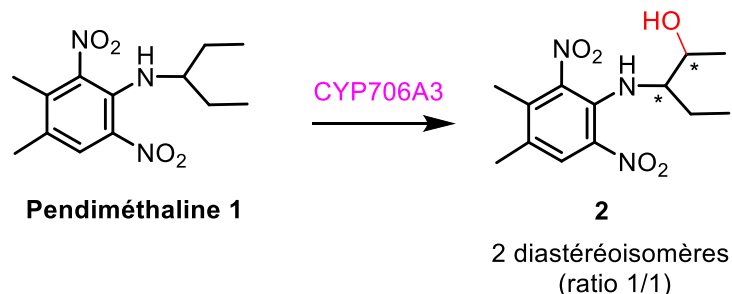


Schéma 1. Conversion de la pendiméthaline par CYP706A3.

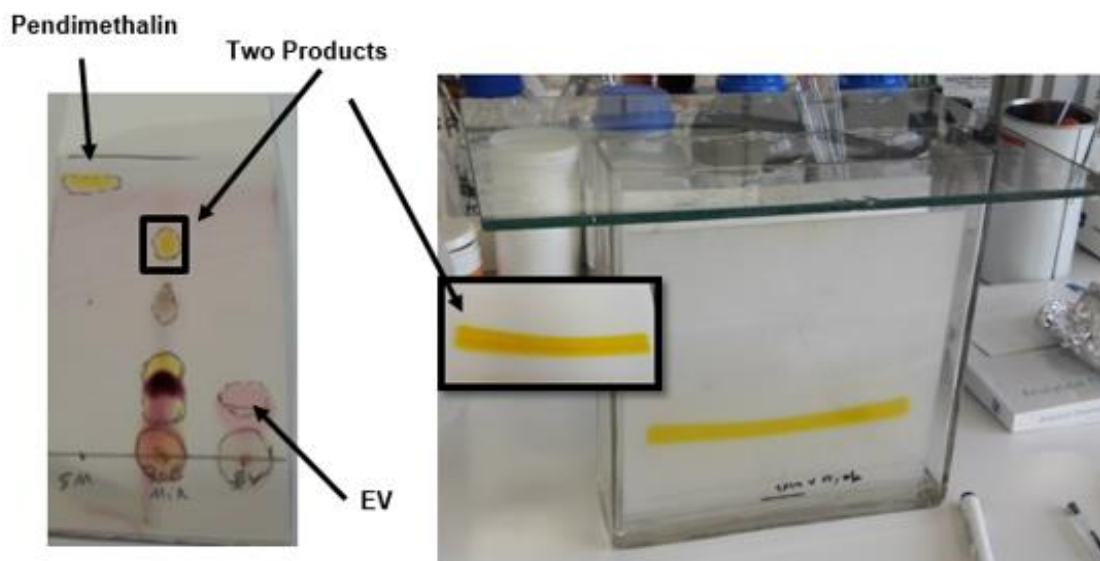


Figure 3. TLC analytique et préparative de la pendiméthaline et des produits de conversion (EV: empty vector).

Le protocole d'incubation des levures entières ensuite été appliqué à une gamme plus large de dinitroanilines, incluant: la pendiméthaline, l'éthalfuraline, la bénéfine, l'oryzaline, la trifluraline et al fluchloraline. A l'exception de l'oryzaline, toutes les dinitroanilines testées ont été converties par CYP706A3, quelquefois en plusieurs produits en fonction du temps d'incubation. CYP706A3 a récemment été décrit comme un P450 qui présente

une très forte promiscuité de substrat, capable de métaboliser un grand nombre de sesqui- et de mono-terpènes (Boachon *et al.*, 2019). Pour mieux comprendre les bases de ce manque de sélectivité et les causes de la capacité de CYP706A3 à oxyder un grand nombre de dinitroanilines, chacune d'entre elles a été arrimée dans un modèle 3D de CYP706A3. Tous les herbicides appartenant à la série des dinitroanilines ont pu être arrimés avec succès, montrant des poses d'arrimage de basse énergie dans le site actif de CYP706A3 ainsi que des orientations compatibles avec les métabolites observés. L'oryzaline a également permis d'obtenir des poses de basse énergie dans le modèle de CYP706A3.

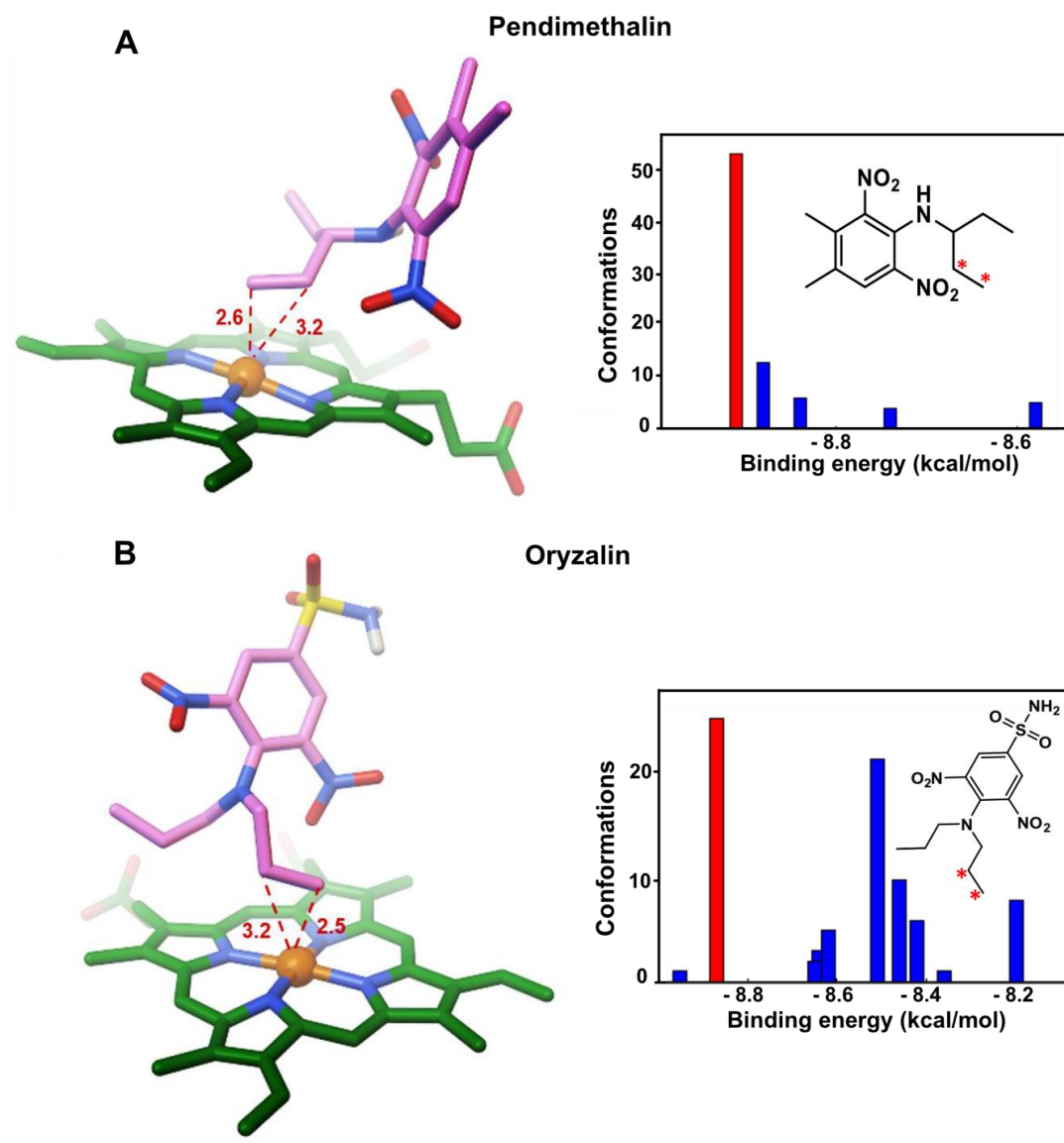


Figure 4. Ancrage de la pendiméthaline et de l'oryzaline dans un modèle moléculaire de CYP706A3.

Les deux herbicides peuvent s'ancrer dans le site actif avec de bonnes affinités prédites et des poses compatibles avec une attaque de leur chaîne latérale par CYP706A3.

Pour mieux comprendre l'absence de métabolisation de CYP706A3, les propriétés physicochimiques des dinitroanilines ont été comparées. Seule l'oryzaline présente un groupement hydrophile, chargé à un pH physiologique. Les canaux d'accès au site actif de CYP706A3, préalablement modélisés sont étroits et fortement hydrophobes. C'est donc une impossibilité d'accès au site actif qui explique la non-métabolisation de l'oryzaline (**Figure 4**).

Le métabolisme des herbicides conduit le plus souvent à la production de dérivés moins toxiques qui peuvent être soit re-métabolisés et complètement dégradés, soit conjugués et stockés dans la vacuole. Dans quelques cas, le métabolisme peut aussi conduire à une activation. Afin de déterminer si l'oxygénation des dinitroanilines par CYP706A3 conduit à une détoxification de ces herbicides, des lignées d'*Arabidopsis* surexprimant *CYP706A3* (expression ectopique sous le contrôle du promoteur *CaMV 35S*) ont été mises à profit. Comme le montre la **Figure 5**, les plantes surexprimant *CYP706A3* deviennent plus résistantes aux dinitroanilines. Ce gain en tolérance aux herbicides est corrélé à leur métabolisme détecté *in vitro*.

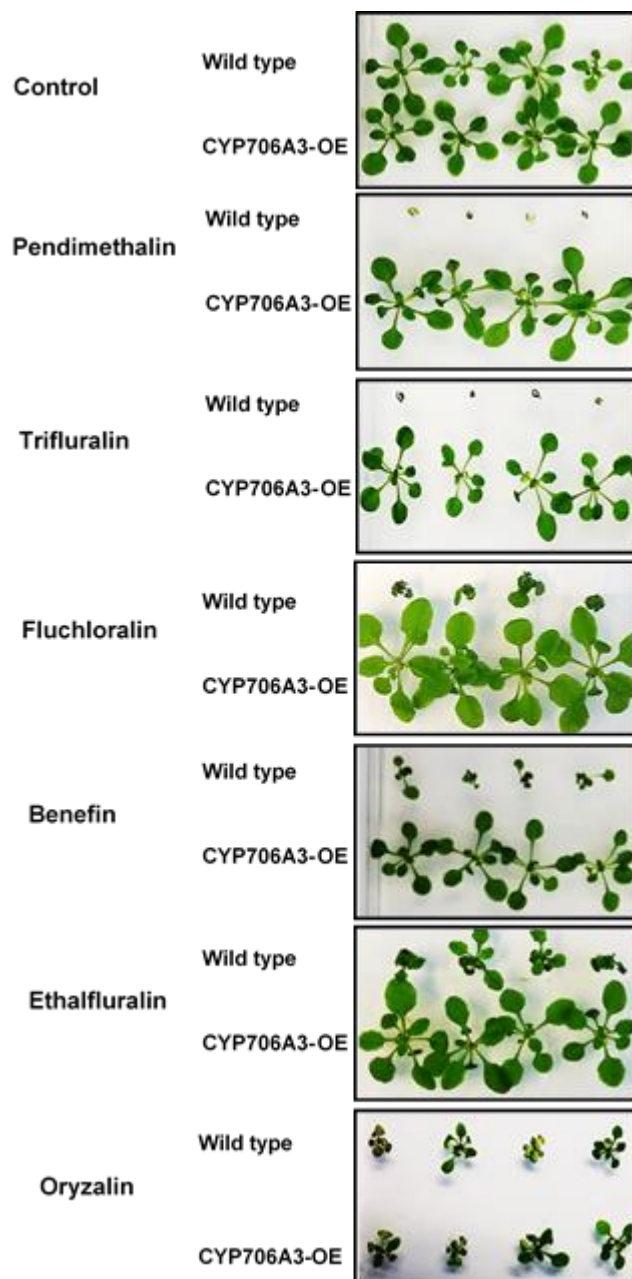


Figure 5. Test de résistance aux dinitroanilines de plantules d'*A. thaliana* sauvages ou surexprimant *CYP706A3*. Les plantes ont été cultivées *in vitro* pendant 15 jours en présence ou en absence de dinitroanilines 1 μ M.

D'autres P450s isolés d'*Arabidopsis* ou d'autres plantes comme le pin, le cèdre de l'Alaska ou l'eucalyptus, et capables de métaboliser les sesquiterpènes, ont enfin été testés pour leur capacité à métaboliser les dinitroanilines. Plusieurs d'entre eux se sont montrés capables de métaboliser au moins l'une des dinitroanilines testées. Les différentes

enzymes génèrent parfois plusieurs produits. Ces produits sont le plus souvent différents en fonction des enzymes testées.

Conclusion générale

Les herbicides exercent une forte pression de sélection sur les agrosystèmes. Il en résulte une évolution de lignées résistantes aux herbicides. Parmi tous les mécanismes de résistance, une augmentation du métabolisme des herbicides constitue la principale menace, car une résistance basée sur le métabolisme concerne généralement non seulement l'herbicide pour lequel la résistance a été sélectionnée, mais aussi des herbicides qui ont un autre mode d'action et n'ont jamais été utilisés sur la culture concernée, y compris de nouveaux herbicides en développement (Powles and Yu, 2010; Iwakami *et al*, 2014; Vrbničanin *et al*, 2017; Alebrahim *et al* 2017). Au cours de ce travail nous avons démontré que le CYP706A3 d'*Arabidopsis thaliana*, un P450 qui montre une forte promiscuité de substrat, est capable de métaboliser la pendiméthaline ainsi que d'autres herbicides de la famille des dinitroanilines. La surexpression ectopique de ce P450 sous le contrôle du promoteur 35S du CaMV conduit à une augmentation d'un facteur 10 environ de la résistance aux dinitroanilines par comparaison aux plantes sauvages. Ceci démontre que les herbicides sont convertis en des composés moins phytotoxiques. Ce travail apporte la démonstration qu'un P450 de forte promiscuité intrinsèque, dont le rôle physiologique est l'oxydation des terpènes pour la défense des fleurs, peut conduire à l'évolution d'une résistance aux herbicides chez les mauvaises herbes ou les plantes de culture lorsqu'il est exprimé dans d'autres organes. Il démontre d'autre part le rôle potentiel des P450 de la famille CYP706A3 dans l'évolution des résistances aux dinitroanilines. Enfin il indique que l'oryzoline pourrait résoudre des problèmes de résistance aux autres dinitroanilines.

Fatemeh ABDOLLAHI

**Analyse des bases moléculaires
de la résistance aux herbicides
chez les plantes**

Résumé

La résistance croissante des adventices aux herbicides est une préoccupation majeure de l'agriculture moderne. Le métabolisme des herbicides par les cytochromes P450 oxygénases est souvent la cause de cette résistance. Dans le foie humain, quelques P450s peu spécifiques détoxiquent la plupart des médicaments. Pour examiner la relation entre promiscuité des P450s chez les plantes et métabolisme des herbicides, la conversion des grandes classes d'herbicides par six P450s de faible à forte spécificité de substrat a été testée. Le moins sélectif, CYP706A3 d'*Arabidopsis thaliana*, s'est montré capable d'hydroxyler la pendiméthaline, ainsi que la plupart des autres dinitroanilines. Il confère également à la plante une résistance à ces herbicides. Seule l'oryzaline n'est pas métabolisée. La modélisation par homologie de CYP706A3 rationalise ces résultats et suggère que l'oryzaline n'a pas accès au site actif. D'autres CYP706s oxydant de petites molécules hydrophobes convertissent aussi les dinitroanilines.

Mots clé : résistance des adventices aux herbicides, métabolisme des herbicides, cytochrome P450 oxygénases, dinitroanilines

Résumé en anglais

Acquired weed resistance to herbicides is an increasing concern in modern agriculture. Herbicide metabolism by cytochrome P450 monooxygenases is a major source of resistance. In human liver, a few promiscuous P450s perform most of drug detoxification. Correlation of herbicide metabolism with plant P450 promiscuity was thus investigated. Major classes of herbicides were tested for oxidation by six plant P450 enzymes with low to high promiscuity. The most promiscuous, CYP706A3 from *Arabidopsis thaliana*, was found to hydroxylate pendimethalin and most other dinitroanilines. CYP706A3-mediated metabolism led to herbicide resistance in Arabidopsis plants. Only oryzalin was not metabolized. Protein homology modelling and dinitroaniline docking in CYP706A3 active site support experimental results and suggest that absence of oryzalin conversion results from impaired access to active site. Dinitroaniline conversion was also observed with other CYP706 enzymes metabolizing small hydrophobic compounds.

Keyword: weed herbicide resistance, herbicide metabolism, cytochrome P450 oxygénases, dinitroanilins